FEASIBILITY AND SYSTEMS DEFINITION STUDY FOR MICROWAVE MULTI-APPLICATION PAYLOAD (MMAP)

GE Report No. 77SDS4220

J.B. Horton, C.C. Allen, M.J. Massaro, J.L. Zemany,
J.W. Murrell, R.W. Stanhouse, G.P. Condon, R.F. Stone

General Electric Company
Valley Forge Space Division
Box 8555
Philadelphia, Pa. 19101

MARCH 1977

Prepared for

GODDARD SPACE FLIGHT CENTER
National Aeronautics and Space Administration
Communication and Navigation Division
Greenbelt, Maryland 20771

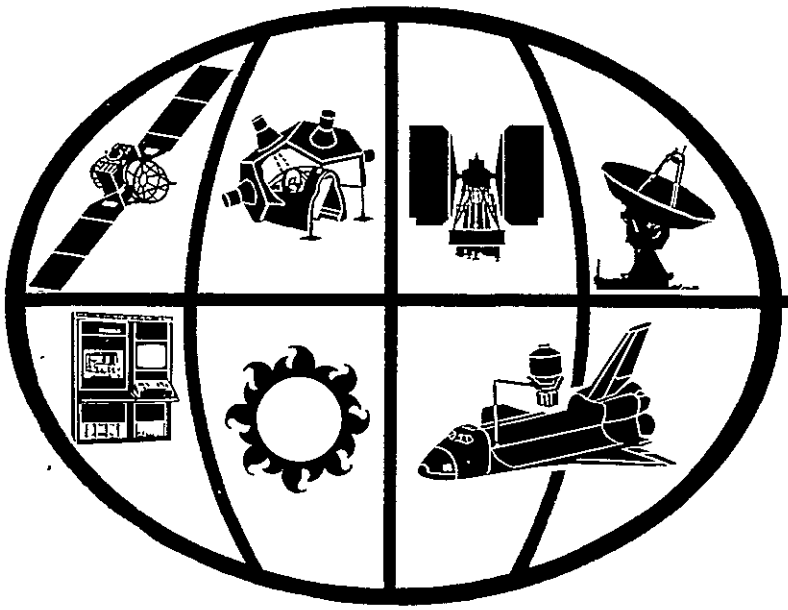

INTERIM REPORT

GENERAL ELECTRIC

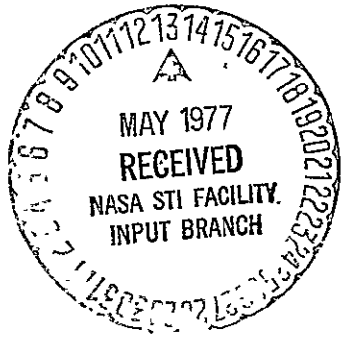

TECHNICAL REPORT STANDARD TITLE PAGE

1. Report No.	2. Government Accession No.	3. Recipient's Catalog No.

4. Title and Subtitle
Feasibility and Systems Definition Study for Microwave Multi-Application Payload (MMAP)

5. Report Date
March 1977

6. Performing Organization Code

7. Author(s)
J. B. Horton, C. C. Allen, M. J. Massaro, J. L. Zemany, J. W. Murrell, R. W. Stanhouse, G. P. Condon, R. F. Stone

8. Performing Organization Report No.
77SDS4220

9. Performing Organization Name and Address
General Electric Company
Valley Forge Space Center
P. O. Box 8555
Philadelphia, Pa. 19101

10. Work Unit No.

11. Contract or Grant No.
NAS-5-23734

12. Sponsoring Agency Name and Address
National Aeronautics & Space Administration
Goddard Space Flight Center
Greenbelt, Md. 20771
John J. Woodruff

13. Type of Report and Period Covered
Interim Report September 1976-March 1977

14. Sponsoring Agency Code
952

15. Supplementary Notes

16. Abstract

This report covers work completed to date on three Shuttle/Spacelab experiments: Adaptive Multibeam Phased Array Antenna (AMPA) Experiment, Electromagnetic Environment Experiment (EEE) and Millimeter Wave Communications Experiment (MWCE). Definition of these experiments has proceeded in parallel. Work on the AMPA experiment was completed. Results included are definition of operating modes, sequence of operation, radii of operation about several ground stations, signal format, foot prints of typical orbits and preliminary definition of ground and user terminals. Definition of the MOD I EEE (121.5 to 2700 MHz) was completed; this work included conceptual hardware designs, spacelab interfaces, preliminary data handling methods, experiment testing and verification, and EMC studies. The MWCE has been defined conceptually for a steerable high gain antenna, work is proceeding on a fixed antenna design.

17. Key Words (Selected by Author(s))	18. Distribution Statement
Shuttle, Spacelab, Microwave, Payloads, Antennas, Receivers, Ground Terminals, Communications	

19. Security Classif. (of this report)	20. Security Classif. (of this page)	21. No. of Pages	22. Price*
Unclassified	Unclassified		

*For sale by the Clearinghouse for Federal Scientific and Technical Information, Springfield, Virginia 22151.

PREFACE

The objective of this study is to provide NASA with a Feasibility and Systems Definition Study for Shuttle/Spacelab Microwave Multi-Applications Payload Experiments (MMAP). This study includes the selection and definition of the system design approach for certain key experiments, and includes the study of equipment requirements, and Shuttle interfaces for each of these experiments. Cost effective design is a major objective in the study. Work to data has been on the definition of the Adaptive Multibeam Phased Array (AMPA) experiment, the Electromagnetic Environment Experiment (EEE) and the Millimeter Wave Communications Experiment (MWCE). Work on the AMPA experiment definition is complete; user and ground terminal definition, and data reduction requirements have started. Definition of the MOD I EEE (121.5-2700 MHz) has been completed; work on MOD II (2.7 to 43 GHz) has started. Work during the next interim period will include continued effort on the AMPA, EEE and MWCE, with emphasis on generic system studies such as equipment reliability versus cost, electromagnetic compatibility, mission operations plan and cost estimates.

Effort will be expeded, as appropriate, on the OSP and suggested new experiments as directed by J. Woodruff.

The authors gratefully acknowledge the contributions of S. Durrani (AMPA), L. Ippolito (MWCE), R. E. Taylor (EEE), and J. Woodruff (MMAP) for their many contributions and suggestions in defining the MMAP experiments.

GLOSSARY

AMPA	Adaptive Multibeam Phased Array Experiment
ARE	Antenna Range Experimen
ATTN	RF Attenuator
BPF	Bandpass Filter
BPF/DIP	Band Pass Filter and Diplexer Combination
BPF/MUX	Band Pass Filter and Multiplexer Combination
bps	Bits per Second
BW	Bandwidth, Refers to Frequency
CMD	Command
CONUS	Continental United States
CRT	Cathode Ray Tube
CSSR	Cooperative Surveillance Spacelab Radar Experiment
CTRL	Control
DCMB	Data Collection With Multi-Beam Experiment
DEMOD	Signal Demodulator
DEMUX	Demultiplexer
DIP	Frequency Diplexer
DN/CNVR	Down Converter
EE	Electromagnetic (interference) Environment
EEE	Electromagnetic Environment Experiment
EIRP	Effective Isotropic Radiated Power
EMC	Electromagnetic Compatibility
F	Frequency
FCC	Federal Communications Commission
Forward Link	Data Link from OCC to Deployed Satellite or Sensor System
GPS	NAVSTAR/GPS Experiment
H	Orbit Height
HDDT	High Density Digital Tape
HPBW	Half Power Beam Width
ID	Identification
I/F	Attitude/Position Location Interferometer
I/O	Input to and/or Output from a Computer
IP	Input
IPD	Information Processing Division
IRAC	Interdepartment Radio Advisory Committee (U.S. Government)
ITU	International Telecommunications Union
K	Kilo-one Thousand
Kbps	Kilo-bits per Second
KM	Kilometers
LHCP	Left Hand Circular Polarization
LNA	Low Noise Amplifier
LNA/DIP	Low Noise Amplifier and Diplexer Combination
LO	Local Oscillator Signal
LOGP	Log Periodic RF Feed

GLOSSARY (Cont)

M	Mega - One Million
Mbps	Mega-bits per Second
METRAD	Meterological Radar
MMAP	Microwave Multi-Application Payload
MUX	Multiplexer
MWCE	Millimeter Wave Communications Experiment
OCC	Operations Control Center, A Ground Facility for Mission Control
OSP	Orbiting Standards Platform
PLI	Position Location Interferometer
POLC	Polarization Control
PS	Payload Specialist
RCVR	Receiver
Record	An Entry in a Data File
Reverse Link	Data Link from a Deployed Satellite or Sensor to OCC
RF	Radio Frequency
RFI	Radio Frequency Interference
RHCP	Right Hand Circular Polarization
S&R	Search and Receive
SMS R/M	Soil Moisture and Salinity Radiometer Experiment
SSR	Surface Spectrum Radar Experiment
STAT(S)	Statistic(s)
STDN	Spaceflight Tracking and Data Network
T&C	Telemetry and Control
TBD	To Be Determined
TCS	Technical Consultation Services
TDRS	Tracking and Data Relay Satellite
TDRSS	Tracking and Data Relay Satellite System
TLM	Telemetry
TT&C	Telemetry, Tracking and Control
WARC	World Administrative Radio Conference (ITU)
WBR	Wide Band Receiver
XMT	Transmitter

TABLE OF CONTENTS

TABLE OF CONTENTS (Cont'd)

LIST OF ILLUSTRATIONS

LIST OF ILLUSTRATIONS (Cont'd)

SECTION 1
INTRODUCTION

The National Aeronautics and Space Administration (NASA) has initiated this study to define a number of Shuttle/Spacelab experiments which are common in technology and which will further the technology goals of NASA in the communication and navigation fields. These experiments all fall within the scope of microwave technology and are grouped to form the Microwave Multi-Application Payload (MMAP) experiments. The experiments are:

1. Electromagnetic Environment Experiment (EEE)
2. Adaptive Multibeam Phased Array Antenna (AMPA) Experiment
3. Millimeter Wave Communications Experiment (MWCE)
4. Orbiting Standards Platform (OSP)
5. Antenna Range Experiment (ARE)
6. Cooperative Surveillance Spacelab Radar (CSSR) Experiment
7. Data Collection with Multibeam (DCMB) Experiment
8. NAVSTAR GPS Experiment (GPS)

During this study, it is planned that most of the effort will be directed toward the EEE, AMPA, MWCE and OSP experiments. These experiments have been partially defined in previous studies[1, 2, 3] and material from these studies has been used extensively in this study. Effort during this study is directed toward definition of experiment instrumentation such as antennas, receivers, data processing equipment, Shuttle interfaces and if required, instrument pointing systems. Other areas of investigation include ground operation and tests, mission operations plans, data handling plan, payload specialists functions, R&QA criteria, an EMC test plan, and listing of critical and long lead items. It is planned that work in the early phases of the study will be concentrated on the EEE, AMPA and MWCE experiments. This report covers work done during the interim contract period September 1976 through March 1977.

1.1 EXPERIMENT OBJECTIVES

The objective of this study is to provide NASA with a Feasibility and Systems Definition Study for the Shuttle/Spacelab Microwave Multi-Applications Payload Experiments. The study includes the selection and definition of the system design approach for certain key experiments, and includes the study of equipment requirements, Shuttle interfaces and ground equipment. Cost effective design is a major objective in the study.

1.2 STUDY APPROACH

The basic approach to defining the MMAP experiments is to apply cost effective design to each experiment, and where practical, to use common equipment designs. Equipment such as antennas, power supplies, control systems and thermal/mechanical systems is expected to be pallet mounted and unique to the MMAP experiments. Data processing equipment, control and display equipment, recorders, and Shuttle interface equipment will probably be located in the Spacelab module and may use common equipment for any experiments. The approach used in this study is to define each experiment for the best cost compromise between unique equipment and Shuttle/Spacelab equipment available to experiments.

Several factors have caused the initial experiment definition to change. These are primarily the role that the payload specialist will have in the experiment, the accessability of the TDRSS real-time data link to the experiment, the amount of operating time an experiment will have, the viewing angle of the experiment antennas, and availability of the Spacelab module. These factors have not necessarily changed the design to cost approach, but have affected the overall philosophy of experiment operation and data management. During the discussion of each experiment, these factors will be included.

Functional definition of each experiment must be carried out to show feasibility of design, and mechanical interfaces with the Shuttle. For the MMAP, all experiments have antennas and associated equipment such as receivers, transmitters, power supplies, etc., and design of the equipment must include field-of-view of the antenna and space to accommodate the associated equipment. Therefore, location of the equipment on the Shuttle is a principal design factor for each experiment. Similarly, other Shuttle related environmental factors; e.g., electromagnetic compatibility (EMC), are considered in the feasibility study.

Ground support equipment is included with each experiment. This includes test equipment for the instrument, and ground terminal equipment for experiment operation. Similarly, supplemental equipment such as data handling and processing equipment is examined for feasibility and to help in devising methods of data reduction. Where practical existing NASA equipment is used for these ground operations.

The overall study approach follows the primary cost effective design approach by using experiment-unique equipment, optimizing operation of this equipment by careful selection of its location in the Shuttle, allowing for maximum operating time when practical, and using existing equipment on the Shuttle and at ground locations whenever practical. This approach should provide the most reliable design and minimum practical cost for each experiment.

SECTION 2

EXPERIMENT DEFINITION

This section includes work completed to date on definition of three MMAP experiments: AMPA, EEE and MWCE. Each of these experiments was studied to determine the feasibility of the instrument design, experiment operation and compatibility of the experiment with the Shuttle[4, 5]. To help in performing operational studies, a 400 km, 57° inclination orbit was assumed. Details of this orbit are included in this section.

2.1 TYPICAL ORBIT PROFILE

A typical orbit profile for the MMAP studies was performed in a previous study to establish operating times for an experiment and to obtain the maximum geographical coverage possible on a typical 7-day Shuttle mission during the 1981-82 time frame.[1] During this time period the Shuttle will be launched from the Eastern Test Range (ETR), Cape Canaveral, Florida, and the maximum orbit inclination being 57°. Results of this study are included here for reference.

To obtain reasonable operation parameters, certain mission guidelines were established. For example, a 7-day orbiter mission is in reality a 6-day mission for EEE, since 1/2 day is needed for orbiter check-out, equipment deployment and experiment check-out, and 1/2 day is needed for orbiter landing preparation. A circular orbit is assumed and orbit altitude is assumed 400 km. Knowing that the launch will be from the ETR, the basic mission parameters for the study can be established as follows:

1. Mission Duration: 6 days
2. Orbit Inclination: 57°
3. Altitude: 400 km
4. Orbit Shape: Circular
5. Insertion Point: ETR (28.5°N, 80.5°W)

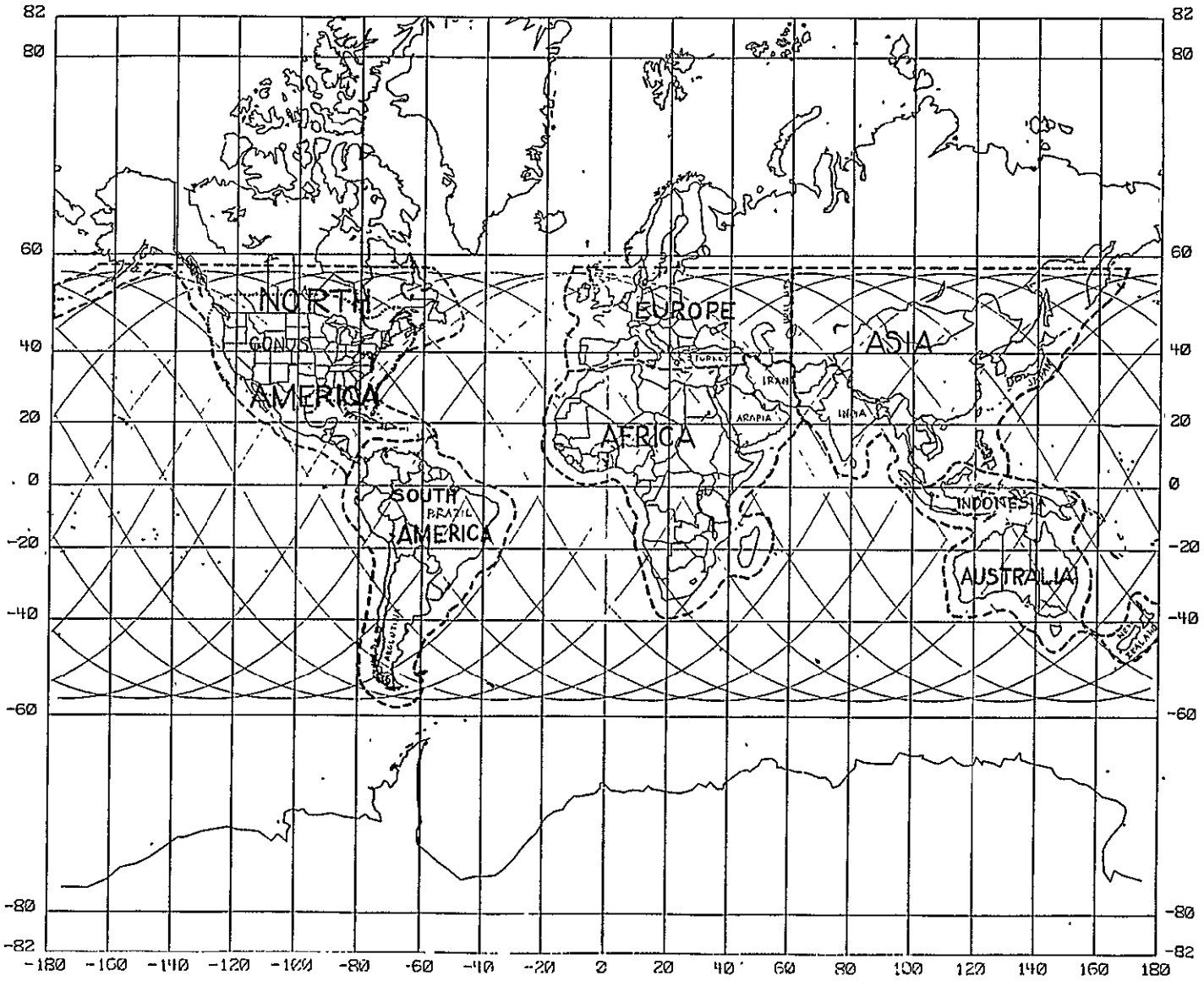

Figure 2-1. Typical EEE Region of Interest/First Day Orbit Traces

The above parameters define a mission profile that covers an area symmetrical about the equator and bounded by $\pm 57^{\circ}$ latitude. Figure 2-1 shows the typical first-day traces of an orbiter inserted in orbit at the ETR and exhibiting these parameters. Characteristics of the profile are:

1. Exact 3 day repeat orbit
2. Orbit period 92.65 minutes (15.54 revolutions/day)
3. Orbits per 6 day missions: 93.34
4. Distance between adjacent orbits 7.8° = 470.4 nm = 871 km (ref. Equator)
5. Orbits over CONUS: 21 per 3 day cycle = 42

Figure 2-1 shows a representative orbit pattern for the first day of a mission. During the second and third days the orbit traces move progressively eastward to fill the area between the traces shown, providing two additional traces between each trace shown in Figure 2-1. The resulting grid over the CONUS is shown in Figure 2-2. This grid and similar grids over the other regions of interest was used to determine fly-over times and EEE operating periods.

Table 2-1 shows typical viewing time for each of the regions outlined in Figure 2-1. Note that the total viewing time for all six geographical regions is 58.93 hours for the entire 6-day mission. Extending this analysis to the CONUS only (Table 2-2), the viewing time is about 50 minutes per day and only 5.15 hours total. Some fly-over times are extremely short, e.g., Nos. 5 and 35 orbits, and no fly-over occurs for orbits Nos. 20 and 66.

The distribution of the CONUS observations times can be seen in Figure 2-3. Shown are the times of orbit coverages for the six days (from Table 2-2 data) plotted on a 24-hour basis starting with the indicated T_0 time reference. Note that all operating times are in nearly the same block of hours each day, thus a six-day mission would not provide for viewing during both daylight and night hours. An early daylight Shuttle launch would be preferred for EEE to obtain viewing during daylight hours, since the major electromagnetic radiation activity occurs during those hours. To cover both day and night on the same mission, a longer mission period is required or orbit parameters must be altered, e.g., change of altitude, orbit inclination and launch site.

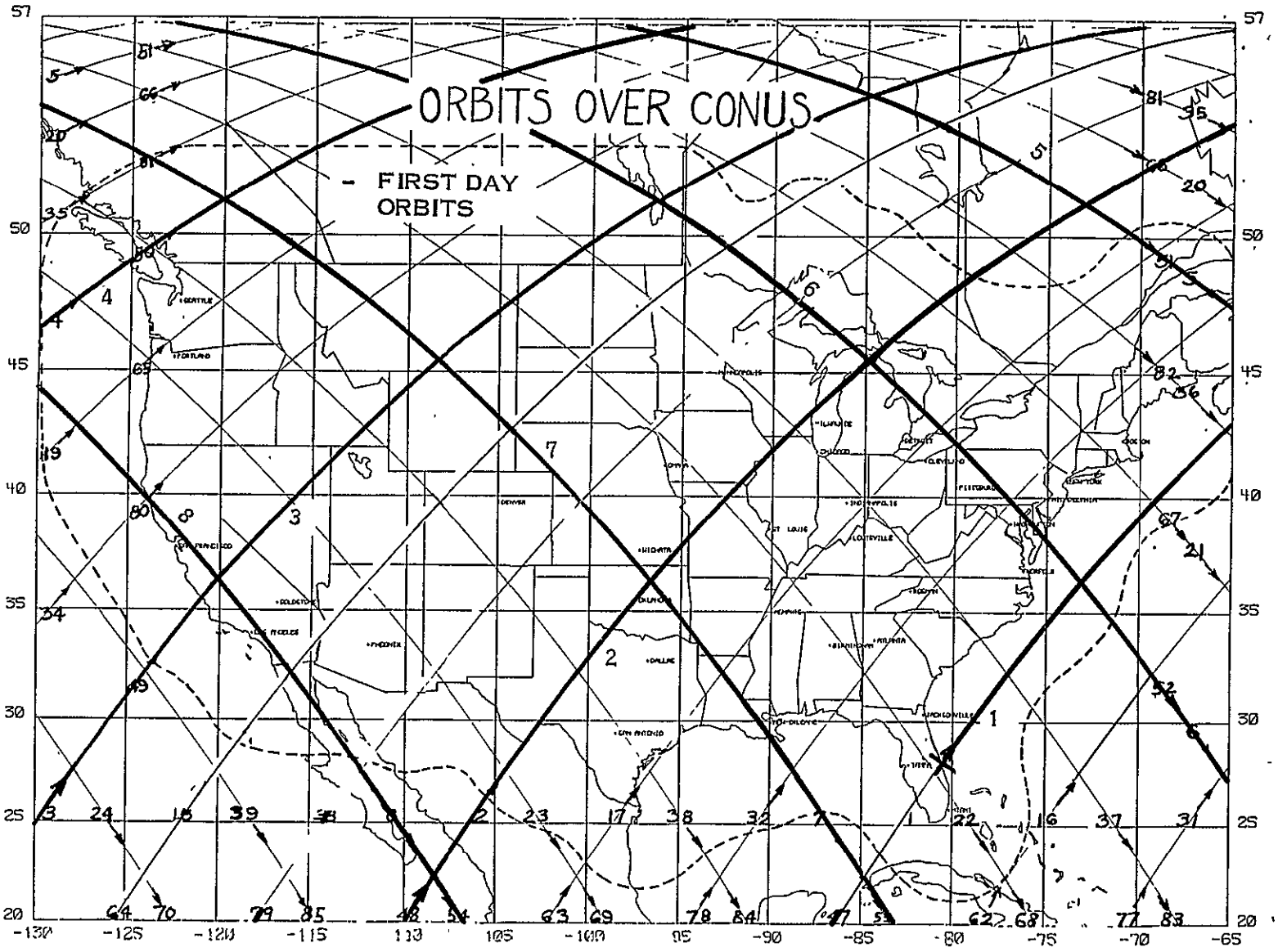

Figure 2-2. CONUS Orbit Pattern (6-Day Mission)

Table 2-1. Estimated Viewing Times* for Global Areas

Areas	Time - 6 Day Mission
CONUS - also included in North America time	5.15 Hours
North America - Includes, Canada, Central America, and Caribbean area as well as CONUS	11.87
South America - As shown	7.12
Europe	7.21
Africa	11.00
Asia	15.44
Australia	6.29
Six-Day Total	58.93 Hours

*Includes one minute operation at each end of each orbit outside applicable boundary or shoreline (See Figure 2-1)

Table 2-2. Operating Time Over CONUS* (Minutes)

Day 1		Day 2		Day 3		Day 4		Day 5		Day 6	
Orbit	Time	Orbit	Time	Orbit	Time	Orbit	Time	Orbit	Time	Orbit	Time
1	7.5	17	9.75	32	4.98	48	8.4	64	8.82	79	8.15
2	8.4	18	8.82	33	8.15	49	7.7	65	4.75	80	6.65
3	7.7	19	4.75	34	6.65	50	2.65	66	x	81	.50
4	2.65	20	x	35	.50	51	1.85	67	6.35	82	3.05
5	1.85	21	6.35	36	3.05	52	7.75	68	11.35	83	8.5
6	7.75	22	11.35	37	8.5	53	9.75	69	8.4	84	9.8
7	9.75	23	8.4	38	9.8	54	5.3				
8	5.3										
										93	7.5
		32	3.0	47	7.5	63	9.75	78	7.98	94	8.4
Total	50.90		52.42		49.13		53.15		50.65		52.55
Six Day Total: 308.80 Minutes 5.15 Hours											

*Assumes one additional minute of operation at each end of orbit path over the U.S. beyond the border/coastline crossings (See Figure 2-2)

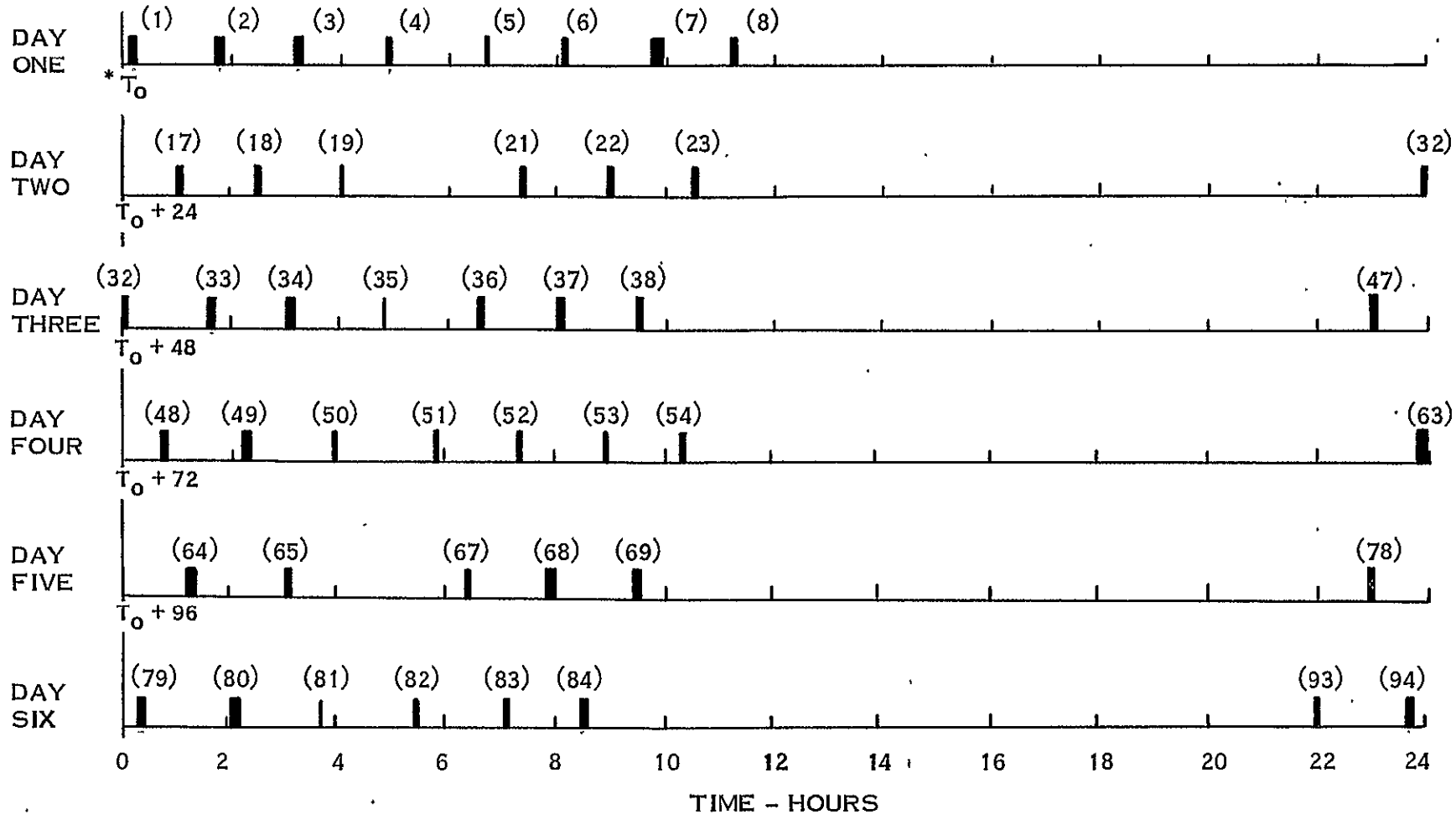

*T_o REFERENCE IS ORBIT NO. 1 CROSSING OF EQUATOR, ASCENDING ORBIT, 57° INCLINATION

( ) = ORBIT NUMBER

Figure 2-3. Operating Times Over CONUS for Six Day Mission

SECTION 3

ADAPTIVE MULTIBEAM PHASED ARRAY (AMPA) EXPERIMENT

Definition of the AMPA experiment is being conducted in four study phases. These are

1. AMPA Experiment Definition. This is the basic definition phase and covers the conduct of the experiment; defining the equipment needed at the Spacelab, ground and user terminals; specifying the parameters to be observed and the method of recording them; and definition of the Spacelab to TDRS link with respect to data transmission and format.

2. User-Terminal Preliminary Design. This phase covers identification of the user-terminal requirements; and preliminary design of the basic user-terminal equipment.

3. Ground Control-Terminal Preliminary Design (JSC). This phase covers identification of the ground control-terminal requirements; preliminary design of the basic ground control-terminal equipment; and specification of calibration beacons.

4. Data Reduction Requirements. This phase covers identifying the data reduction requirements during flight and after flight; and specifying the format, amount, and method of data reduction and analysis.

Effort during the first interim period has been concentrated primarily on the experiment definition. Some preliminary effort was applied to user terminal definition in order to establish the user-terminal parameters assumed for communications link calculations.

Work on experiment definition was done in several related areas. An expansion of the operational concepts for the AMPA Experiment was conducted in order to better define the operational modes and sequence of operations for each. An analysis was made of AMPA radii of operation and footprints on earth for typical orbits. Typical AMPA operating times were determined from the radii of operation. A set of assumed experiment parameters and operating conditions was established for the communications link, the adaptive beamforming control link, and the user ground stations. Link calculations were made to determine carrier-to-noise (C/N) ratios for both the communications link and the adaptive beamforming control link for the assumed operating conditions. Signal modulation and format were proposed for both the communications signal and the pilot signal.

3.1 AMPA EXPERIMENT DEFINITION

3.1.1 AMPA EXPERIMENT CONCEPT AND PURPOSE

The basic concept of the AMPA Experiment is the use on a spacecraft of independently steerable high-gain agile beams that can be formed adaptively on those low power users that signal a valid address or user code. Simultaneously, undesired interfering signals that are not properly coded will be adaptively rejected. By providing high EIRP on the spacecraft portion of the overall communications system and rejecting interference, the Adaptive Multibeam Phased Array (AMPA) system enables many small user applications to be met, such as low-power point-to-point communications between small users, data collection from widely distributed low power sources, emergency aid to users in distress, search and rescue operations, hospital/medical data relay, etc. The basic AMPA L-band Communications Experiment configuration is illustrated in Figure 3-1, which was generated during the AMPA Phase A Feasibility Study.[2]

The general purpose of the AMPA Experiment on Spacelab is to provide a test bed for demonstrating and verifying the feasibility of adaptively establishing such a two-way (duplex) communications link at L-band between typical low-power user terminals via a low orbiting spacecraft. Ultimately, such a system could be used as a free flyer or at synchronous geostationary orbit and tailored to specific applications. The heart of the AMPA Experiment is the Adaptive Multibeam Phased Array, which as presently envisioned would have only two adaptively formed transmit/receive beams. Two beams are sufficient to conduct the experiment and minimize the AMPA equipment costs. The use of two beams is not limiting, however, and the experimental results will be directly applicable to expanded AMPA systems for applications requiring 6, 8, 12 or more simultaneous, independently steerable, adaptively formed beams. Such an expanded AMPA system would use the same phased array radiating elements, microwave distribution networks, and RF amplifiers as the two-beam array, but would have additional adaptive beamforming circuits and transponders for the added channels.

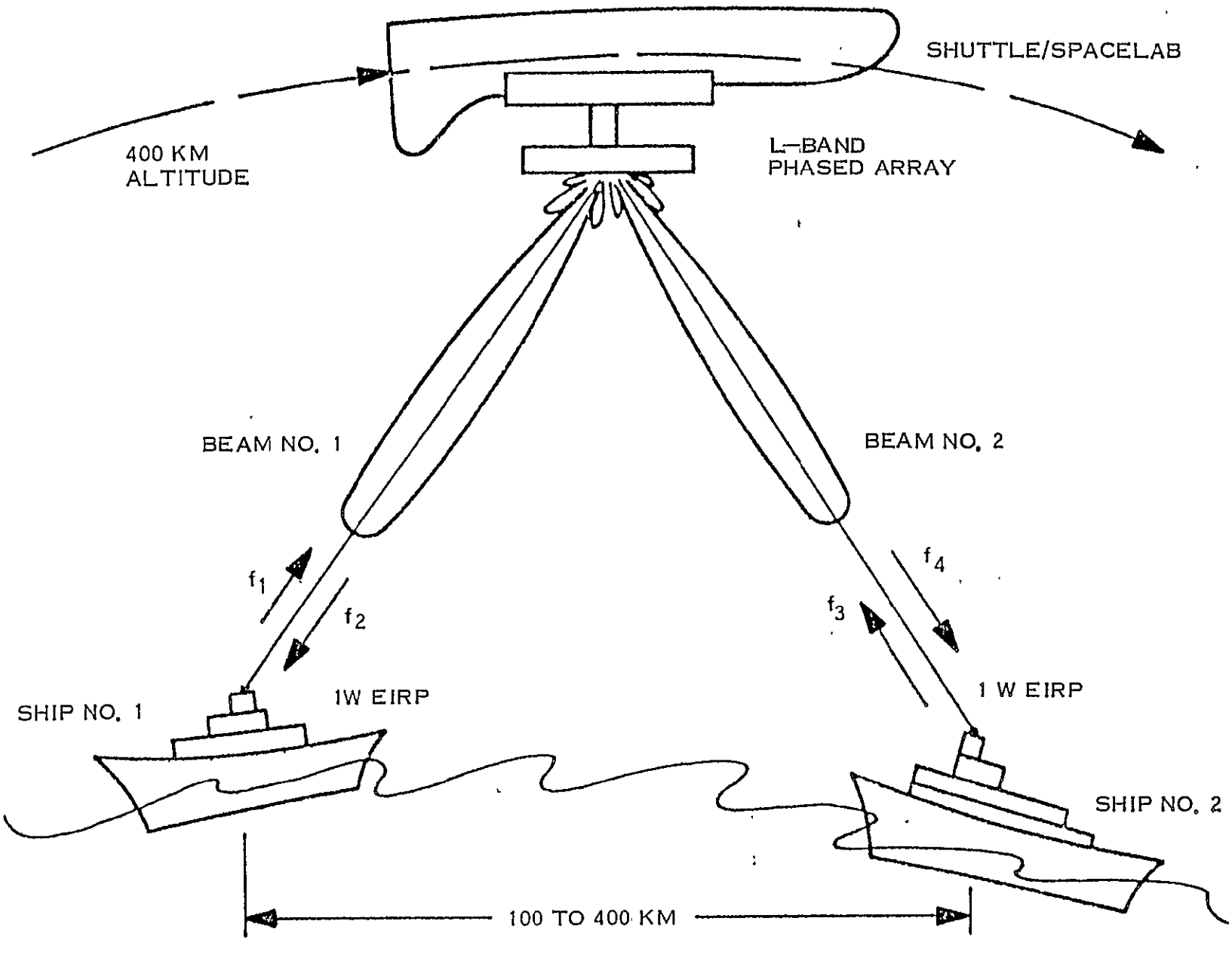

Figure 3-1. AMPA L-band Communications Experiment Configuration

3.1.2 AMPA EXPERIMENT OPERATIONAL CONCEPTS

Two major operational concepts have been considered for the AMPA Experiment. The first uses fully-adaptive beamforming and interference rejection, as described briefly in paragraph 3.1, and is by far the most versatile and effective operational use of the AMPA system, since it fully utilizes the inherent AMPA capabilities.

The second operational concept for the AMPA Experiment uses a programmed search or commanded beam steering to acquire and track each valid user with a beam, and only uses the adaptive circuitry to reject interference. This operation of the AMPA system is less versatile than the first since it requires some prior knowledge of the user locations in order to function efficiently. An undue amount of time could be used up in the search mode without such a priori information.

It is assumed here, therefore, that the AMPA equipment is capable of fully-adaptive operation for both beamforming and interference rejection. It is also assumed, however, that the adaptive beamforming mode of operation can be switched to a programmed search or commanded beam steering mode of operation for operational flexibility. Both operational concepts can thus be employed for the AMPA Experiment.

3.1.2.1 Fully-Adaptive AMPA Experiment Operational Modes

Four fully-adaptive operational modes are currently envisaged for the AMPA Experiment. These are listed below:

1. User/User Operation (paired AMPA Beams)/Duplex Comm Link without interference
2. User/User Operation (paired AMPA Beams)/Duplex Comm Link with interference
3. User/Spacelab Operation (independent AMPA Beams)/Duplex Comm Link
4. User/Spacelab Operation (independent AMPA Beams)/One-Way Comm Link

Adaptive operation in all four modes would consist of:

1. Acquisition of valid User
2. Beamforming on User
3. Tracking of User
4. Retrodirected transmit beam
5. Interference rejection

For all four full-adaptive modes, it is assumed that each user terminal has a unique identification code and frequency, that each user terminal has hemispheric coverage antennas, and that the normal to the AMPA on Spacelab is pointed along the nadir.

The first mode in the above list is a basic operational mode for the AMPA system and is that pictured in Figure 3-1 for duplex communications between two user terminals. For this mode, the AMPA system would adaptively form two receive beams and two corresponding transmit beams to establish a duplex communications link between two co-operating shipboard or mobile terminals within the coverage area. The data relayed via the AMPA antenna system would be recorded on board the Spacelab or be relayed to ground in order to evaluate the received and relayed signal quality. The signals received by each user terminal would also be recorded for evaluation. Other key measurement parameters to be recorded for evaluation are the user acquisition time, the tracking accuracy, the signal-to-noise (S/N) ratio at Spacelab and at the user terminals, and the Doppler compensation achieved at Spacelab.

The second mode is a variation of the first, in which interference of a controlled type and level is present from a third user terminal whose signal does not have a valid user code. The purpose of this mode is to permit evaluation of the AMPA adaptive interference rejection in a systematic manner for various levels and types of interfering signals. The data recorded would be the same as that for the first mode plus measures of the interference rejection/cancellation under the different controlled conditions and the degree to which signal-to-noise plus interference, S/(N+1), is maximized for the desired transmission.

The third mode listed is likewise a variation of the first in which a duplex communications link is established adaptively between a single user terminal and the AMPA system, which is used as a Spacelab terminal in this mode rather than as a relay. Controlled interference could be introduced with this mode, as was described for the second mode, to permit further evaluation of the AMPA adaptive interference rejection capability.

The fourth mode is similar to the third except that the single beam is used for receive only in a one-way communications link. This mode could be used for such experiments as data collection from buoys and platforms having suitable beacon terminals or search and rescue operations with a suitable distress beacon terminal.

Both the third and fourth modes could be used also as special check-out modes for each beam of the AMPA system to evaluate its technical performance as an instrument, as compared to its operational performance. In such a checkout mode, antenna performance parameters such as acquisition time, S/N at Spacelab, Doppler compensation achieved, and angle tracking would be recorded for analysis.

A typical sequence of operation for the AMPA Experiment operated in its User/User dual-beam duplex communications link mode is as follows:

1. Shuttle/Spacelab flies into Radius of Operation of User Terminal
2. Adaptive Loops Acquire User Identification Signal and Form Beam No. 1
3. AMPA sends Verification Signal to User
4. Shuttle/Spacelab flies into Radius of Operation of 2nd User Terminal, Acquires, Forms Beam No. 2, and Verifies Contact to both Users.
5. AMPA Relays Data Transmission between Users simultaneously, sequentially, or responsively during contact.
6. Adaptive Loops Track Users and Reject Interference
7. AMPA Alerts Users when Contact Termination is imminent.
8. Sequence Repeats for Next User as Shuttle/Spacelab enters its Radius of Operation.

3.1.2.2 Programmed AMPA Experiment Operation

The programmed search or commanded beam steering mode is an alternative mode of operation for AMPA to fully-adaptive signal acquisition, beamforming, and tracking. Prescribed search patterns can be generated for special purposes with this mode, while the adaptive array circuitry only provides interference rejection. This is a desirable feature to provide for the AMPA system, since it permits either adaptive beamforming or commanded beam steering for greater operational versatility.

Programmed operational modes for the AMPA Experiment would be similar to the four listed in paragraph 3.1.2.1 for fully-adaptive AMPA operation. User terminal locations would have to be known priori to use these modes for duplex communication links, however, and this would limit their utility. It is more likely that the programmed operational modes would be found useful in search operations for user terminals that do not have the identification codes required for adaptive beamforming operation of the AMPA system.

3.1.3 AMPA COVERAGE AREA/RADIUS OF OPERATION

A study was made of AMPA radii of operation for typical Shuttle/Spacelab earth orbits to determine the geographic area coverage obtained and the typical times of operation. Calculations were made for a 5° ground-station elevation angle, which represents the lowest practical ground-station elevation angle, and also for a 23° ground-station elevation angle, which corresponds to a 60° scan angle of the AMPA from the normal to the array face. A 400 km orbit altitude is assumed with a nadir-pointing beam at 0° scan. A scan angle of 60° represents the practical limit usually used for phased-array scan angles. Since the AMPA is adaptive, however, and can self-compensate to some extent for the detrimental effects of mutual coupling etc. at large scan angles, it should be possible to scan beyond 60° somewhat and thus achieve greater coverage area and operating time. The AMPA scan angle only increases to 69.6° for a 5° ground-station elevation angle and the 400 km orbit altitude, but the corresponding increase in coverage area is large because of the earth curvature, and total operating time is increased 5 to 7 times.

Typical operating areas over the CONUS (Continental United States) are shown in Figure 3-2 for ground stations located at NASA/GSFC, Rosman, NASA/Lewis, and Goldstone. NASA sites were selected for more convenient experiment planning and operation. The lighter contour line about each location is for a 23^{o} ground-station elevation angle, while the heavy contour line is for a 5^{o} elevation angle. For general information, a horizon contour line is also included for the Goldstone location and corresponds to an AMPA scan angle of 70.2^{o}. The Shuttle/Spacelab orbits shown are for a 400 km. orbit altitude at an inclination angle of 57^{o}, which results in a series of orbits that progress from east to west (see orbit numbers) and repeat every 3 days.

For the User/Spacelab single-beam modes of AMPA system operation with a ground station (the third and fourth modes discussed in paragraph 3.1.2.1), each radius-of-operation contour defines the area of coverage under the specified conditions. Any orbit passing through this area will permit a User/Spacelab single-beam communications link to be established with the ground station during the time the Shuttle/Spacelab is within the area. While the radii-of-operation contour lines are slightly egg-shaped on a Mercator projection, they are true circles about the ground-station locations. Arc radius is indicated in Figure 3-2 for three contours about Goldstone.

AMPA User/Spacelab operating times are given in Table 3-1 for the 23^{o} elevation-angle contours about NASA/Goddard, Lewis, and Rosman and for the 5^{o} elevation-angle contour about Rosman. The table gives the daily number of orbits through each coverage area and the total contact time per day, as well as the total six-day contact time. A comparison of the two sets of figures for Rosman shows that the average time per orbit with a 5^{o} elevation angle is roughly twice that for the 23^{o} elevation angle and that the average number of orbits per day is more than doubled, thus the total contact time is nearly 5 times as great. The total 6-day experiment operational time would be 680 minutes for four stations and 1020 minutes with 6 stations.

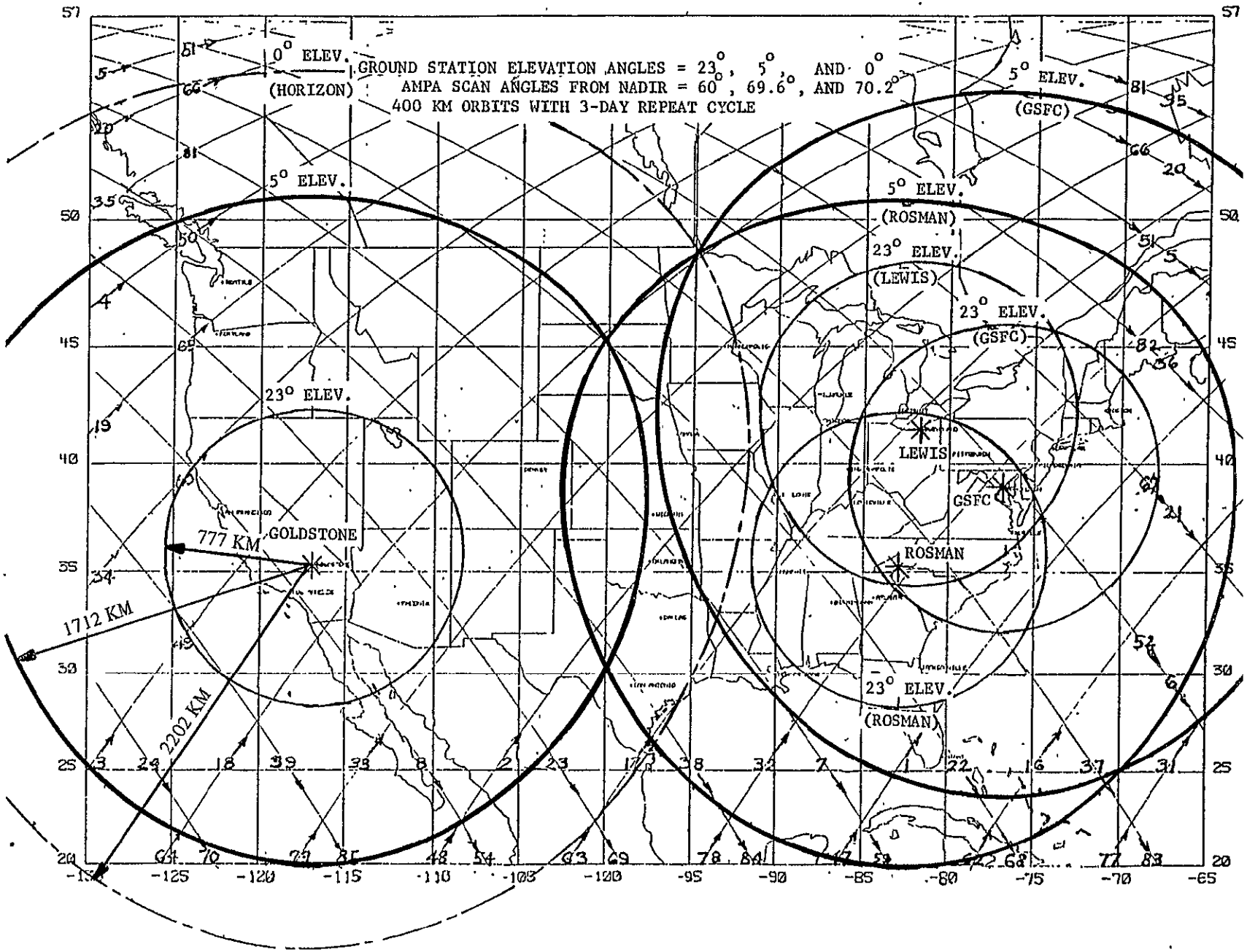

Figure 3-2. Typical Operating Areas Over CONUS

Table 3-1. Typical AMPA User/Spacelab Operating Times for 5° and 23° Ground Station Elevation Angles

(TIME IN MINUTES; # = NO. OF ORBITS)

STATION	DAY 1		DAY 2		DAY 3		DAY 4		DAY 5		DAY 6		6 DAY TOTAL TIME	AVE. TIME PER ORBIT	AVE. NO. OF ORBITS/DAY
	#	MIN.	#	MIN.	#	MIN.	#	MIN.	#	MIN.	#	MIN.			
GSFC (23°)	2	6.6	3	8.8	2	5.8	2	6.2	2	6.2	1	2.8	36.4	3.03	2.00
LEWIS (23°)	2	6.1	3	9.0	1	3.3	3	9.7	2	5.4	1	3.3	36.8	3.07	2.00
ROSMAN (23°)	2	3.5	3	9.8	2	5.5	2	4.5	2	6.8	1	3.5	33.6	2.80	2.00
ROSMAN (5°)	4	28.5	6	36.6	5	27.1	5	34.2	4	23.3	4	19.5	169.2	6.04	4.67

For the User/User dual-beam modes of AMPA system operation with a pair of ground stations (the first and second modes discussed in paragraph 3.1.2.1), the area common to two overlapping radius-of-operation contour lines defines the User/User region of operation for the two ground stations under the specified conditions. Any orbit passing through this region will permit a dual-beam communications link to be established between the two ground stations during the time the Shuttle/Spacelab is within the region.

Referring to Figure 3-2, it is seen that very little contact time would be available between Goldstone and Rosman even with 5^{o} ground-station elevation angles. For Rosman and Goddard, however, as well as for Rosman and Lewis and for Goddard and Lewis, there is a relatively large region of operation with 23^{o} ground-station elevation angles and an even larger region with 5^{o} elevation angles. For Goddard, Rosman, and Lewis, a part of their coverage areas is common to all three ground stations and defines a potential region in which three-beam operation could be performed or in which a User/User two-beam communications link could be established between two of the three stations while controlled interference was transmitted from the third (i.e., the second mode discussed in paragraph 3.1.2.1).

In order to obtain greater total operating time for the AMPA Experiment with the User/User mode of operation, more ground stations could be provided. Typical operating areas over the CONUS are shown in Figure 3-3 for ground stations located at Goldstone, White Sands, Johnson Space Center, St. Louis, Rosman, and Goddard. For clarity, the radius-of-operation contour lines are shown only for the 23^{o} ground-station elevation angle; however, much larger regions of operation can be visualized with the overlapping contours for 5^{o} elevation angles.

AMPA User/User operating times are given in Table 3-2 for the adjacent station pairs (Goldstone/White Sands, White Sands/Johnson, Johnson/St. Louis, St. Louis/Rosman, and Rosman/Goddard) for the 23^{o} ground-station elevation angle. Also included in the table are the User/User operating times for the Rosman/Goddard station pair for a 5^{o} elevation angle, as obtained from Figure 3-2. Comparison of the two sets of figures for the Rosman/Goddard station pair shows that the average time per orbit with a 5^{o} elevation angle is over three times that for the 23^{o} elevation angle and that the average number of orbits per day

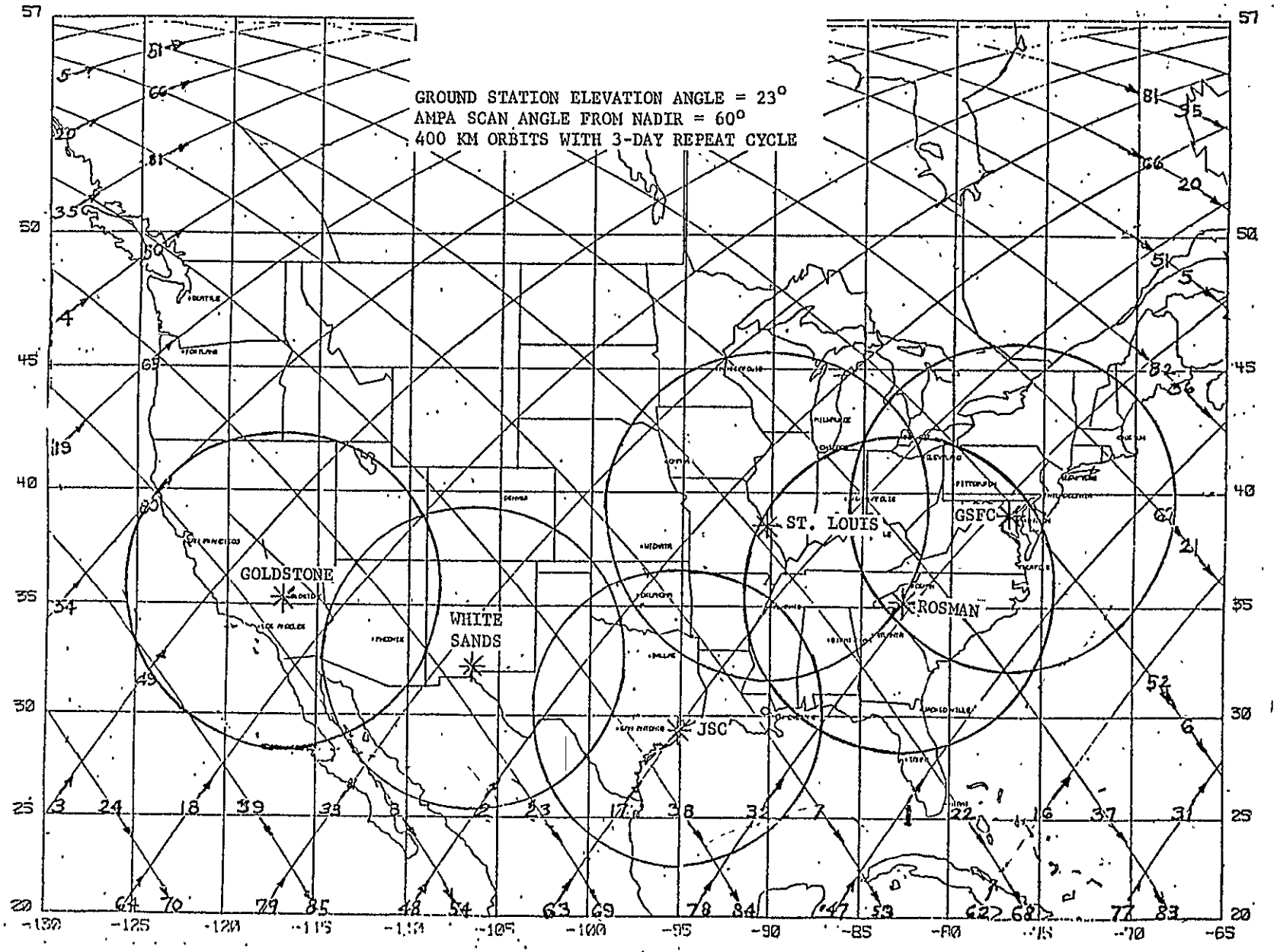

Figure 3-3. Typical Operating Areas Over CONUS

Table 3-2. Typical AMPA User/User Operating Times for 5° and 23° Ground Station Elevation Angle

(TIME IN MINUTES; # = NO. OF ORBITS)

STATION PAIR	DAY 1		DAY 2		DAY 3		DAY 4		DAY 5		DAY 6		6 DAY TOTAL TIME	AVE. TIME PER ORBIT	AVE. NO. OF ORBITS/DAY
	#	MIN.	#	MIN.	#	MIN.	#	MIN.	#	MIN.	#	MIN.			
GOLDSTONE/ WHITE SANDS (23°)	0	-	2	3.2	0	-	0	-	2	3.2	0	-	6.4	1.60	0.67
WHITE SANDS/ JSC (23°)	1	1.7	0	-	1	1.2	1	1.7	0	-	1	1.2	5.8	1.45	0.67
JSC/ ST. LOUIS (23°)	2	2.0	1	1.1	0	-	3	3.1	0	-	0	-	6.2	1.03	1.00
ST. LOUIS/ ROSMAN (23°)	0	-	2	4.6	1	1.6	1	2.8	1	1.8	1	1.6	12.4	2.07	1.00
ROSMAN/ GSFC (23°)	2	2.5	2	3.2	2	3.8	2	2.6	1	2.1	1	2.8	17.0	1.70	1.67
ROSMAN/ GSFC (5°)	4	20.5	5	29.4	4	20.6	5	25.0	3	18.7	3	14.4	128.6	5.36	4.00

is more than doubled, thus the total time for User/User operation is over 7 times as great. The total 6-day experiment operational time for the User/User mode would then be 640 minutes for the five pairs of stations.

3.1.4 AMPA FOOTPRINT ON EARTH

The footprint of the AMPA beams on earth was studied to determine the combined effects of beam broadening with angle of scan from nadir and increased space attenuation with greater slant range. For a 2 meter by 2 meter array aperture, the -3 dB beamwidth at 0° scan is about 7.5° at 1500 MHz. The beamwidth increases in the plane of scan inversely as the cosine of the scan angle, to a first approximation. At a 60° scan angle, therefore, the -3 dB beamwidth is about 15° in the plane of scan, which places the -3 dB angles at about 52.5° and 67.5°. Because of the rapidly increasing space attenuation with increasing scan angle in this region, the relative -3 dB levels on earth occur at angles that are somewhat smaller than given above and the 0 dB reference level also occurs at a smaller angle than the scan angle.

Footprints of the AMPA -3 dB contours on earth are shown in Figure 3-4 for scan or viewing angles of 0°, 15°, 30°, 45°, and 60° from nadir. The footprints are plotted against radial arc length on earth from nadir, and the central earth angle from nadir is also indicated for reference. Shown dotted for comparison are the -3 dB beamwidth contours without space attenuation (path loss) for the 45° and 60° scan angles. For any point on an orbit within an AMPA single-beam coverage area or dual-beam region of operation, the footprint on the earth about the ground-station location can be obtained by interpolation from Figure 3-4 and placed on the operating area maps shown in Figures 3-2 and 3-3.

3.1.5 AMPA PARAMETERS, OPERATING CONDITIONS, AND LINK CALCULATIONS

A set of assumed parameters and operating conditions was established for the AMPA system in order to permit link calculations to be made for the AMPA Experiment operation. These assumed operating conditions are shown in Table 3-3 for the AMPA antenna system and in Table 3-4 for the User Terminals (ground stations that will be used to simulate small user terminals). The variation in AMPA receive and transmit gain was assumed to vary as the

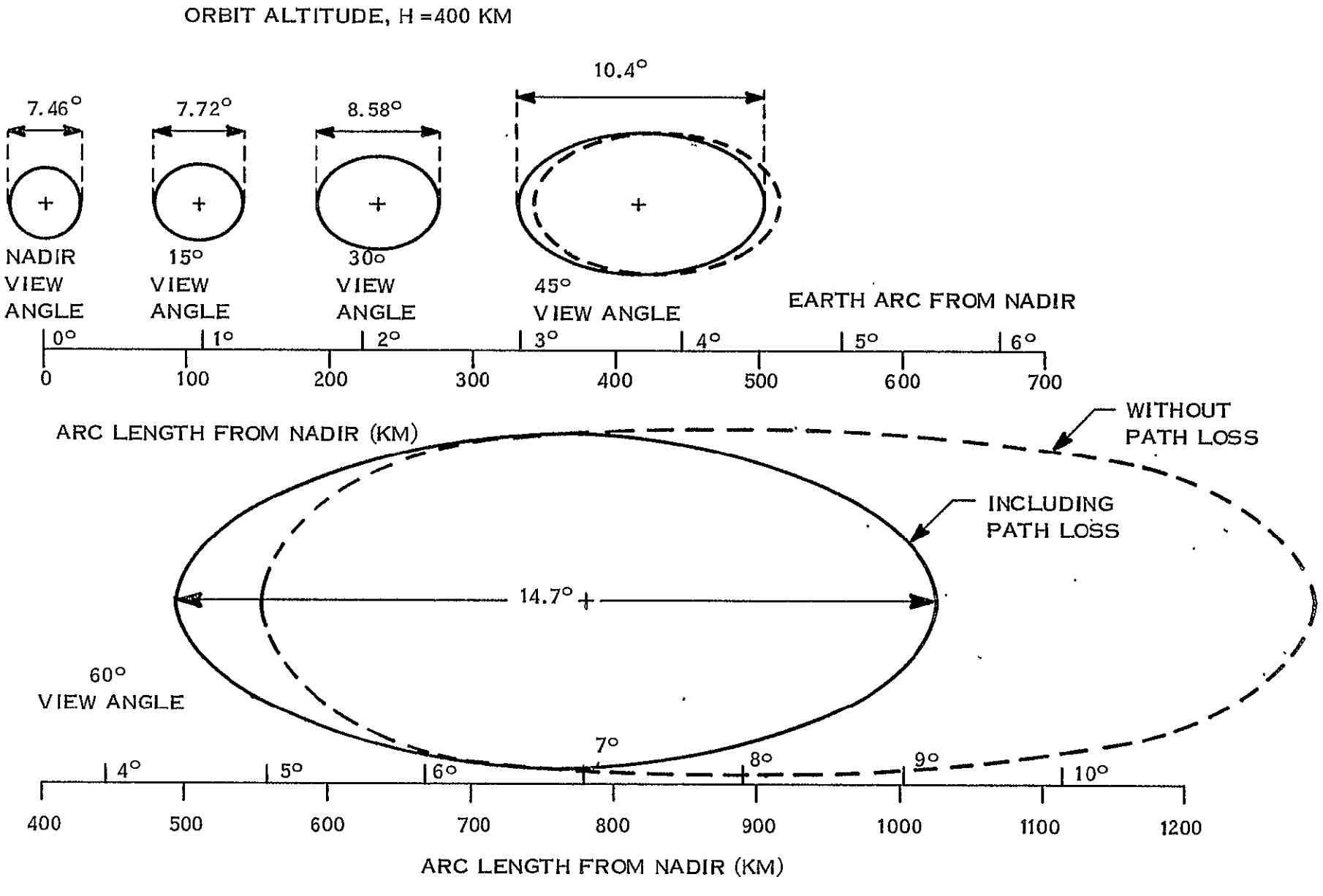

Figure 3-4. Footprint of AMPA -3 dB Contour on Earth for Several View/Scan Angles from Nadir

cosine of the scan angle. The full array gain is assumed for transmit, and the radiated power per beam takes into account the beam-splitting loss incurred with simultaneous independent beams. The system noise temperature assumes a receiver noise figure of 5 dB (627^{o}K) plus 83^{o}K for circuit losses and a 290^{o}K antenna/ground temperature.

Table 3-3. AMPA Experiment Parameters and Operating Conditions

AMPA Antenna System
• Number of Radiating Elements = 32
• Field of View = $\pm 70^{o}$
• Gain (Beams Formed) = 19.2 dB/Beam at 0^{o} Scan
• Radiated Power = 6.6 Watts/Beam (8.2 dBW)
• System Noise Temperature = 1000^{o}K*
• Transmit Frequency = 1.54 GHz
• Receive Frequency = 1.64 GHz
• RF Bandwidth = 7.5 MHz (3 Bands of 2.5 MHz)
• Comm Signal Bandwidth = 50 KHz
• Pilot Signal Bandwidth = 1 KHz

*Note: $T_S = T_A + T_R$

Table 3-4. AMPA Experiment Parameters and Operating Conditions

User Terminals
• Antenna Coverage = Hemispheric
• Radiated Power = 1 Watt EIRP Above 23^{o} Elevation Angle (5 Watts EIRP for 5^{o} Elevation Angle)
• System Noise Temperature = 860^{o}K*
• Transmit Frequency = 1.64 GHz
• Receive Frequency = 1.54 GHz

*Note: $T_S = T_A + T_R$

Link calculations were made for the AMPA communications channel and for the adaptive beamforming channel. The carrier-to-noise ratio (C/N) for the communications channel was calculated for the uplink from a ground station to Spacelab, for the downlink from Spacelab to a ground station, and for the total dual-beam link between two ground stations having the same elevation angle to Spacelab. The results are shown plotted against AMPA view/scan angle in Figure 3-5 with the corresponding ground-station elevation angles also indicated. The available C/N margins above a 10 dB minimum are also indicated. It is seen that the assumed operating conditions are adequate out to an AMPA view/scan angle of 62^{o}, and that an additional 7 dB of ground station power (5 Watts EIRP) would permit operation out to 69.6^{o}, which corresponds to a 5^{o} ground-station elevation angle.

The carrier-to-noise ratio for the adaptive beamforming channel was calculated only for the uplink, since the corresponding transmit beam is retro-directed by an algorithm that uses the adapted radiating-element weights of the receive beam. The results are shown plotted against AMPA view/scan angle in Figure 3-6. It is seen that the assumed operating conditions are adequate in this case out to an AMPA view/scan angle of over 66^{o}, thus the adaptive beamforming channel is not the limiting link in the AMPA Experiment.

3.1.6 AMPA EXPERIMENT EQUIPMENT

The AMPA Experiment requires equipment on Spacelab, at user terminals, at the ground control terminal, and at the data processing facility. The equipment required on Spacelab has received the most attention to date. Preliminary designs of the User Terminal and of the Ground Control Terminal are covered in paragraphs 3.2 and 3.3, while special equipment needed for data reduction is covered in paragraph 3.4.

A block diagram of the AMPA L-band antenna system on Spacelab is shown in Figure 3-7. Part of the AMPA antenna system equipment is located on a Spacelab pallet and the rest is inside the Spacelab module, as indicated by the dashed line on the block diagram. When the adaptive loops are at the array as shown here, the pallet equipment consists primarily of the L-band radiating element modules, the adaptive beamforming network and control, and

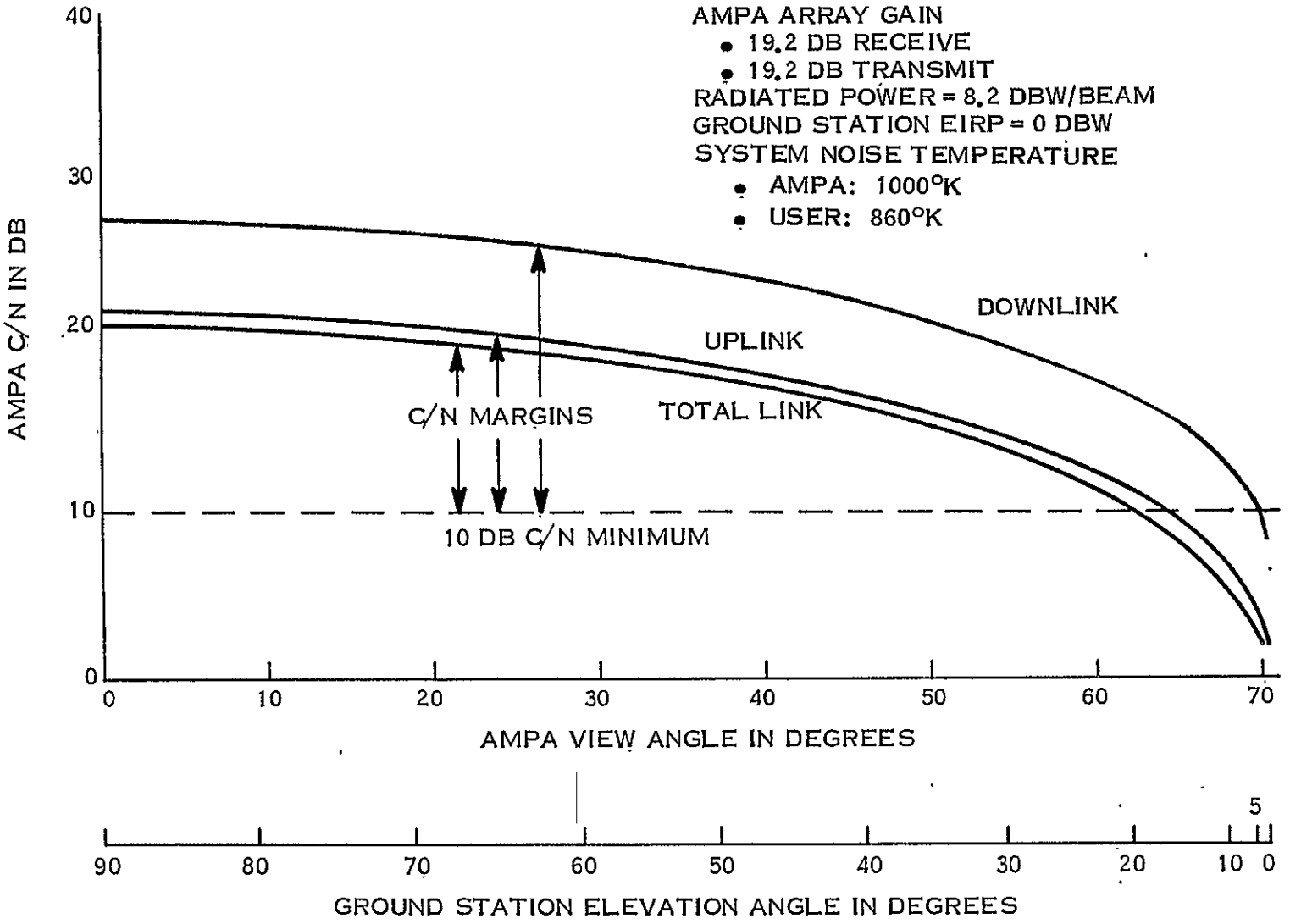

Figure 3-5. AMPA Carrier-to-Noise Ratio for 50 KHz Communication Channel

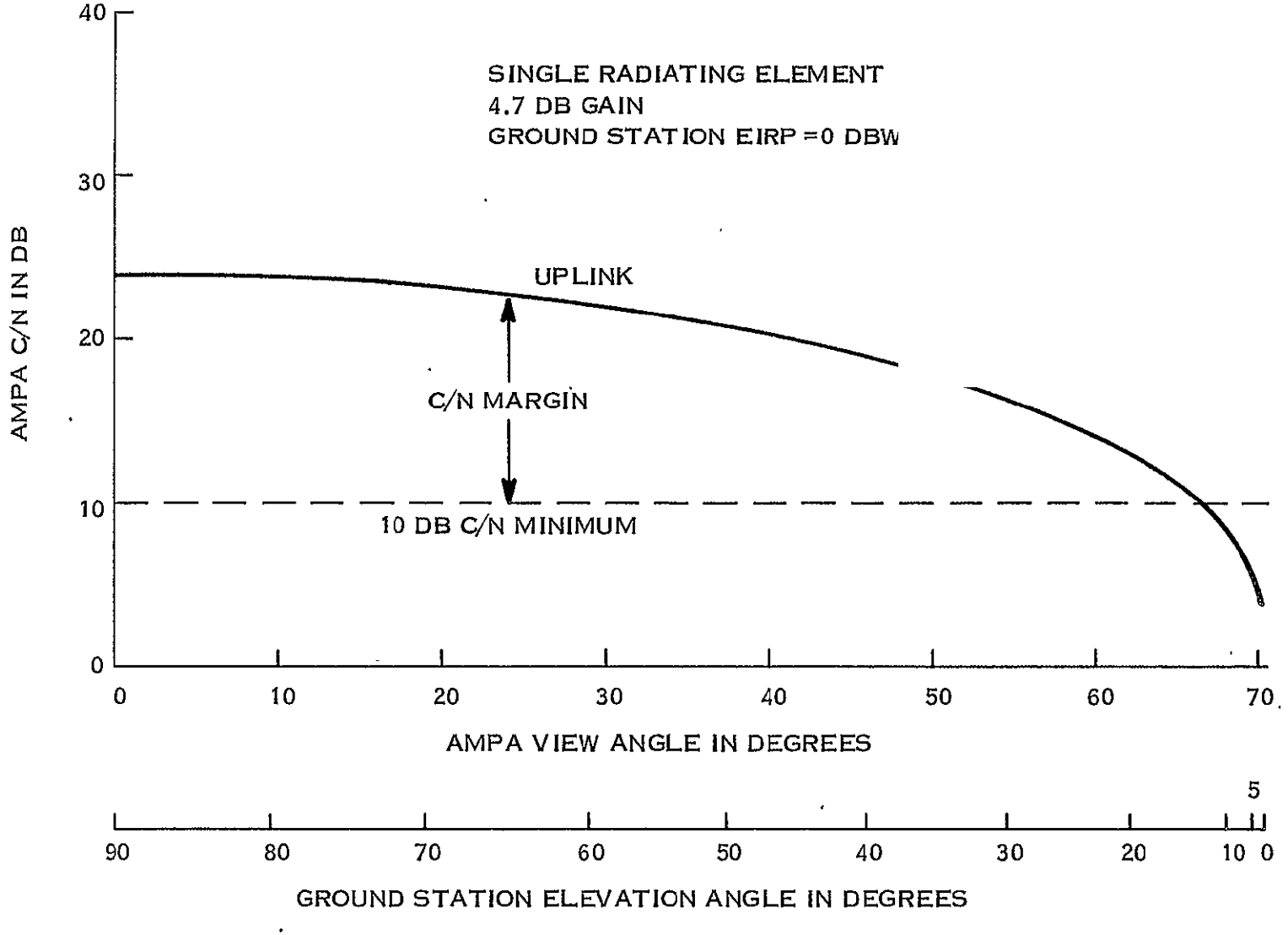

Figure 3-6. AMPA Carrier-to-Noise Ratio for 1 KHz Adaptive Beamforming Channel

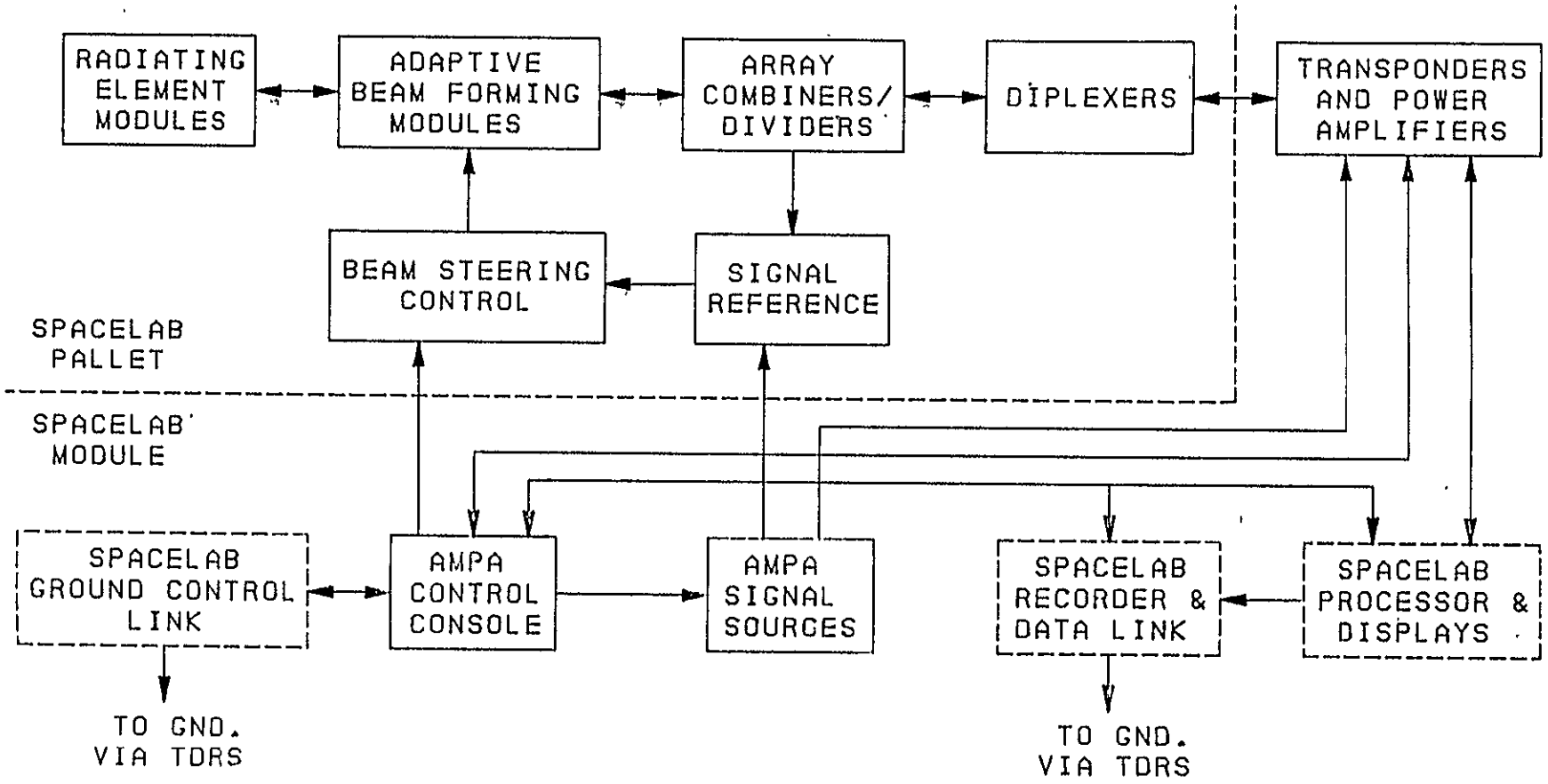

Figure 3-7. AMPA L-Band Antenna System Block Diagram

the diplexers. Equipment inside the Spacelab module consists of the beam-level receivers and transmitters, the AMPA signal sources, and the AMPA control console. Alternatively, the adaptive circuitry could be placed inside the module, in which case only the radiating element modules would be on the pallet. Interfaces with Spacelab equipment are also indicated in the AMPA antenna system block diagram for on-board data recording, processing, and display, for a data link to ground via TDRS, and for a control link to ground via TDRS.

Figure 3-8 shows one configuration of the L-band AMPA Experiment pallet equipment mounted on a standard Spacelab pallet. Alternative configurations are being considered to permit this equipment to occupy only one half of a pallet.

3.2 AMPA USER-TERMINAL PRELIMINARY DESIGN

Some preliminary work was done on User Terminal design to establish the user-terminal parameters assumed for the link calculations and to permit initial systems analysis. The initial assumptions are 1 Watt EIRP with hemispheric coverage, as shown in paragraph 3.1.5. A ground terminal receiver noise figure of 5 dB (627^{o}K) was assumed, with circuit losses of 83^{o}K and an antenna temperature of 150^{o}K. Practical ground-terminal antennas will have more gain overhead and fall off at low elevation angles, thus more user transmitter power may be needed to maintain 1 Watt EIRP at low elevation angles.

3.3 AMPA GROUND CONTROL-TERMINAL PRELIMINARY DESIGN

Preliminary consideration of this phase has been limited to the AMPA control link, which would be via the TDRS (Tracking and Data Relay Satellite) to/from White Sands as shown in Figure 3-9. AMPA control signals would then be transmitted by land line between White Sands and the Ground Control Terminal located at NASA/Johnson Space Center.

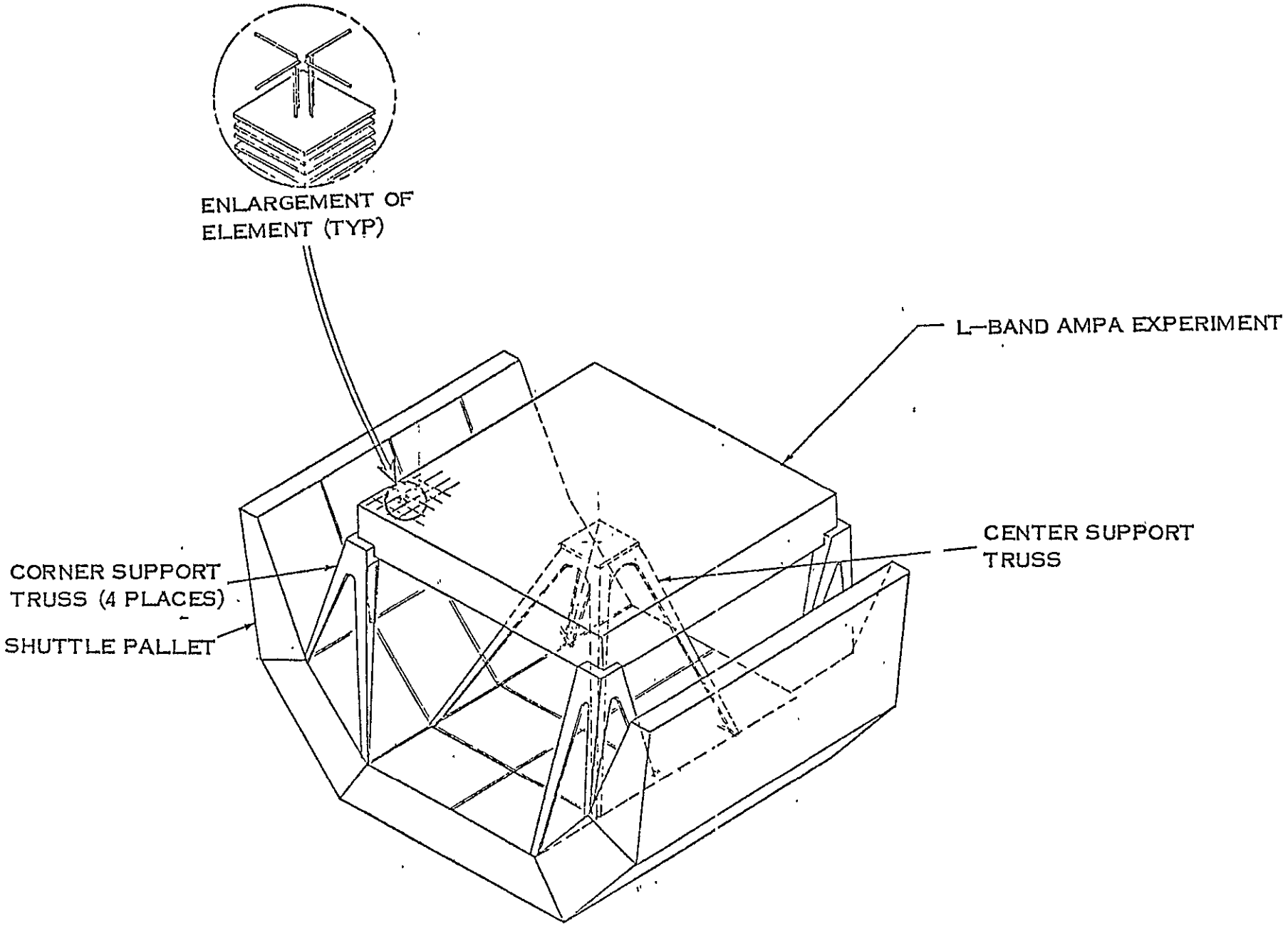

Figure 3-8. L-band AMPA Experiment Pallet Complement

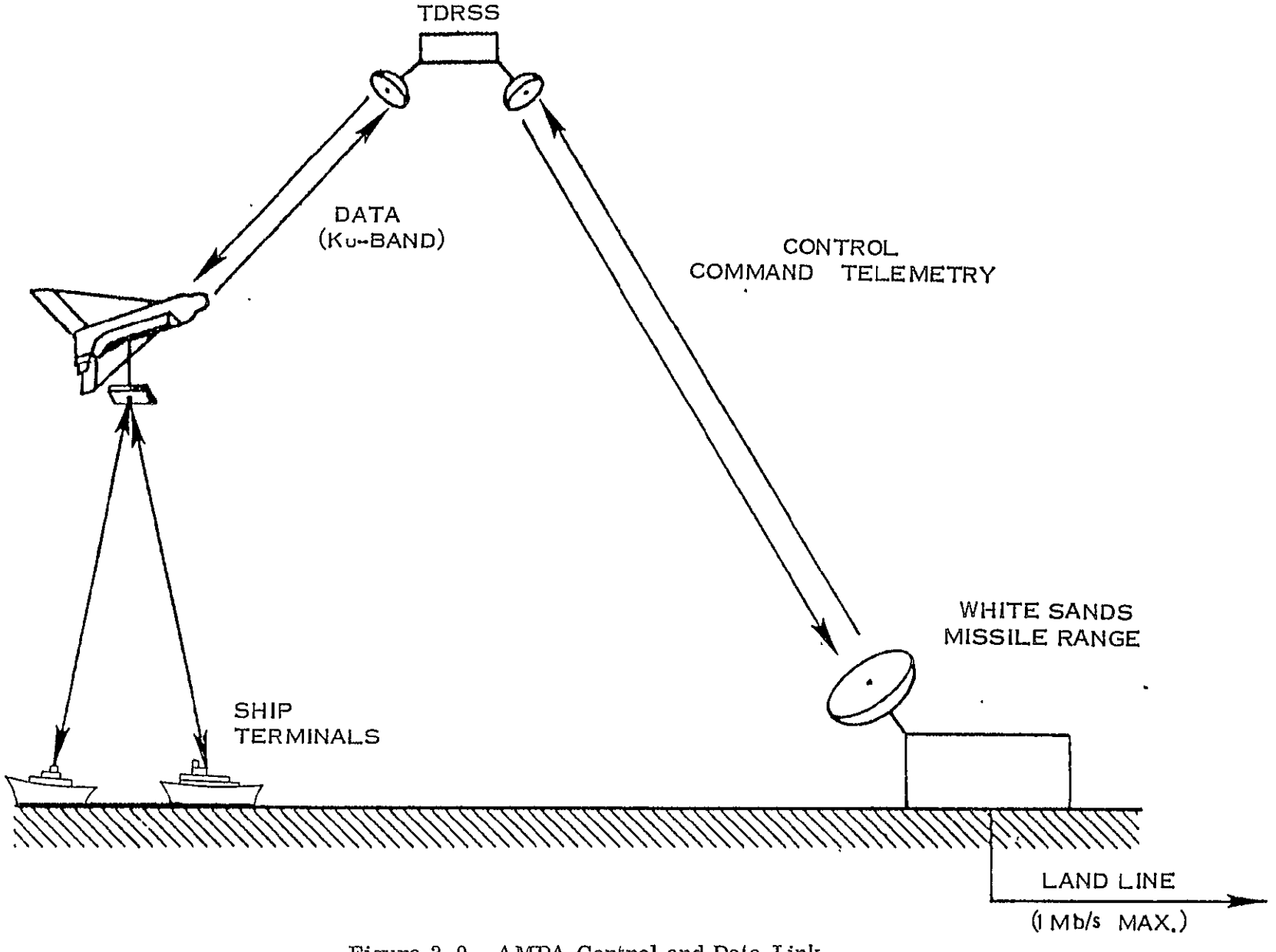

Figure 3-9. AMPA Control and Data Link

3.4 AMPA DATA REDUCTION REQUIREMENTS

Some of the AMPA Experiment data will be recorded, processed, and displayed during the Shuttle/Spacelab flight. The payload specialist will be involved with the data and displays particularly when the AMPA Experiment operation is involved. For example, experiment operation may involve changes in type of user code or modulation during orbit passes through ground-station coverage areas and regions of operation.

Other AMPA Experiment data will be relayed directly to ground via TDRS. Some of these data will be transmitted by land line to the AMPA Ground-Control Terminal at NASA/Johnson Space Center when related to experiment operations, while other data will be routed via land line to the IPD (Information Processing Division) at NASA/Goddard Space Flight Center for recording and processing. These two areas of AMPA Experiment control and data handling are indicated in Figure 3-10.

3.5 ADDITIONAL AMPA MATERIAL GENERATED

Payload Data Sheets (Level A and B Data) for the AMPA Experiment were revised on November 5, 1976 and submitted to NASA/GSFC.

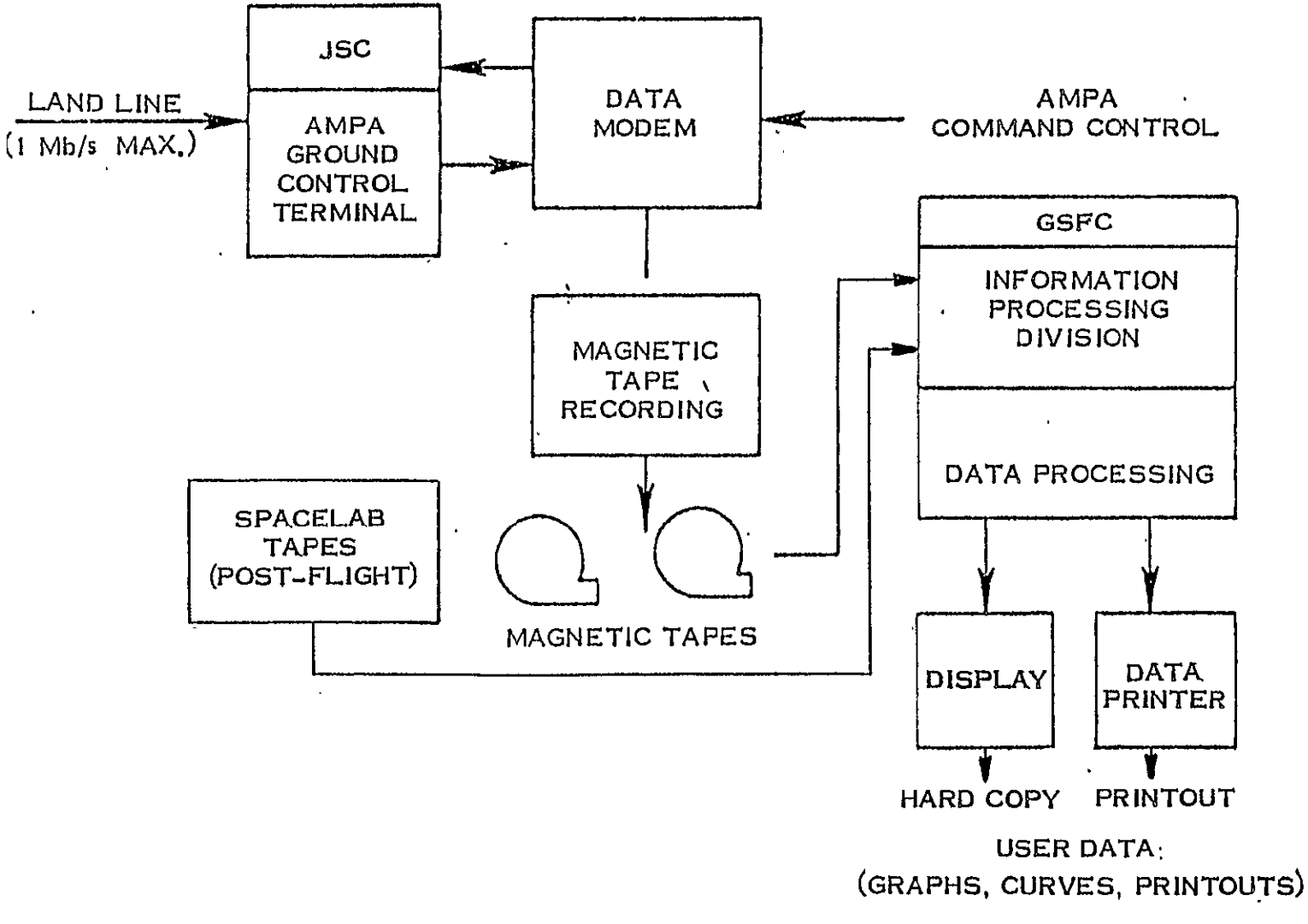

Figure 3-10. AMPA Experiment Control and Data Handling

SECTION 4

ELECTROMAGNETIC ENVIRONMENT EXPERIMENT (EEE)

Definition of the EEE is being conducted in three phases: MOD I design (121.5 to 2700 MHz), MOD II design (2.7 to 43 GHz), and preparation of a listing of terrestrial emitters within the NASA bands. Work during this period was concentrated on the MOD I EEE design.

The MOD I EEE definition work has included several aspects of the experiment, but was concentrated in the following areas:

1. EEE Operation and Sensitivity
2. Payload Configuration
3. Operational Environment and Data Management
4. Instrument Tests During Development

4.1 EEE OPERATION AND SENSITIVITY

The Electromagnetic Environment Experiment is designed to monitor radio frequency interference emitters located on the earth. Figure 4-1 shows the EEE concept and the major functional parts of the experiment. The Shuttle/Spacelab segment is composed of the antennas, the receiver, associated Spacelab equipment such as displays, a magnetic tape recorder, and interface equipment to control the experiment and transmit data to the ground station. The TDRSS is the principal means of transmitting real-time data to the EEE Ground Processing Center. Final processing of data and distribution of information to Users will be accomplished at the Processing Center.

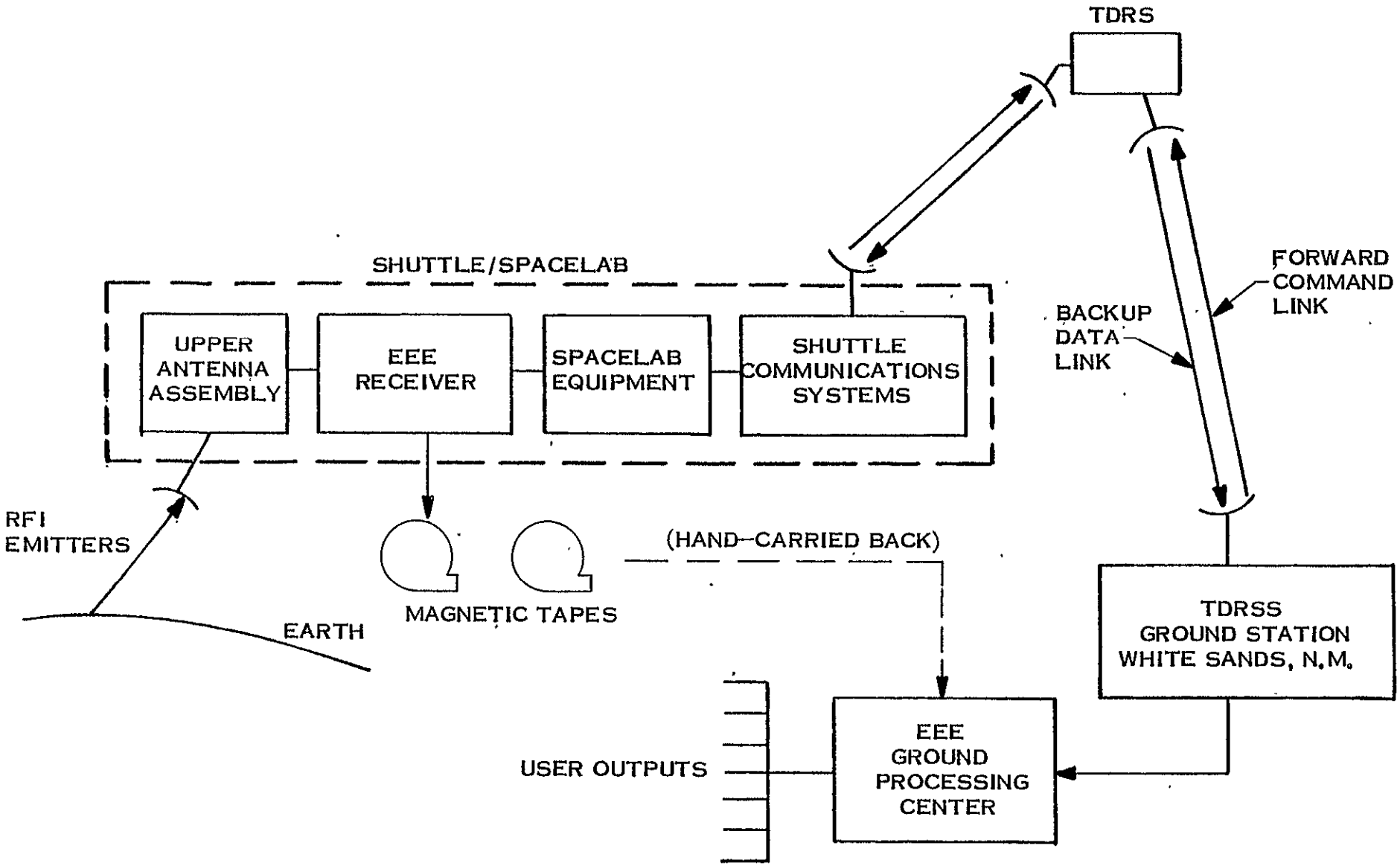

Figure 4-1. EEE Functional System

Control of the EEE will be by three different modes: via ground command, by programmed automatic procedures, or by manual control by the payload specialist. Figure 4-2 shows the principal functions of the EEE and the Spacelab equipment involved in operation of the on-board equipment. Control via command from the ground station will be routed through the TDRSS, and involves a decoder located in the EEE receiver. Similarly, status of the equipment will be sent to the ground station through the encoder and TDRSS.

The Spacelab computer and payload specialist are directly involved in the programmed/automatic control mode. This mode will be controlled almost totally by the special EEE software maintained in the Spacelab computer. The payload specialist will be involved in this mode, but probably only to activate the mode and to monitor the operation of the experiment on the Spacelab displays and/or the EEE data display panel located on the EEE receiver.

The manual control mode is provided as a back-up mode and specifically for operation of the experiment by the payload specialist. A control keyboard is provided at the EEE receiver for command inputs and status monitoring. The data display is provided for monitoring of incoming data and equipment checkout.

Operation of the EEE is centered about two main functional parameters, the frequency bands of interest and the receiver sensitivity to earth emitter electromagnetic signals. Figure 4-3 shows the RF frequency bands to be covered in the MOD I design of EEE. The frequency range covered is 121.5 to 2700 MHz in specific bands of interest to NASA. The specific allocated use of these bands is shown in Figure 4-3.

Sensitivity of the EEE is shown in Figure 4-4. The RF frequency bands are grouped according to the proposed antenna designs listed. Receiver bandwidths are typical minimum and maximum bandwidths expected to be used. Sensitivity is given as Effective Isotropic Radiated Power (EIRP) from the earth. Note that the sensitivity varies

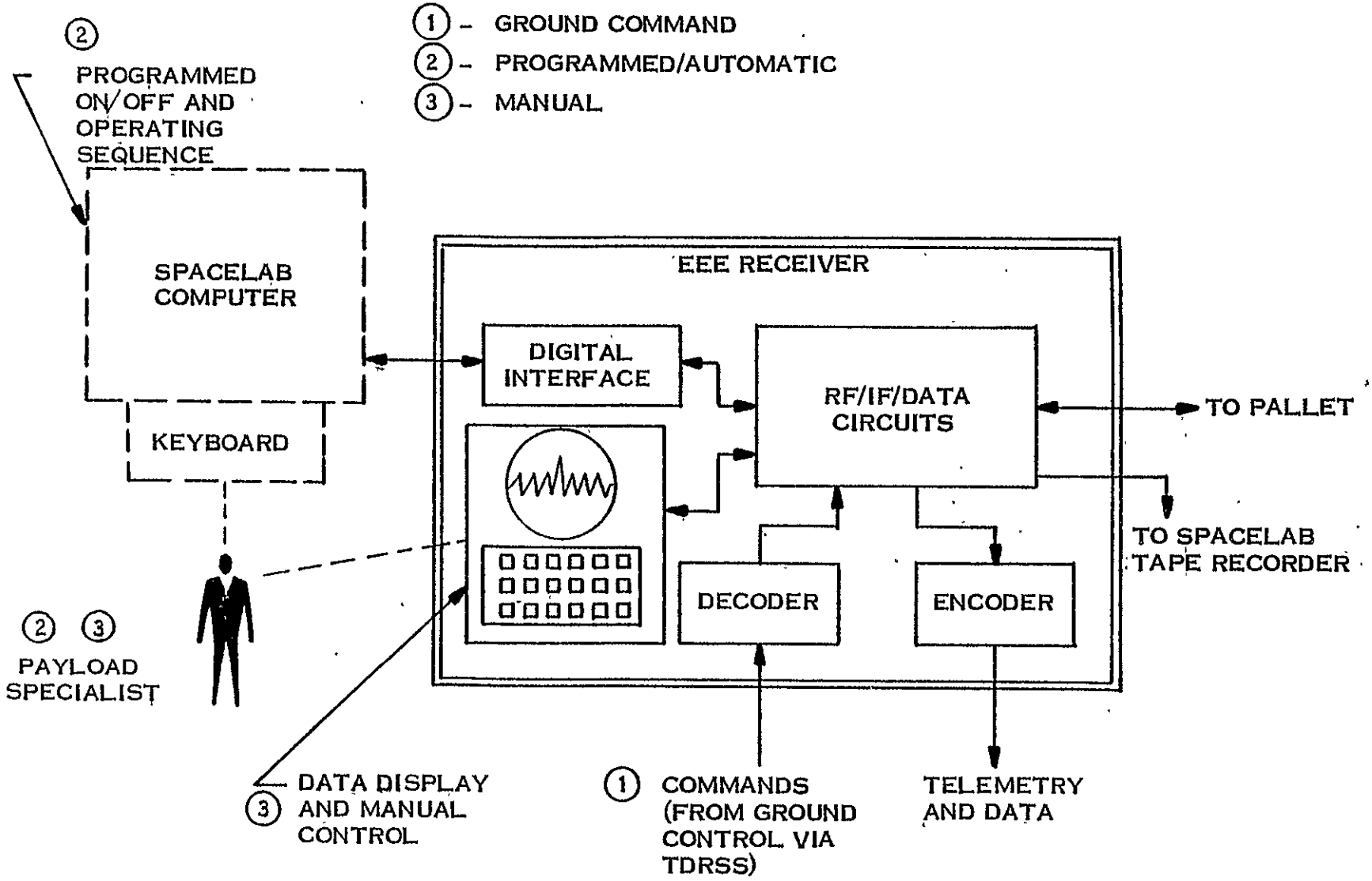

Figure 4-2. EEE Receiver Operation Modes

Frequency Band	Planned Mission Bands	BW	Use
1	121.5 MHz	±25 kHz	Emergency and Distress, Aeronautical and Maritime Mobile
2	243.0 MHz	±25 kHz	Emergency and Distress, Aeronautical and Maritime Mobile
3	150 - 174 MHz	24 MHz	"High Band," Land Mobile Service, Radio Astronomy, Region 1 (150.05-153 MHz)
4	399.9 - 410.0 MHz	10.1 MHz	NASA Space Operation, Data Collection, Radio Astronomy (406.1-410 MHz), 406.05 MHz ± 50 KHz EPIRB
5	450.0 - 470.0	20	NASA Meteor. Sat. Data Collection, Land Mobile
6	806.0 - 947.0	141	Land Mobile
7	1220 - 1285	65	SSR Experiment, NASA Seasat, SAR (1275 ± 9.5 MHz)
8	1350 - 1450	100	SMS R/M Experiment, Internationally protected Exclusive Radio Astronomy (H Line) (1400-1427 MHz)
9	1636.5 - 1670	33.5	Maritime/Aeronautical Mobile Sat., Radio Astronomy OH line (1660-1670 MHz)
10	2040 - 2110	70	NASA Earth to Sat. Data/Telecommand/Ranging
11	2200 - 2300	100	NASA Sat. Data Relay (TDRSS S-Band)
12	2655 -2690	35	Fixed Sat. (Earth to Space)
13	2690 - 2700	10	Internationally protected Exclusive Radio Astronomy

ACRONYM DEFINITIONS

SSR	Surface Spectrum Radar	Seasat SAR	Seasat (Spacecraft) Synthetic Aperture Radar
SMS R/M	Soil Moisture and Salinity Radiometer	EPIRB	Emergency Position - Indicating Radio-Beacon

Figure 4-3. RF Frequency Bands for the EEE

Band	Frequency Band[1] (MHz)	Antenna	Beamwidth (degrees)	Gain (dB)	Efficiency (%)	Free Space Loss[2] (dB)	System Temp.[3] (K)	RCVR Bandwidth	Sensitivity[4] Min. Detectable EIRP (dBW)	In-Orbit Power-Flux Density[2] (dBW/m^2)
1	121.5	Log Periodic (1.3 dia x 1.8 ht)	70	8	40	126	900	±25 kHz	-21	-144
2	243.0	↓	70	8	40	132	900	±25 kHz	-15	-138
3	150-174	↓	70	8	40	129	900	20 kHz 1 MHz	-22 -5	-145 -128
4, 5	390.9-470.0	UHF Array (1.0 x 1.3 m)	43	13	70	137	1400	20 kHz 100 kHz 1 MHz	-17 -10 0.0	-140 -133 -123
6-13	806-2700	0.7 m Parabolic	37-11	11-22	40	143 to 153	1800	20 kHz 1 MHz	-8 +9	-131 -114
6-13	806-2700	Conical Helix (0.17 dia x 0.17 m)	70	6	-	143 to 153	1800	20 kHz	-3 to 7	-126 to -116

[1] Calculations except beamwidth are at mid-band frequency.

[2] Altitude of 400 km referenced to nadir.

[3] System Noise Temperature $T_S = T_R + T_A$, where T_R = Receiver noise temperature and $T_A = 290^O$ = effective antenna noise temperature.

[4] Includes 10 dB Signal to Noise Ratio, Antenna Gain at HPBW. EIRP is referenced to Earth's surface.

Figure 4-4. EEE Sensitivity Analysis Summary

from -22 to +9 dBw, depending on the band and bandwidth selected. In-orbit power-flux density gives the expected power density incident on the antenna. These values can be used to evaluate the effects of Shuttle generated RF interference signals on the EEE sensitivity.

The type of signals expected to be received by the EEE is shown in Figure 4-5 from Reference 6. These data are typical and are representative of one form of user outputs. Typical user data outputs will be generated in graphs, charts and tabular form, examples* of which are:

EIRP versus Frequency

% Channel Occupancy versus Frequency

Channel Occupancy Tabular Ranking

Power-Flux Density (In Orbit)

4.2 PAYLOAD CONFIGURATION

The equipment located on the Shuttle represents the basic EEE payload configuration. Figure 4-6a shows the block diagram for the antennas, receiver and Spacelab interface equipment. This particular design shows four basic antennas:

1. UHF Array (1.0 x 1.3m)
2. Parabolic Dish (0.7m)
3. Conical Helix (0.17m Dia x 0.17m HT)
4. Cavity Backed Spiral (1m Dia x 1m HT)

Signal level control and receiver protection are provided by the attenuator and limiter shown at the receiver input. The bandpass filter (BPF) provides band integrity and protection from out of band jamming. Signal downconversion is provided by the series of low noise amplifiers (LNA) and downconverters. Signals are conducted from the pallet

*Examples suggested by R.E. Taylor.

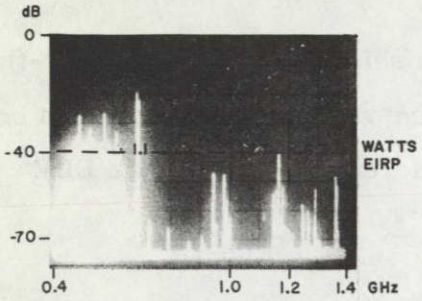

(a) Chicago, Morning, May 1, 1975
Time: 081741 (Start Run)

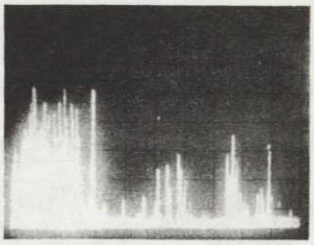

(b) Chicago, Morning, May 1, 1975*
Time: 081842 (4 Mile Point)

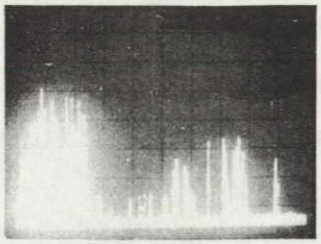

(c) Chicago, Morning, May 1, 1975*
Time: 082009 (10 Mile Point)

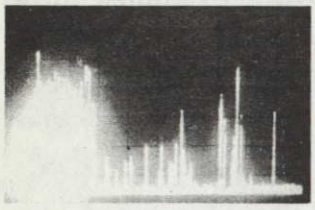

(d) Chicago, Night, May 1, 1975*
Time: 223035 (Start Run)

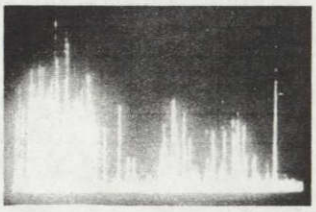

(e) Chicago, Night, May 1, 1975*
Time: 223746 (Run Midpoint)

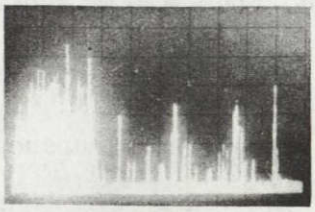

(f) Chicago, Night, May 1, 1975*
Time: 224427 (End of Run)

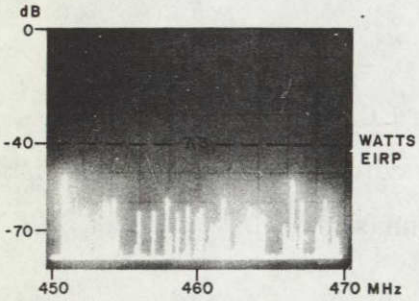

(g) Chicago, Afternoon, May 1, 1975
Time: 150111 (Start Run)

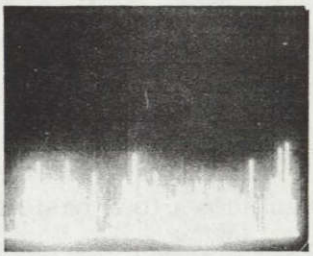

(h) Chicago, Afternoon, May 1, 1975**
Time: 150234 (6 Mile Point)

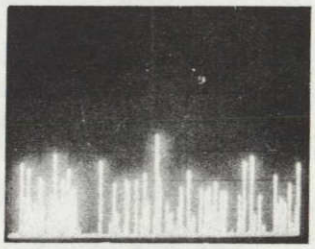

(i) Chicago, Afternoon, May 1, 1975**
Time: 150406 (10 Mile Point)

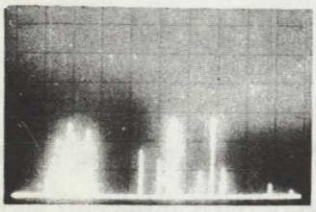

(j) Chicago, Night, May 1, 1975**
Time: 230120 (Start Run)

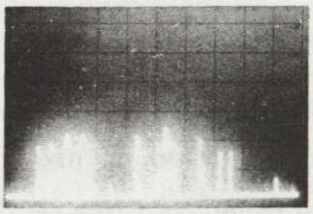

(k) Chicago, Night, May 1, 1975**
Time: 230251 (5 Mile Point)

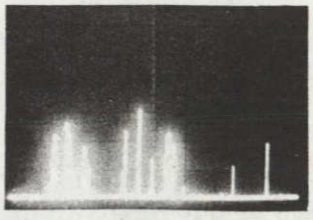

(l) Chicago, Night, May 1, 1975**
Time: 230422 (10 Mile Point)

Figure 11. Chicago (Morning-Nighttime) -0.4 to 1.4 GHz and 450 to 470 MHz
Scale: *Same as (a) Altitude: 10,5[illegible] ft Analyzer Bandwidth: Antenna: NADIR
**Same as (g) Aircraft Headi[illegible] North Fig. 11a to 11f -30kHz
Fig. 11g to 11l -10kHz

Figure 4-5. Typical EIRP versus Frequency Data Display

equipment to the Module/Aft Flight Deck equipment by coaxial cables. The IF signal frequencies are typical frequencies, but are consistent with keeping the IF signals low; i.e., no greater than 500 MHz, to avoid high signal loss. Figure 4-6(b) shows typical Spacelab equipment needed to route the detected signals to the TDRSS downlink, the recorder and/or the EEE displays. The equipment shown in Figure 4-6(b) represents the operational modes shown in Figure 4-2.

Layout of the EEE pallet mounted equipment is shown in Figure 4-7. The antennas shown are those depicted in Figure 4-4, and are representative of antennas needed to cover the EEE bands. In this design space is left for additional antennas for bands above 2700 MHz.

RF electronics will be located below the antenna platform. Figure 4-8 shows the vertical locations of the components and clearance angles for each antenna. Note that the center-of-gravity (CG) range for the vertical profile is below the top of the pallet. Figure 4-9 shows the pallet equipment mounted in the Shuttle bay. Similarly, Figure 4-10 shows a typical EEE receiver package* that could be used for Aft Flight Deck equipment. Figure 4-11 shows the weight, size and power required for the EEE payload equipment.

Location of the pallet equipment in the Shuttle bay could affect the antenna patterns if the Shuttle blocks a portion of the pattern. Figure 4-12 shows two locations which would offer almost no pattern distortion by the Shuttle. These positions represent the closest that the equipment can be located to the ends of the bay. A nominal interference as shown by the tail in the widebeam antenna patterns is not considered serious.

*Suggested by R.E. Taylor.

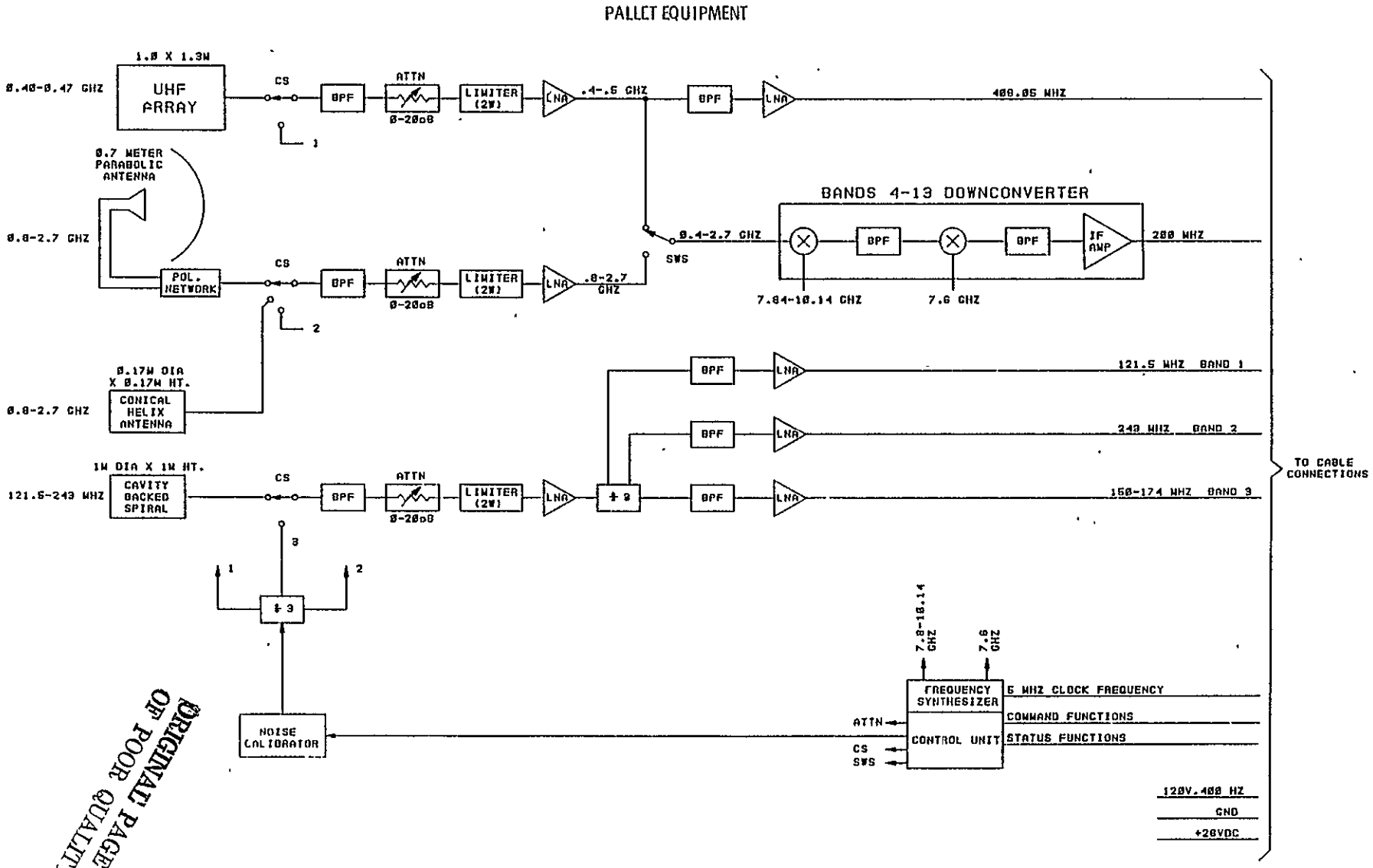

Figure 4-6a. EEE System Block Diagram

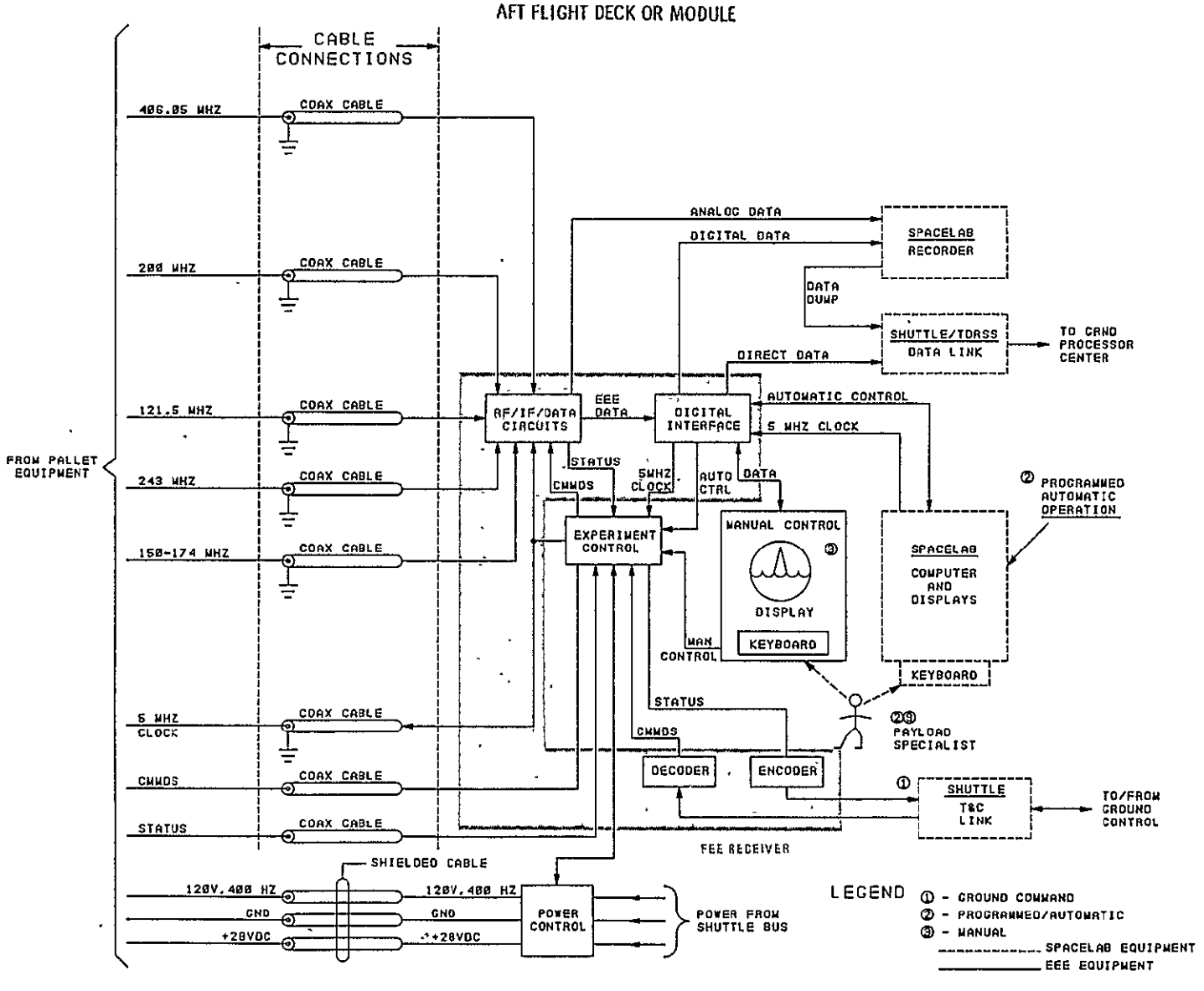

Figure 4-6(b). EEE System Block Diagram

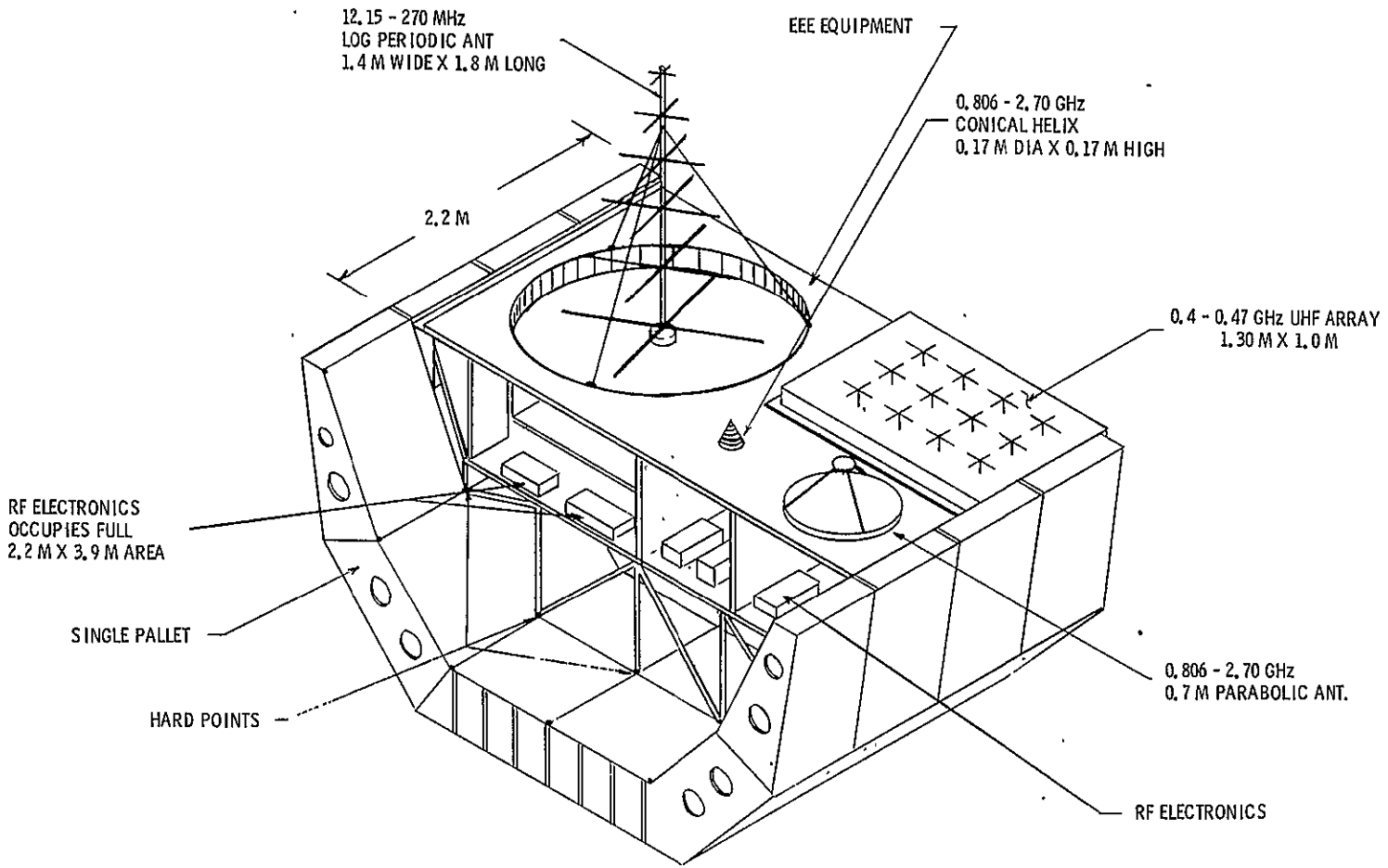

Figure 4-7. EEE Pallet Mounted Equipment

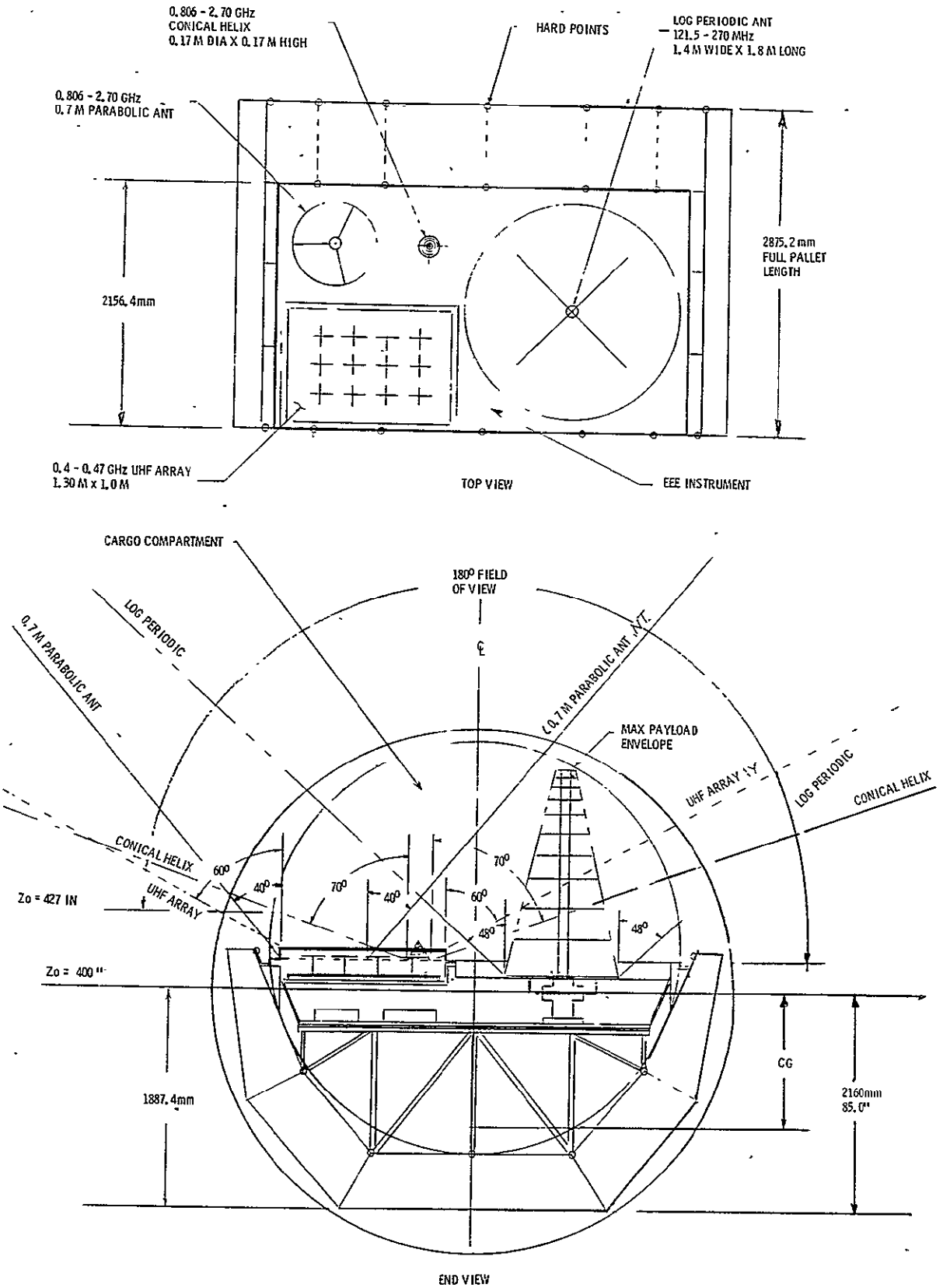

Figure 4-8. EEE Pallet Layout and Antenna Field of View

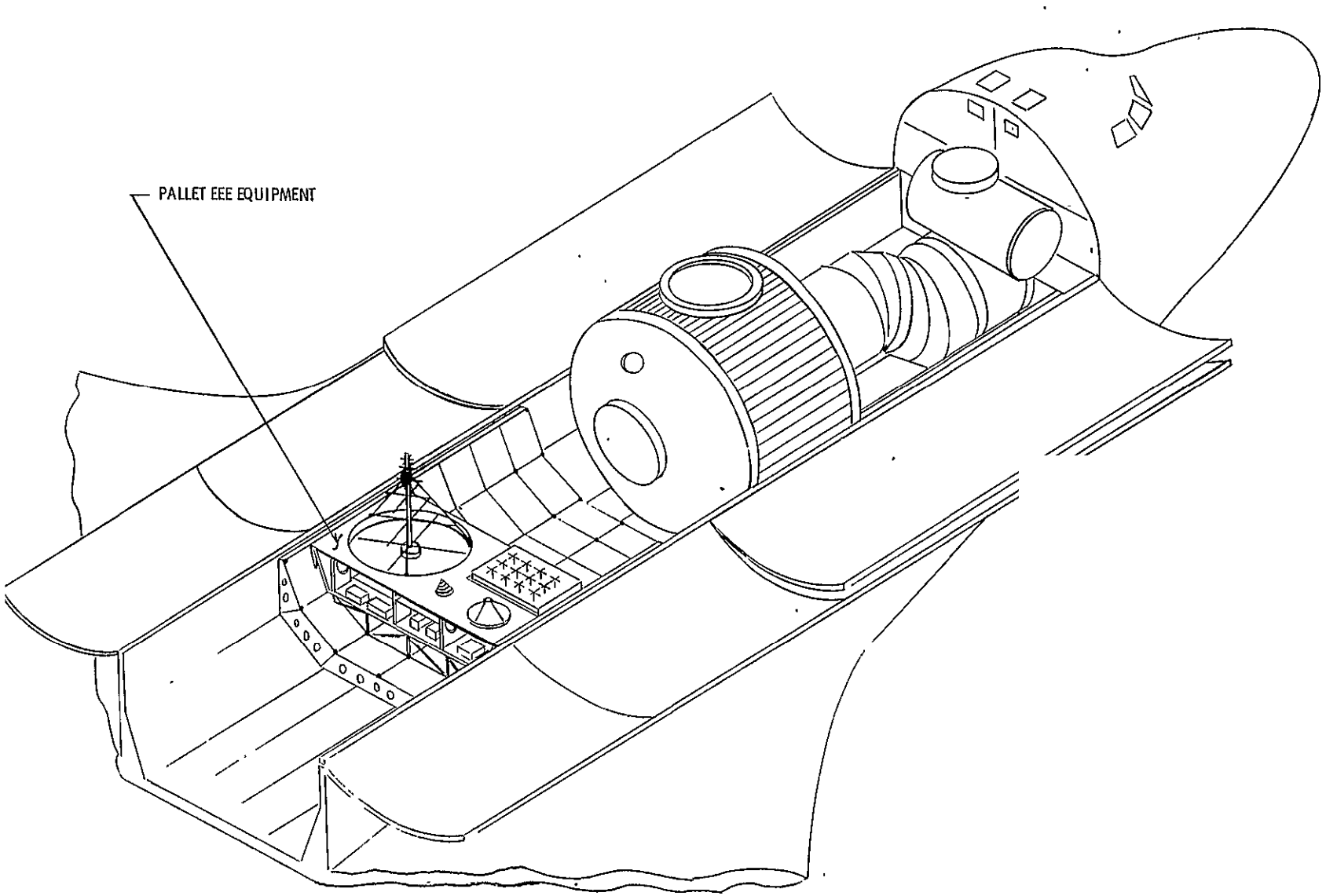

Figure 4-9. EEE Spacelab Flight Configuration

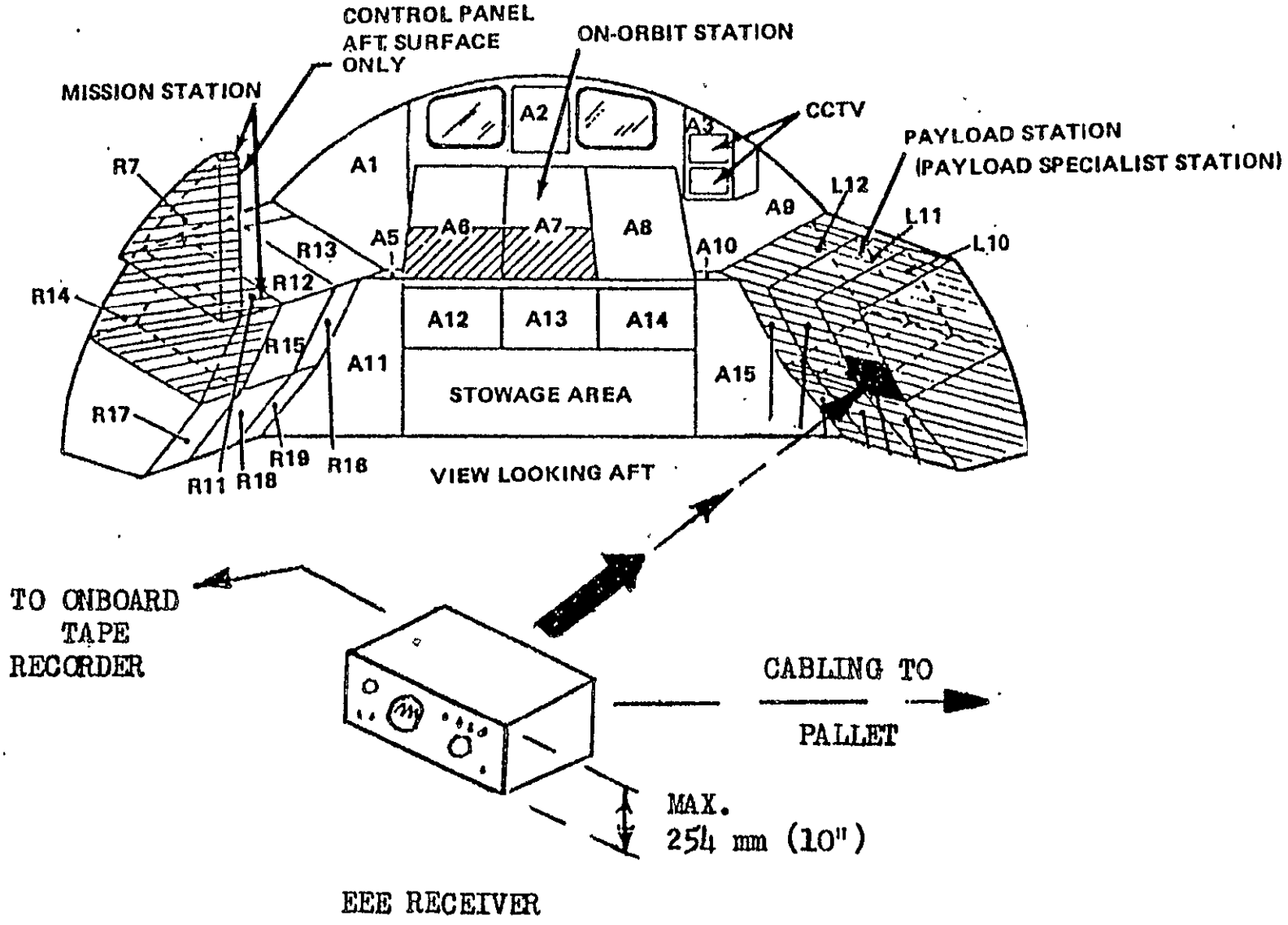

Figure 4-10. EEE AFD Equipment

LOCATION	WT (kg)	SIZE (CM)
PALLET	128	350 W X 180 D X 250 H
AFD/MODULE	28	48.3 W X 50.8 D X 25
TOTAL	156	VOLUME = 15.81 M^3

Figure 4-11(a). EEE Weight & Size

POWER	400 HZ, 120 VAC (W)	28 VDC (W)
PALLET	150	25
AFD/MODULE	40	5
TOTAL	190	30
STANDBY	20	3

TYPICAL SINGLE CYCLE OPERATION SEQUENCE

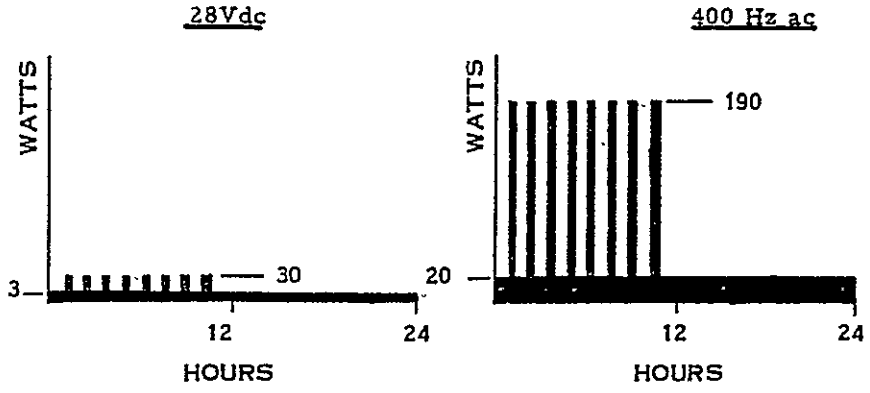

Figure 4-11(b). EEE Power Requirements

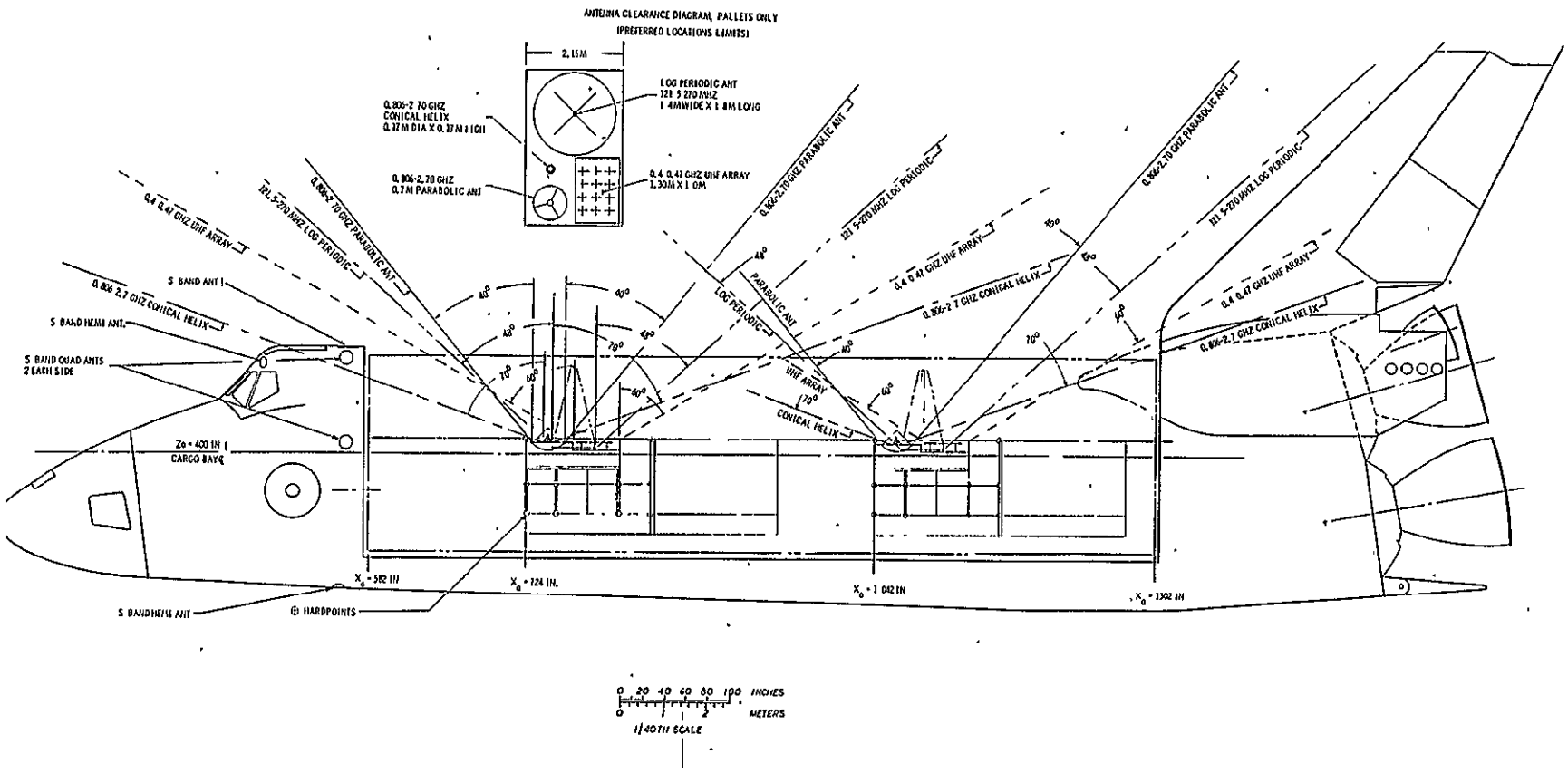

Figure 4-12. Antenna Clearance Diagram, Pallets Only

4.3 OPERATIONAL ENVIRONMENT AND DATA MANAGEMENT

Figure 4-6(b) shows the functional interfaces for the EEE, and the conceptional approach to the experiment control and operation. Further definition of the interfaces and environment was carried out to determine the physical and RFI (radio frequency interference) environment the equipment will be exposed to, and to define a data management scheme. This work has included a study of the expected environment related to the Shuttle[5], interfaces with the Spacelab on-board systems[4], and a proposed method of managing the EEE data. Experiment control is intimately involved in data management and experiment operation and is included here to show involvement of the payload specialist and ground control personnel.

4.3.1 EEE ENVIRONMENT CONSIDERATIONS

After a study of the Shuttle bay payload environment conditions and the types of equipment that could be used on EEE, a set of physical operating parameters was formulated. These parameters include temperature, humidity, acoustic limits, acceleration, radiation and RFI susceptibility. These parameters and the expected limits are shown in Figure 4-13.

In general, the limits for temperature and humidity shown in Figure 4-13 are those normally expected for military equipment and weatherized commercial equipment. Acoustic and acceleration limits are those required for Shuttle launch and landing, but are reasonable for microwave equipment, also. However, it is not expected that the EEE equipment will survive a crash landing, except to stay in contact with the pallet.

PARAMETERS	LIMITS	
	AFD MODULE	PALLET
TEMPERATURE		
TYPE CONTROL	AIR	PASSIVE (COATING,ETC.)
OPERATING	0 TO 50°C	-65 TO 65°C
(PREFERRED)	(25)	(25)
NON-OPERATING	-65 TO 65	-65 TO 65
HUMIDITY		
OPERATING	40 TO 60%	40 TO 60% (TEST)
NON-OPERATING	0 TO 100	0 TO 100
ACOUSTIC LIMITS		
NON-OPERATING	145 dB	145 dB
ACCELERATION		
NON-OPERATING	5.0 G	5.0 G
OPERATING	1×10^{-2}	1×10^{-2}
RADIATION (NUCLEAR)	NOT A PROBLEM	
RFI SUSCEPTIBILITY		
ELECTROMAGNETIC	EMC ANALYSIS	DERIVED FROM JSC-07700, VOL. XIV
GENERATED RFI	NOT A PROBLEM	

Figure 4-13. EEE Environment Considerations
(Ref: Spacelab Accommodation Handbook)

Nuclear radiation is not expected to be a problem to the EEE, since the flights are short and no equipment is susceptible to normal nuclear environment experienced during a low orbit Shuttle flight. RFI susceptibility is a different type of problem, however, and must be dealt with in depth. The generated RFI from the EEE will be very low, since the EEE is primarily a receiver, which does not produce RFI.

The RFI susceptibility problem was studied to determine the effect the Shuttle bay RFI will have on principal EEE operating parameters such as sensitivity. Figure 4-14 shows the RFI specification limits imposed by the Shuttle payload requirements[4] and the expected EEE sensitivity levels for each frequency band. An additional RFI level that could be caused by digital logic radiation is shown at the bottom of the graph.

The major significance of Figure 4-14 is that the EEE sensitivity levels are far below the Shuttle cargo bay specification limits. Figure 4-15 shows the range of isolation needed to allow EEE to operate at its maximum sensitivity levels. The significance of the levels shown in Figure 4-15 is very apparent when it is realized that the typical

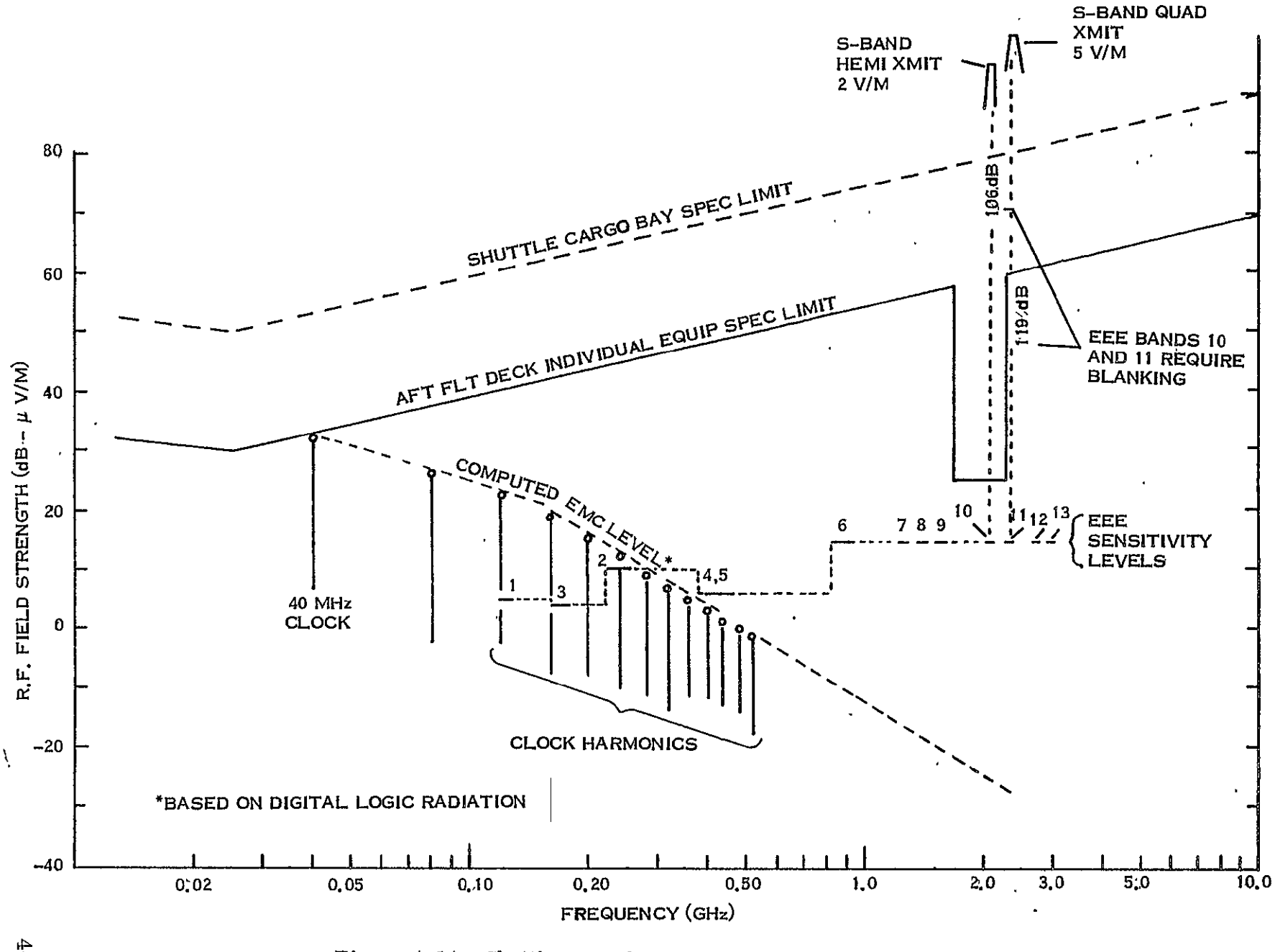

Figure 4-14. Shuttle Bay Electromagnetic Compatibility Environment (Other On-Board Experiments Excluded)

EEE BANDS	FREQUENCY MHz	SOURCE OF RADIATION: SHUTTLE LIMIT dB	SOURCE OF RADIATION: EQUIPMENT LIMIT dB	DIGITAL LOGIC* (1 M DISTANCE)
1	121.5	57	37	21 dB
2	243.0	55	35	5 dB
3	150–174	60	40	18 dB
4	399.9–410	64	44	0 dB
5	450–470	64	44	0 dB
6	806–947	59	39	–15 dB
7	1220–1285	62	42	–20 + dB
8	1350–1450	63	43	–20 + dB
9	1636.5–1670	64	44	–20 + dB
10	2040–2110	106 dB BLANKING REQ. – S-BAND HEMI		
	OTHER	10 dB	10	–20 dB +
11	2200–2300	119 dB BLANKING REQ. – S-BAND QUAD		
	OTHER	10 dB	10	–20 dB +
12	2655–2690	67	47	–20 dB +
13	2690–2700	67	47	–20 dB +

*DIGITAL LOGIC RADIATION

RADIATED ENVELOPE OF 40 MHz, 5 VOLT CLOCK SIGNAL

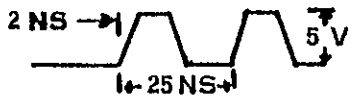

BASED ON
- TWISTED SHIELDED PAIR – ≈ 50 dB ATTENUATION
- PATH LOSS = 50 dB 1ST METER OF SPACING

Figure 4-15. Shuttle Bay to EEE EMC Isolation Required

isolation provided by a receiver antenna (back radiation) is on the order of 20-25 dB. For the Shuttle limit and individual equipment limit, the EEE sensitivity will be affect greatly, raising the detection levels of the receiver. For a normal digital logic level, however, the receiver should be able to operate without loss of sensitivity.

In addition to the random noise levels specified by the Shuttle specifications, individua Shuttle communications transmitters will cause receiver saturation and will be blocke from the receiver by filters.

It should be noted that this study does not take into account the RFI generated by other experiments. At this time, other experiments have not been specified. However, whe serious interference is expected from another experiment, time sharing of operation time must be arranged.

4.3.2 EEE DATA MANAGEMENT AND MONITORING

Management of the EEE involves both data management and control of the experiment from detection of signals to user outputs. Organization of received data is also a principal factor in all phases of data management and control. Work completed on this aspect of EEE includes a preliminary estimate of received data, a proposed arrangement of the data format and a method by which these data can be controlled by any one of the three proposed operation modes.

Figure 4-16 shows the expected data rates needed to manage and operate the EEE. Receiver data is estimated to be 70 kbps and will be buffered and formed into a serial bit-stream. These data are from bands 3-13 of the receiver (see Figures 4-3 and 4-6). The search and receive (S&R) bands will not be frequency scanned, and will be monitored using analog detection. These channels are to be recorded as separate channels. Capacity required for the S&R channels is expected to be less than 100 kHz. All data will be recorded on magnetic tape.

TYPES OF DATA	DATA RATE
RECEIVER OUTPUT	DIGITAL: 70 kbps TYPICAL
	ANALOG: 10^5 Hz MAX (3 S&R CHANNELS)
ON-BOARD DATA STORAGE	DIGITAL/ANALOG MAGNETIC TAPE
COMMAND	2 kpbs MAX
TELEMETRY (EQUIP. STATUS)	64 kbps MAX
EPHEMERIS DATA	
DAY TIME LONGITUDE LATITUDE ALTITUDE SHUTTLE ATTITUDE	SHUTTLE SUPPLIED (REF: AIRBORNE DIGITAL DATA ACQUISITION SYSTEM-ADDAS)

Figure 4-16. EEE Data Management and Control

Experiment control via TDRSS will be by command and telemetry. Estimated command link capacity is 2 kbps. Equipment status should require no more than 64 kbps for telemetry and monitoring.

Ephemeris information to be supplied with the receiver data will provide information needed to reduce the detected receiver data to user formats. Examples of ephemeris data are: calendar day, time of day, Shuttle position (longitude and latitude), Shuttle altitude, Shuttle attitude (reference to radii), and other experiment operational inputs such as reference signals.

Figure 4-17 shows a proposed arrangement of detected receiver data. This scheme could apply to other experiments as well as EEE and contains initial identification of the experiment and the type of data being recorded (record). For the EEE, band number, band resolution and frequency will provide the parameters to define sensitivity. Information about the attenuator setting at the receiver input is being supplied with the band number. Using the minimum cell size of 20 kHz, a five-filter bank is proposed for MOD I EEE. This allows for 0.1 MHz frequency steps by the receiver. All bands are to be serially stepped; e.g., in the normal mode, starting at band 2, each band will be searched for power output until band 13 is completed, and the scan repeats. Alternate modes can be set up by preprogramming a manual control, allowing specific bands to be searched. S&R bands are to remain open and sampled periodically, without frequency scanning. Data from these channels will be recorded without conversion to digital format.

The proposed control monitoring method for EEE is shown in Figure 4-18. Provision is made for monitoring data, test information and equipment status at the EEE receiver on the Shuttle, at the Spacelab display panel, by the Experiment Specialist at NASA JSC and at NASA GSFC. Data will be monitored near-real time, with displays of the type shown in Figure 4-5.

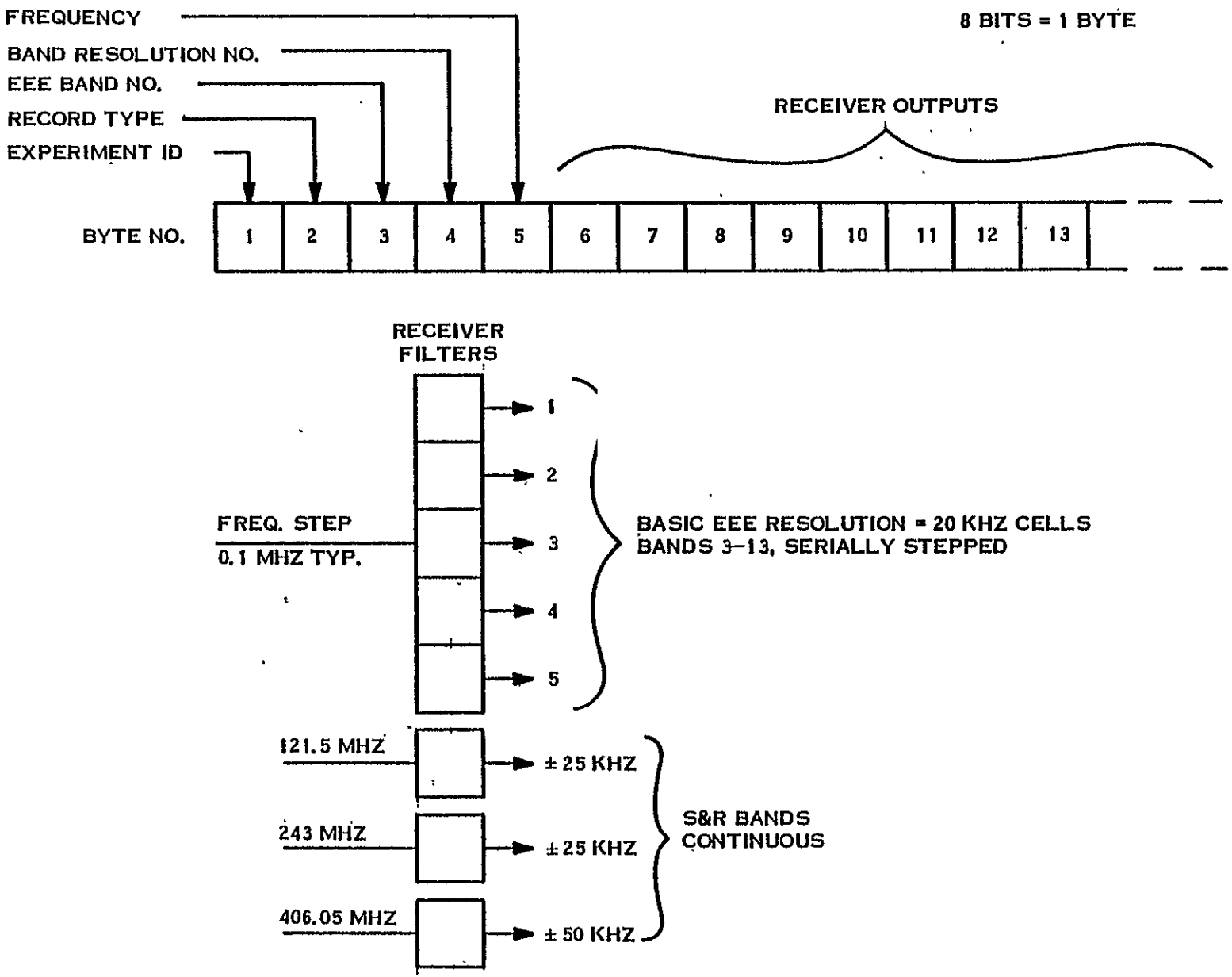

Figure 4-17. EEE Receiver Data Management

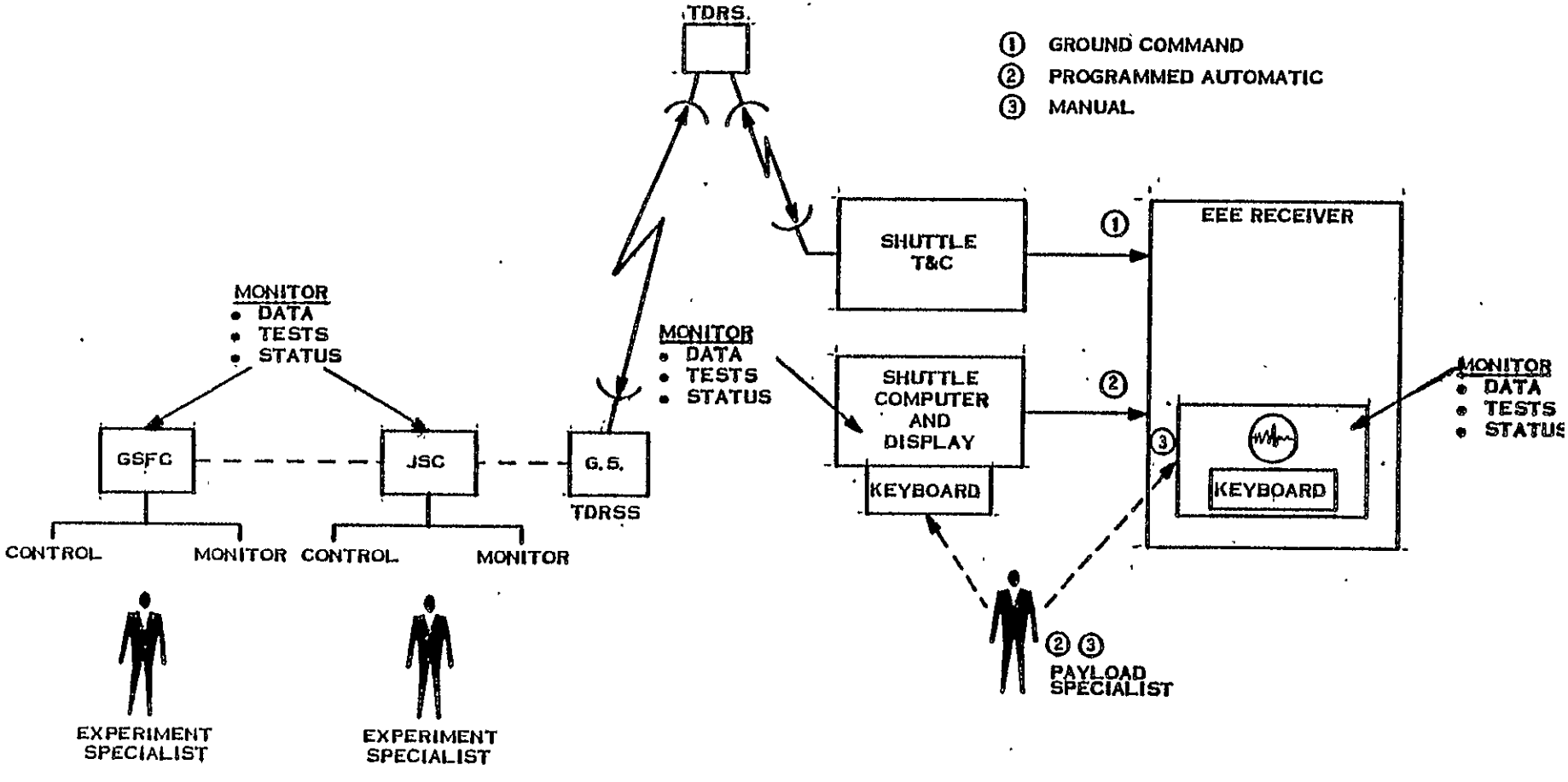

Figure 4-18. Receiver Control and Monitoring

Further definition of the data management system is shown in Figure 4-19. Data received by the TDRSS ground station will be sent to the GSFC EEE Control Center via Houston, and recorded on magnetic tape. Data are then turned over to the Data Processing Center at GSFC for processing into user formats.

4.4 INSTRUMENT TESTS DURING DEVELOPMENT

It is not expected that the EEE equipment will be fully space qualified. The level of qualification is still being studied, but will depend to a large extent on the type of testing to be done on the equipment and on the system. Therefore, a testing plan is key to defining the development and verification of the equipment at each phase of the EEE equipment development. This plan will cover tests at the factory, at the initial integration stage, and integration on the Shuttle, and when in flight.

The overall philosophy for development of the EEE is that a system contractor will manage the initial equipment procurement, and will be responsible for testing at the factory and at each level of integration. It is also assumed that some type of built-in test equipment will be designed into EEE; e.g., the noise source shown in Figure 4-6(a).

4.4.1 FACTORY TESTS

Figure 4-20 shows a typical test program that could be used for EEE. The basic acceptance tests will not be fully defined at this stage of definition, but are essentially those tests to verify that the equipment will meet EEE equipment specifications. Types of tests and test environment are shown in Figure 4-20b. It is expected that major components such as antennas will be tested by the subsystem supplier. The EEE equipment could be assembled in an RF lab, but must be tested in a shielded room or Anechoic chamber to measure low levels of sensitivity. Mechanical tests will be completed in a typical mechanical laboratory, as normally used by a spacecraft manufacturer. It follows that special tests such as thermal/vacuum will be conducted in a vacuum chamber, probably in conjunction with electrical performance tests. Test

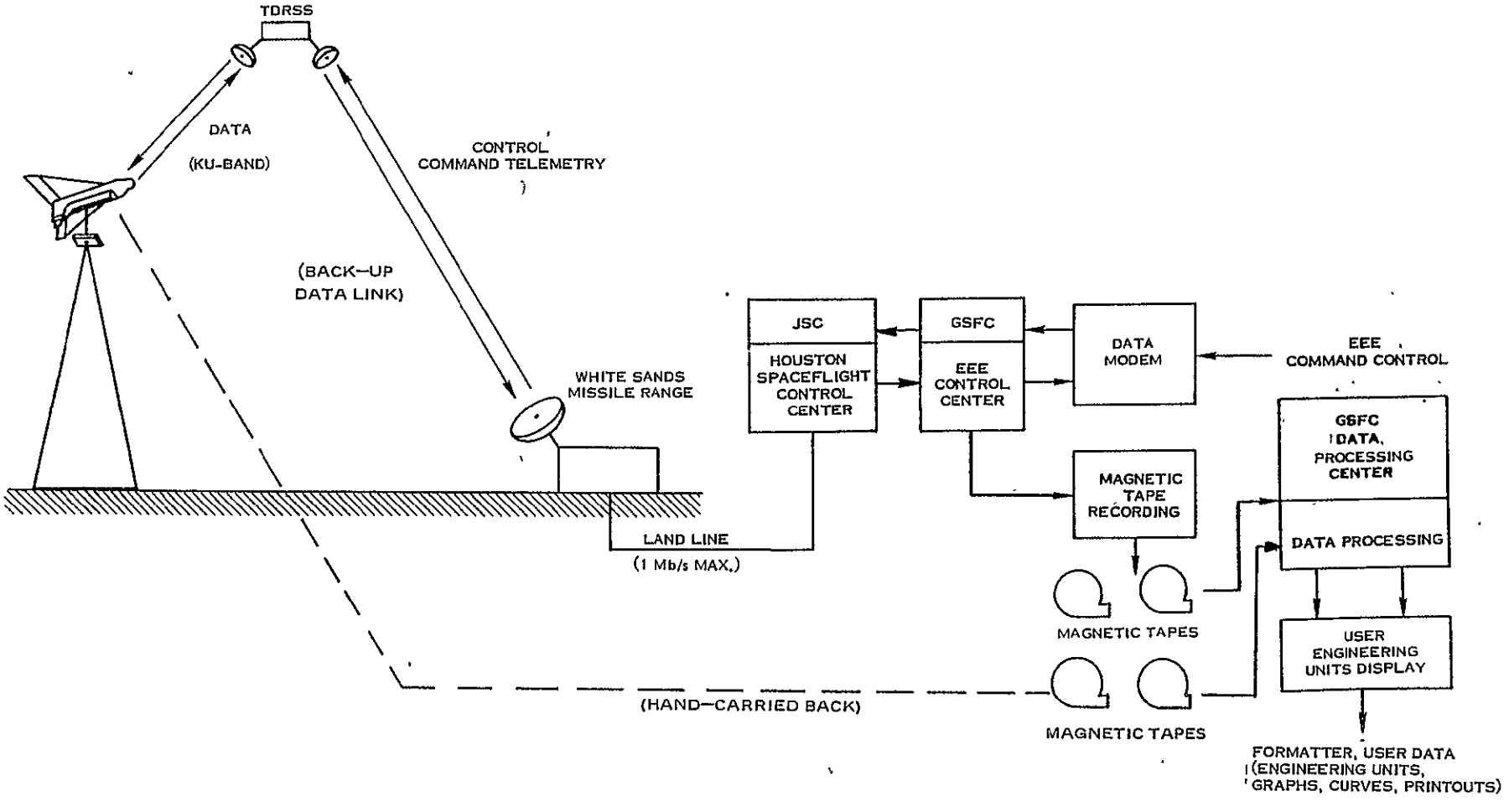

Figure 4-19. Experiment Data Processing

TEST PROGRAM

- BASIC ACCEPTANCE TESTS TO BE PERFORMED AT FACTORY
- FIRST EEE INTEGRATION AND TESTS AT FACTORY
- FULL PERFORMANCE TESTS AT FACTORY
- CALIBRATE BUILT-IN NOISE SOURCE

TEST EQUIPMENT

- CONSTRUCT EEE ELECTRICAL TEST EQUIPMENT - PORTABLE RACKS
- ANTENNA RANGE (120 - 2700 MHz)
- SHIELDED ROOM (120 - 2700 MHz)
- MECHANICAL TEST EQUIPMENT INCLUDING THERMAL VACUUM
- BUILT-IN TEST EQUIPMENT (NOISE SOURCE)
- MECHANICAL FRAME OR PALLET

(a)

TYPICAL TESTS	TEST ENVIRONMENT	COMMENTS
ELECTRICAL ACCEPTANCE		
- ANTENNA	RANGE	MEASURED BY ANTENNA SUPPLIER
- RECEIVERS	RF LAB	SUBSYSTEM LEVEL
- CONTROL	RF LAB	WITH RECEIVERS
- INTERFACE	RF LAB	FULL SUBSYSTEM
- SUBSYSTEM	SHIELDED ROOM	FULL SUBSYSTEM, EMC
MECHANICAL ACCEPTANCE		
- VIBRATION	MECH. LAB	INDIVIDUAL BOXES, SUBSYSTEMS, PALLET EQUIP. IN FIXTURE
- SHOCK		
- ACCELERATION		
- THERMAL VAC		INDIVIDUAL BOXES, SUBSYSTEMS
- ACOUSTIC		EQUIP. IN FIXTURE
- TEMPERATURE	RF/MECH. LAB	COMBINED WITH ELEC. TESTS

(b)

Figure 4-20. EEE Factory Tests

equipment for electrical performance tests will be experiment unique, and it is proposed that portable racks containing test equipment be constructed and used at various stages of test and integration. Similarly, built-in test equipment should be used in all stages of testing to calibrate the test equipment and develop experience in use of the equipment.

4.4.2 EQUIPMENT CERTIFICATION

The first level of EEE integration onto the Shuttle will be on the pallet. This phase of integration is still being defined, but could take place at a NASA center. Equipment verification will involve some basic performance tests and verification of crucial interface criteria; e.g., electromagnetic compatibility (EMC). It is proposed that these tests be performed using the portable test equipment supplied with the instrument and the built-in noise source. Figure 4-21 identifies some of the basic tests to be done at certification.

TEST PROGRAM

- BASIC PERFORMANCE TESTS TO VERIFY EQUIPMENT STATUS
- EEE INTEGRATION TESTS WITH PALLET INTERFACE
- EMC TESTS - VERIFICATION
- VERIFY BUILT-IN NOISE SOURCE CALIBRATION

TEST EQUIPMENT

- EEE ELECTRICAL TEST EQUIPMENT - PORTABLE RACKS
- SHIELDED ROOM (120 - 2700 MHz).
- BUILT-IN TEST EQUIPMENT (NOISE SOURCE)
- PALLET AND MODULE RACK FOR INTEGRATION

Figure 4-21. EEE Equipment Certification

Similarly, Shuttle integration tests are shown in Figure 4-22. Since this is the first full-up equipment and integration tests, the portable test equipment is still required, although the Spacelab equipment and built-in test equipment can be used for many of the tests. It should be noted, however, that this may be the first time that crucial integration and EMC tests are run.

4.4.3 INFLIGHT CALIBRATION AND TESTING

Testing and equipment calibration during the EEE flight will make use of the built-in noise source and beacons located at NASA sites shown in Figure 3-2, page 3-9 for Goldstone and Rosman. By switching in the noise source shown in Figure 4-6a, receiver sensitivity can be measured. This technique can be used to set attenuator levels as well as monitoring system noise level. Calibration of the EEE instrument, however, requires a known ground source. It is proposed that unmanned beacons emitting 10W EIRP be set up at several NASA sites. These emitters, along with other known sources, provide the sources for calibration inflight and data received can be used in checking user data after processing. Figure 4-23 shows the tests and test equipment suggested for these tests.

TEST PROGRAM

- PERFORMANCE TESTS TO VERIFY EQUIPMENT STATUS
- EEE INTEGRATION WITH MODULE AND SHUTTLE
- EMC TESTS USING BUILT-IN NOISE SOURCE
- EXPERIMENT OPERATION TESTS (MODES 1 , 2 , 3)

TEST EQUIPMENT

- EEE ELECTRICAL TEST EQUIPMENT - PORTABLE RACKS
- BUILT-IN TEST EQUIPMENT

Figure 4-22. EEE Integration and Prelaunch Tests

TESTS

- MONITOR EEE OUTPUTS FOR NOISE POWER INPUTS
- MEASURE EEE OUTPUTS FOR ON/OFF NOISE INPUTS
- CALCULATE SENSITIVITY AND NOISE BASE

TEST EQUIPMENT

- BUILT-IN TEST EQUIPMENT

Figure 4-23a. EEE Noise Calibration

TEST PROGRAM

- MEASURE 10W EIRP BEACONS AT NASA SITES
- MONITOR KNOWN SOURCES
- OPERATE RECEIVER ATTENUATORS FOR SIGNAL REDUCTION

TEST EQUIPMENT

- UNMANNED 10W EIRP BEACONS

Figure 4-23b. EEE Inflight Calibration with Beacons

SECTION 5

MILLIMETER WAVE COMMUNICATIONS EXPERIMENT (MWCE)

Definition of the MWCE is being conducted in five phases: MWCE instrument design, experiment implementation, operations support, implementation schedule, and MWCE test plan. Work completed this period has included a review of earlier studies[3], and extension of these studies to include a preliminary design of a full up MWCE experiment using a steerable pointing antenna system. Work on experiment implementation has included study of the ground systems as well as the Shuttle equipment and a radius of operation analysis to show operating times over specific stations. Work reported this period is in the following areas:

1. MWCE Experiment
2. MWCE Instrument Description (Steerable Antenna)
3. Preliminary Data Reduction Analysis
4. System Performance Analysis

5.1 MWCE EXPERIMENT

In the design of space communications and microwave sensing systems at millimeter wavelengths, consideration must be given to the effects of precipitation on the earth-space propagation path. At frequencies above 10 GHz, absorption and scattering caused by hydrometeors (rain, hail, or wet snow) can cause a reduction in signal level (attenuation) which will reduce the reliability of the link. Other effects can be generated by precipitation events. They include: depolarization, amplitude and phase scintillations, and bandwidth decoherence. All of these factors can have a degrading effect on space communications and microwave sensing at millimeter wavelengths.

Over the last decade or so, direct measurements of earth-space attenuation above 10 GHz have been accomplished, first with radiometers and sun-trackers, then with the ATS earth satellites. More refined models were proposed, and the first steps in acquiring long term attenuation statistics were begun at a number of frequencies and locations. Recently, data from the ATS-5, ATS-6 and CTS satellite experiments have become available. Results from the MWCE will extend the scientific and engineering data base into the millimeter wave frequency bands, specifically the 30/20 GHz communications bands.

5.1.1 EXPERIMENT OBJECTIVES

The primary objective of the Millimeter Wave Communication Experiment (MWCE) is to evaluate advanced wideband communications techniques for space applications in the millimeter wavelength bands. The techniques will include the measurement and evaluation of digital and analog communications utilizing frequency reuse techniques. A second objective is to measure atmospheric affects and provide a data base for design of future millimeter wave communications systems.

The significant and unique aspects of the MWCE are:

1. High rate (500 Mbps) data links at 20 GHz (downlink) and 30 GHz (uplink).
2. Frequency re-use using right and left-hand circular polarized signals.
3. Provide an additional downlink for Spacelab data.
4. Data transmissions are to be evaluated as a function of local ground station elevation angle to evaluate scintillation and effects characteristics of low elevation angles.
5. Evaluate sub-synchronous communications link capabilities.
6. Wideband analog and digital techniques.

Two major advances of the MWCE are:

1. Actual wideband communications will be conducted along with beacon-type experimentation.

2. The measurements will be the first conducted from a non-synchronous orbit, thus allowing the variables of ground station elevation angle and satellite antenna pointing accuracy to be evaluated.

Results of the MWCE would be utilized in the development of system design requirements for NASA projects, for the development of spectrum utilization, frequency management and sharing criteria, and for the evaluation of domestic distribution and communications satellite questions under the GSFC TCS (Technical Consultation Services) Program.

A vast number of organizations and agencies are actively involved in the evaluation of millimeter wave data and system analysis. A partial list of these organizations interested in MWCE is presented below:

1. NASA Programs
   a. CTS, ATS - Telecommunications Users
   b. Nimbus/Landsat - Sensor Development
   c. Space Shuttle - EVAL, IUS Payload Development
   d. Next Generation NASA Operations
2. WARC Support
   a. IRAC Inputs for Position Papers
   b. Significant Interest for Frequencies Above 20 GHz
3. Technical Consultation Services (TCS)
   a. Provide support for frequency use and spectrum management under GSFC TCS Program

4. Other Government Users

   a. Federal Communications Commission (FCC)

   b. U.S. Dept. of Commerce, Office of Telecommunications, Institute for Telecommunications Sciences (OT/ITS)

   c. Office of Telecommunications Policy (OTP)

   d. National Oceanic and Atmospheric Administration (NOAA)

5.1.2 OPERATIONAL MODES

The MWCE will be flown on the Shuttle to simulate low-orbit satellite communications links from the MWCE to designated principal ground stations at GSFC, Greenbelt, Md. and GSFC, Rosman, N. C. STDN Sites. Additional ground stations might include Blacksburg, Virginia (Virginia Polytechnic Institute and State University), Columbus, Ohio (Ohio State University) and Austin, Texas (University of Texas). The location of these ground stations requires a 57^{o} inclined orbit; nominal altitude is planned for 400 km.

The operational links of the MWCE will provide a direct evaluation of critical design requirements for millimeter wave space systems. The areas of investigation include: frequency re-use techniques employing orthogonal polarization; propagation characteristics and low elevation angle effects; wideband analog and digital techniques.

The MWCE will be operated in several modes in order to demonstrate the feasibility of high data rate, millimeter wave, satellite communication links:

1. Transponder Mode
2. Spacelab Mode
3. Beacon Mode

The modes are illustrated in Figure 5-1.

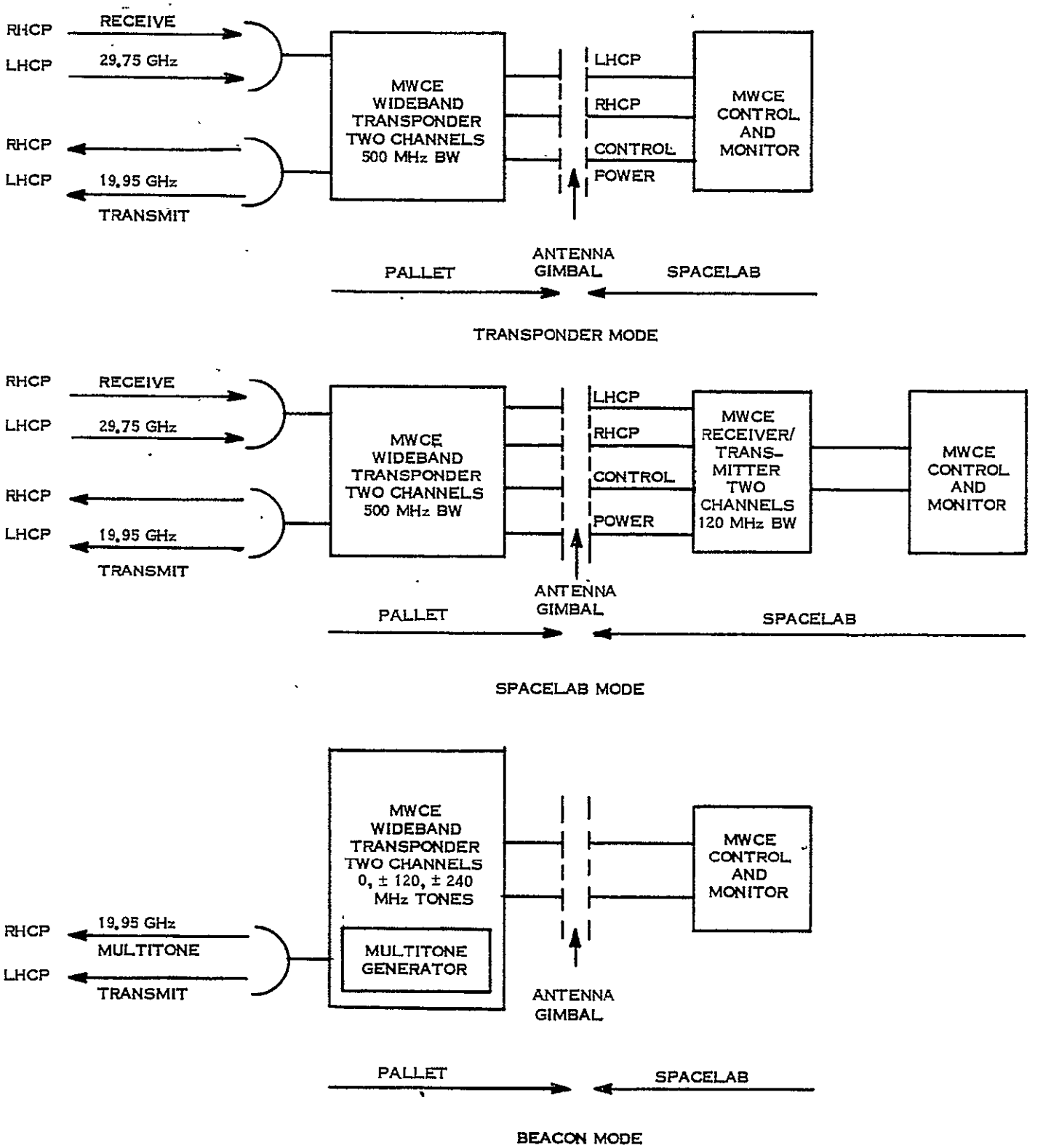

Figure 5-1. MWCE Modes of Operation

In the transponder mode the MWCE acts as a frequency-converting "bent-pipe" communications link. In this mode it is planned to use two circularly polarized channels each with 500 MHz bandwidth through the transponder using separate receive and transmit antennas.

In the Spacelab mode of operation the MWCE Payload Specialist (PS) will be an active participant. For example, unlinked data will be recorded, cross-correlated between channels, retransmitted via the TDRSS (limited to 50 Mbps), etc., with close coordination between the PS and the responsible ground station personnel. The PS may also be transmitting data such as random generated data, TDRSS data, video data, multitone signal, and CW. Simultaneously, antenna pointing, time sharing with other experiments and experiment monitoring will be being conducted.

The beacon mode consists of continuously operating 20 and 30 GHz test signals (Shuttle to earth) for the evaluation of propagation and low elevation angle effects.

A summary of the principal measurement parameters is given below:

1. Transponder Mode

    a. Bit Error Rate (BER) on LHCP channel, RHCP channel no signal, channels isolation measurements

    b. BER on RHCP channel, LHCP no signal, channel isolation measurements

    c. BER on both channels, same signal and clock rate - cross-correlation between channels (a measure of channel isolation)

    d. BER on both channels, different clock rates

    e. BER as a function of elevation angle

    f. Phase lock loop lock-in, slewing, loss-of-lock

    g. Signal amplitudes

2. Spacelab Mode

   a. BER of known Spacelab digital data, correlate with TDRSS downlinked data, both channels

   b. BER for single channels only

   c. Spacelab data on one channel, uncorrelated data on other channel, measure BER, correlate with TDRSS downlinked data

   d. BER versus elevation angle

   e. Phase lock loop lock-in, slewing, loss-of-lock

   f. Signal amplitudes

3. Beacon Mode

   a. Attenuation and depolarization caused by rain

   b. Low elevation effects caused by the atmosphere

5.2 INSTRUMENT DESCRIPTION

The major instrument systems of the MWCE are illustrated in Figure 5-2. Figure 5-3 shows the MWCE pallet mounted equipment. A gimballed mount will be used with $\pm 70^{\circ}$ FOV from NADIR. The mount will be stowed as shown in Figure 5-3 during launch and landing.

Pallet mounted equipment will be enclosed in a rectangular structure of 290 x 280 x 264 centimeters. This structure will be mounted on gimbals as shown in Figure 5-3 to provide $\pm 70^{\circ}$ field of view for ground station tracking. A light weight structure will house the two 0.7 m parabolic antennas, the two widebeam acquisition horns, and the RF electronics including the traveling wave tube amplifiers, down converters frequency synthesizer and power supplies. This arrangement provides compact packaging, weight reduction and short waveguide runs. A six inch diameter X-Y gimbal will be used to provide tracking. Flexible coaxial cables will be used for IF signal connections, control signal lines, and power connections to the pallet equipment.

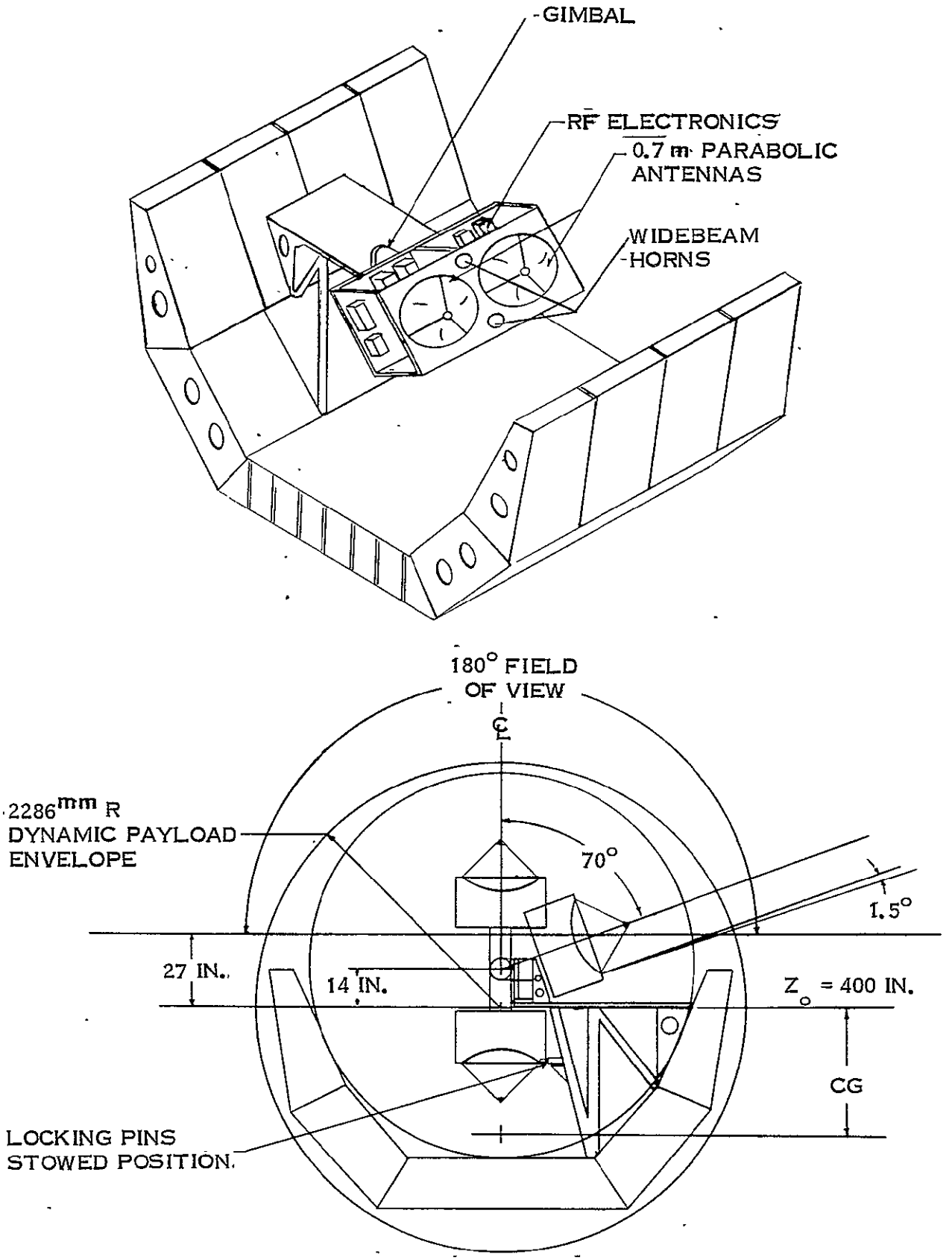

Figure 5-3. MWCE Pallet Mounting Configuration

The $\pm 70^{o}$ FOV is obtained by mounting the pallet equipment enclosure on a cantilever structure as shown in Figure 5-3. During launch and landing the Y-axis gimbal rotates to the full down position and is locked into position. This stowed position is needed to comply with center of gravity constraints for launch and landing. Solenoid operated locking pins will be used to lock the gimbal and the structure in its stowed position.

The pallet based RF systems consist of two dedicated antennas, two transponders, and two stages of IF down/up conversion. The two transponders are designed to receive at 29.75 ± 0.25 GHz and transmit at 19.95 ± 0.25 GHz. There is a separate antenna for transmitting and receiving and each antenna is capable of simultaneously handling both right- and left-hand circularly polarized signals. A passive microwave polarizer is employed to separate the polarized signals upon reception and combine the orthogonal polarizations for transmission.

The transmit antenna system consists of a Cassegrain 0.7 meter parabolic dish, 9 cm hyperbolic sub reflector, and dual polarized feed system capable of generating RHCP and LHCP. The horn aperture will be designed such as to efficiently illuminate the sub reflector for optimum aperture illumination and minimum spill over loss. The polarized section creates right-hand and left-hand circular polarizations, the quality of which is a function of power division quality, 90^{o} phase shift and internal match in the feed circuit. An axial ratio of less than 0.5 dB is achievable. Areas of concern in maintaining the polarization purity are tolerances, maintaining symmetry, reflections from the sub reflector and off axis cross polarized components introduced by the curvature of the main reflector.

The receive antenna system consists of an identical Cassegrain configuration except for the tracking mode and additional filtering which may be required. The sum mode circuit in the receive antenna (as well as in the transmit) will consist of the horn, orthogonal coupler and a short slot hybrid which creates the power combination (or division) and a 90^{o} phase differential. The quality of circular polarization is a function

of the accuracy of power division equality and 90° phase shift in the short slot hybrid and the internal match in the feed circuit.

In the transponder mode of operation each transponder acts as a double conversion RF/IF/RF repeater with a 1.35 GHz IF frequency. After conversion the received dual polarized signals are retransmitted by a 10W TWTA operated at saturated power. Because of the high data rates to be transmitted, i.e., on the order of 500 Mbps, the amplitude and phase characteristics of the transponder components must be designed for minimum distortion. In the spacelab mode, additional IF conversion stages translate the received left-hand circularly polarized signal (LHCP) to an IF frequency of 425 MHz and the right-hand circularly polarized signal (RHCP) to an IF frequency of 330 MHz. The two orthogonal polarized signals are then sent to the display console for analysis by the Payload Specialist. Similarly, digital or analog signals generated at the control console by the Payload Specialist are converted to 425 MHz and 330 MHz IF frequencies for LHCP and RHCP signals, respectively, and then translated to the 1.35 GHz IF frequency for transmission to the ground stations.

In the beacon mode of operation, a CW beacon or a multitone generator will supply signals at 1.35 GHz which are then up-converted for transmission to the ground station. The CW beacon frequency is 19.95 GHz and the tones generated are spaced around the center frequency of 19.95 GHz at $\pm$120 MHz and $\pm$240 MHz.

In the console control area there are five specific experiment display and control functions under the supervision of the Payload Specialist during the spacelab mode of operation. For each circularly polarized signal there is a QPSK demodulator with phase lock loop. The constituent quadrature I and Q channel data streams are processed to determine the overall BER and the resulting BER is recorded. Alternately, the quadrature data streams can be recorded or retransmitted via TDRSS. The phase lock loop error signal is displayed to determine lock-in or loop lock loss. The received signal amplitude variation is determined by an envelope detector. An analog strip-chart

recorder for recording the amplitude variations is available to the Payload Specialist. The signal amplitude is also sampled, digitized in a PCM format and recorded for later analysis.

There are two transmitted information signals under the direct control of the Payload Specialist, a video signal that originates in the shuttle and a coded QPSK modulated data stream. In the former case, various parameters of the video signal are controlled directly by the Payload Specialist, e.g., the type of test pattern transmitted. The modulation format for the video information can be chosen to be some form of angle modulation (FM, PM, etc.). In the digital transmission mode, a PN code generator and its effective data rate are controlled by the Payload Specialist to determine variation of channel BER with respect to data rate.

5.3 DATA REDUCTION AND ANALYSIS

Due to the high data rates that will be transmitted, storage of the received 500 Mbps digital signal originating from the ground or the Shuttle will be prohibitive. Consequently, all high digital data rate information must be processed and the processed information stored. For example, the BER results can be digitized and stored rather than storing the received digital stream. The amplitude variations of the received signals are strip-chart recorded directly and sample digitized in a PCM format and stored.

Data received by the MWCE will be sent to the ground control/processing center in real time via the TDRSS and existing land lines. Figure 5-4 shows the steps to be taken to process data received at the control center. All data are expected to be initially recorded on magnetic tapes for storage and eventually transferred to GSFC Information Processing Division (IPD) data processing system. Similarly, data received at the tracking stations will be recorded and sent to the GSFC IPD.

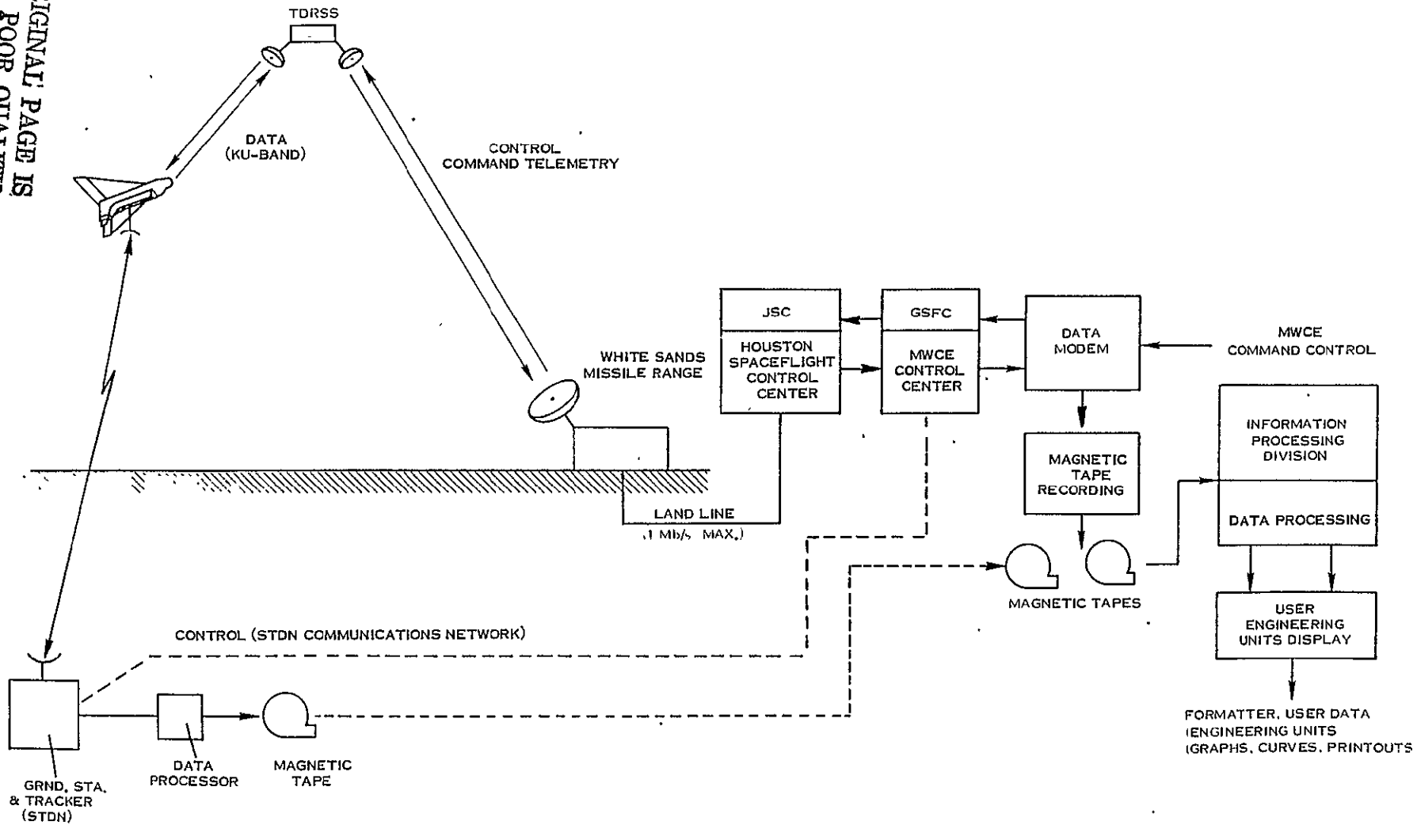

Figure 5-4. MWCE Data Processing

5.4 SYSTEM PERFORMANCE ANALYSIS

5.4.1 RADIUS OF OPERATION AND OPERATIONAL TIME

The radius of operation is defined as the maximum great circle arc distance from an earth station at which a desired communication system performance is achieved. The radius of operation can be limited either by geometrical factors such as the maximum allowable ground station elevation angle or the maximum shuttle antenna viewing angle or by communication performance parameters such as receiver sensitivity or antenna gain. The practical operating elevation angle for most ground stations is about 5^{o}. For ground stations located in very flat areas with no ground obstructions such as trees or mountains, it may be possible to operate at or near 0^{o} elevation angle. For most stations the radius of operation is the great arc circle distance to the sub-shuttle point for a 5^{o} ground station elevation angle. The Shuttle-Ground Station geometry is illustrated in Figure 5-5.

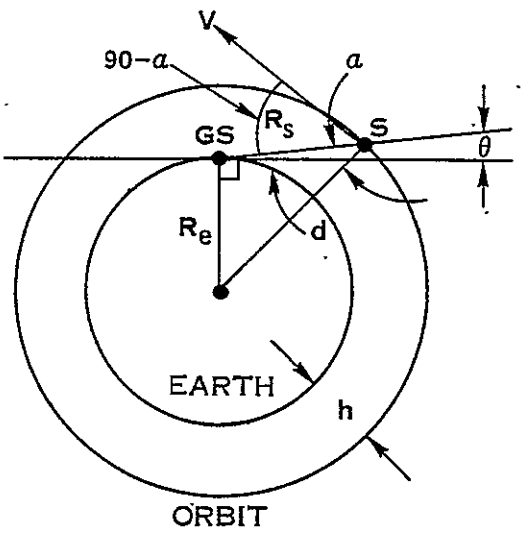

S = SHUTTLE
GS = GROUND STATION
R_e = EARTH RADIUS = 6374 km
h = SHUTTLE ALTITUDE
θ = ELEVATION ANGLE
a = MWCE ANTENNA VIEWING ANGLE
R_S = SLANT RANGE
d = ARC DISTANCE TO SUB-SHUTTLE POINT ON EARTH'S SURFACE

Figure 5-5. Satellite-Ground Station Geometry

For a given ground station elevation angle the MWCE antenna view angle from Figure 5-5 can be expressed as

$$\alpha = \sin^{-1}\left[\frac{R_e}{R_e + h}\,(\cos\theta)\right] \tag{1}$$

where

α is the MWCE antenna view angle from nadir

R_e is the earth's radius = 6374KM

h is the Shuttle altitude

θ is the ground station elevation angle.

The slant range one-way communication distance between the shuttle and the ground station is

$$R_S = \frac{\cos(\theta + \alpha)}{\cos\theta}\,(R_e + h) \tag{2}$$

where R_S is the slant range distance between the shuttle and the ground station. The great-arc distance between the ground station and the sub-shuttle point is

$$d = \frac{\pi R_e}{180}\,(90 - \theta - \alpha) \tag{3}$$

and the radius of operation r, is given by

$$\gamma = d(\theta_{MAX}) \tag{4}$$

The radius of operation and the MWCE antenna view angle from NADIR are given in Table 5-1 for various values of the maximum ground station elevation angle. Also, the same results are presented in graphical form in Figures 5-6 and 5-7.

Table 5-1. Radius of Operation and Total Link Margin for Various Ground Station Elevation Angles*

ELEVATION ANGLE (°)	ANTENNA VIEW ANGLE FROM NADIR (°)	REQUIRED S/N (dB)	RECEIVED S/N (dB)	MARGIN (dB)	RADIUS OF OPERATION (km)
5	69.6	15.7	29.5	13.8	1713 (925 nm)
10	67.9	15.7	34.0	18.3	1344 (726 nm)
20	62.2	15.7	38.5	22.8	873 (471 nm)
30	54.6	15.7	41.3	25.5	603 (326 nm)
40	46.1	15.7	43.3	27.6	431 (233 nm)
45	41.7	15.7	44.1	28.4	366 (198 nm)

* ORBIT: 400 KM, 57° INCLINATION

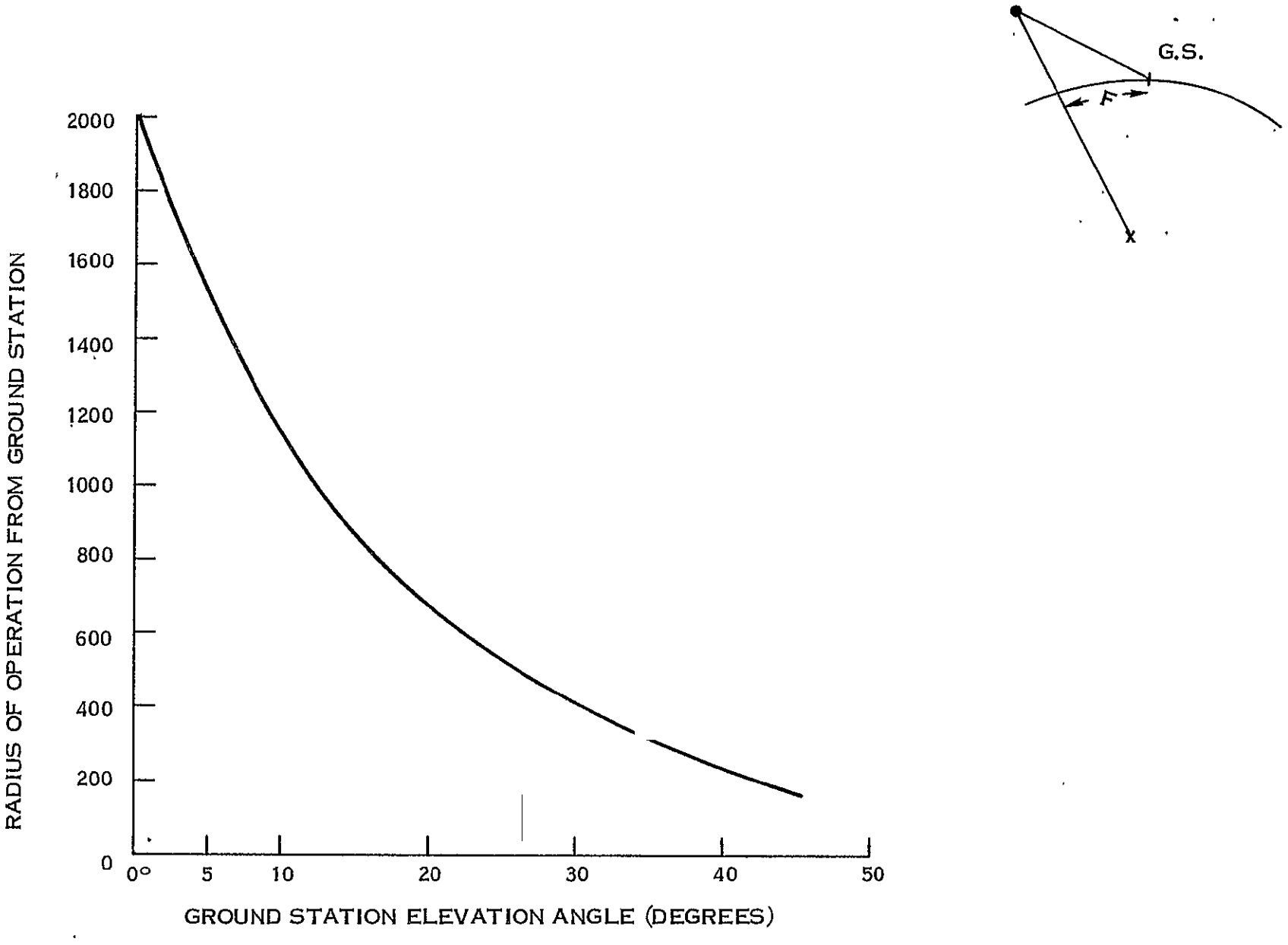

Figure 5-6. MWCE Maximum Radius of Operation as a Function of Ground Station Elevation Angle

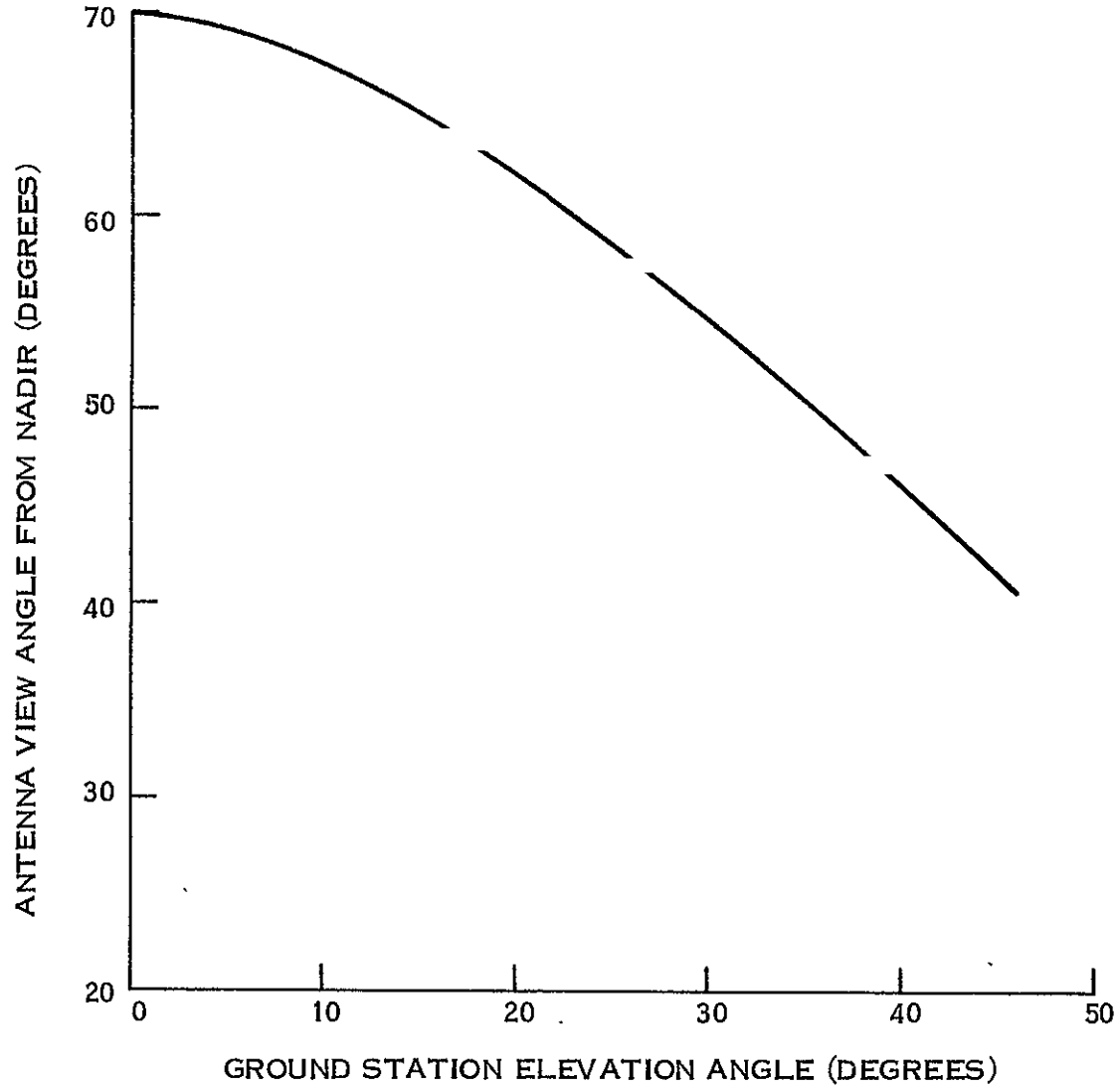

MWCE Antenna View Angle from NADIR as a Function of Ground Station Elevation Angle

The extent of the radii of operation for the Rosman, N.C. and Austin, Texas ground stations is illustrated in Figure 5-8. The radii of operation, corresponding to a 5^{o} elevation angle (1713 km), were drawn around the both ground stations and a radius of operation, corresponding to a 20^{o} elevation angle (873 km), was drawn around the Rosman, N.C. facility. The CONUS shown in the figure as well as the longitudinal and latitudinal scales are MERCATUR projections of their actual spherical shapes.

The cross-hatched lines represent the orbital paths of the Shuttle for a 400 km orbit with a 57^{o} inclination traced over a full, six day period. Approximately 94 orbits are traced in a six day mission with an orbitral period 92.65 minutes. The numbers at the bottom of Figure 5-8 correspond to the sequential orbit number of the trace. The operational time for a particular ground station represents the total orbital time within the radius of operation of the ground station, that is, the sum of all of the orbit trace times within the radius of operation. The operation time is determined by first computing the great arc circle length of each orbital trace of interest.

The calculation of the great arc circle length is illustrated in Figure 5-9. The points A and B are the intersection points of the orbital trace and the radius of operation and $\hat{p}$ is the great circle arc distance between the intersection points. The coordinates of A are given by λ_a and η_A and those of B are given by λ_B and η_B. The terms $\hat{a}$ and $\hat{b}$ are minor arcs of a great circle and together A, B and point P, the North Pole, form a spherical triangle. The great-circle arc distance is given by

$$\hat{p} = \cos^{-1} \left[\cos \hat{a} \cos \hat{b} \times \sin \hat{a} \sin \hat{b} \cos \hat{P}\right] \tag{5}$$

where

$$\hat{a} = \pi/2 - \lambda_A \tag{6}$$

$$\hat{b} = \pi/2 - \lambda_B \tag{7}$$

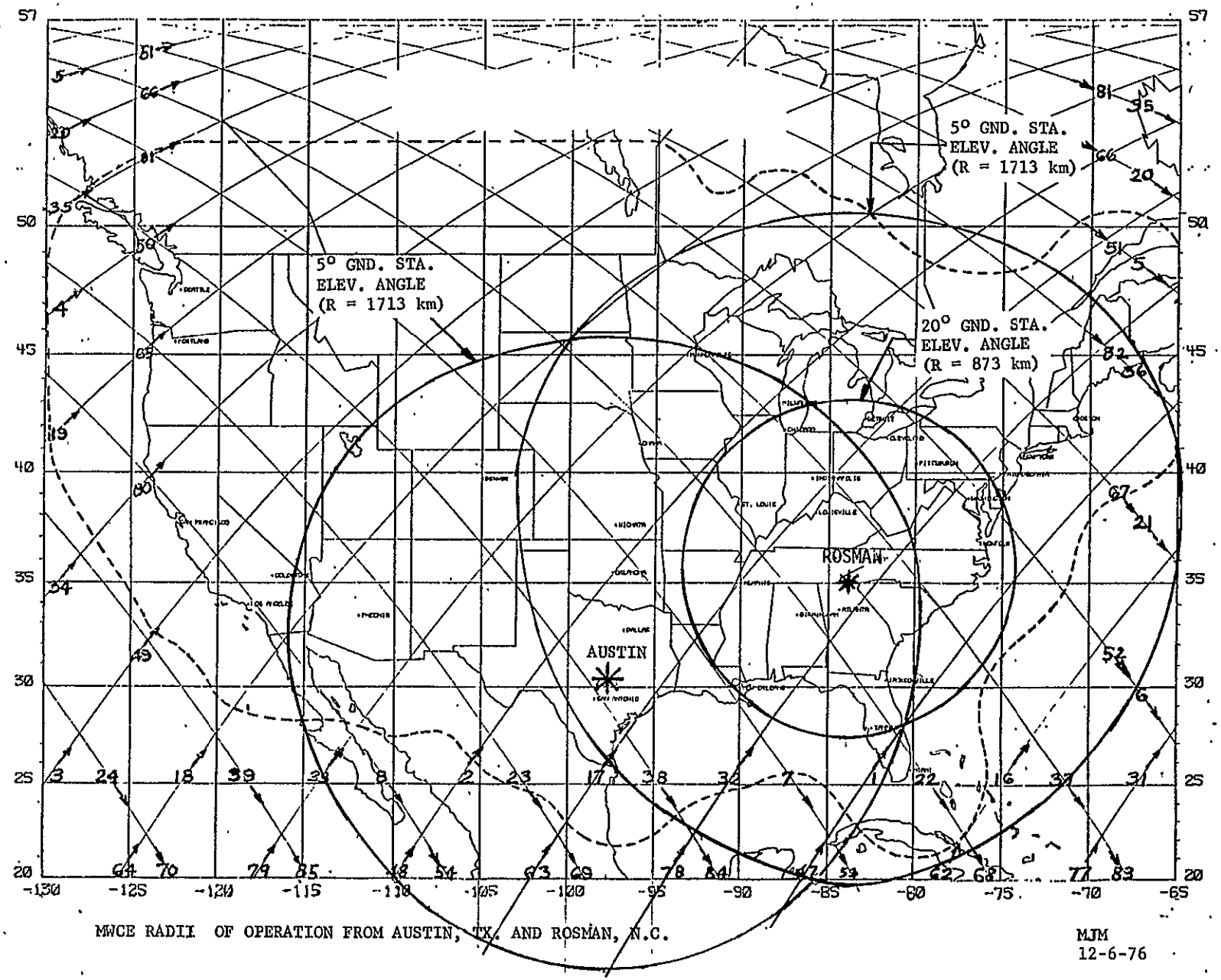

Figure 5-8. MWCE Radii of Operation from Austin, TX. and Rosman, N. C.

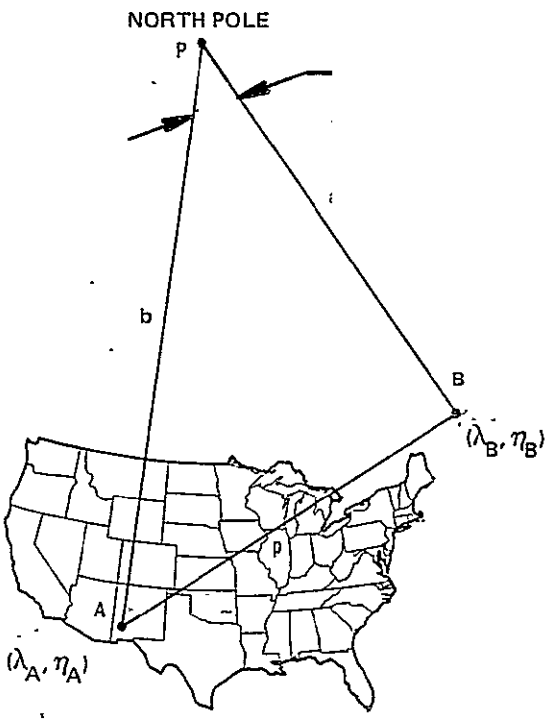

Figure 5-9. Spherical Geometry for Computation of Orbital Trace Time

and

$$\hat{p} = \left| \eta_B - \eta_A \right| \tag{8}$$

The operational time corresponding to the great-circle arc length $\hat{p}$ is

$$t = \frac{\hat{p}}{\pi} T \tag{9}$$

where

t is the operational time

$\hat{p}$ is the arc length in radians

and

T is the orbital period

The total operation times for the Rosman N. C. Facility for a 20^{o} and a 5^{o} ground station elevation angles is presented in Tables 5-2 and 5-3, respectively. It can be seen that the operation time increases considerably when going from a 20^{o} elevation angle (873 km) to a 5^{o} elevation angle (1713 km). The operating time over Austin, Texas is shown in Table 5-4 and is slightly less than the operating time over Rosman, N. C. The operating time for a given elevation angle should not vary widely with respect to the particular ground station location. The operating time using both ground stations is presented in Table 5-5.

5.4.2 COMMUNICATION PERFORMANCE ANALYSIS

Of the three modes of operation the transponder mode of operation for QPSK represents the worst-case operation in terms of overall link performance; consequently, only this case will be analyzed. It was assumed that a bit error rate (BER) of 10^{-5} was the desired probability of error performance. The required bit energy to noise density ratio to obtain a 10^{-5} BER for ideal QPSK detection is 9.6 dB. Since there are two bits of information for every QPSK symbol, the ideal detection signal-to-noise ratio for QPSK is given by adding 3.0 dB to the required E_b/N_o ratio. From General Electric's experience in the design, testing, and simulation of QPSK modems, it is known that the ideal performance is not difficult to achieve. Due to the practical implementation of QPSK detection and non-linear amplification there is a difference between the actual versus the ideal BER performance. It has been found that there is a 3.1 dB difference between actual and ideal BER performance. Some of the causes for this "digital demodulation loss" are intersymbol interference, carrier recovery phase errors, non-linearities in the MWCE/Shuttle TWTA, sampling jitter noise, etc. Thus, the total signal-to-noise ratio needed at the input to the detector is 15.7 dB and the results are presented in Table 5-6.

All of the equations needed to determine the system performance will now be derived. The actual received signal-to-noise ratio is determined by combining the noise contributions produced by the up-link transmission and reception in the shuttle and by the

Table 5-2. MWCE Operating Time Over Rosman, N.C. for 20° Ground Station Elevation Angle

DAY 1		DAY 2		DAY 3		DAY 4		DAY 5		DAY 6	
ORBIT	TIME (MIN.)	ORBIT	TIME (MIN.)	ORBIT	TIME (MIN.)	ORBIT	TIME (MIN.)	ORBIT	TIME (MIN.)	ORBIT	TIME (MIN.)
1	2.2	17	3.3	37	3.8	52	1.9	68	3.8	83	3.8
6	1.9	22	3.8	47	2.2	63	3.3	78	3.9		
		32	3.9								
TOTAL	4.1		11.0		6.0		5.2		7.7		3.8

SIX DAY TOTAL: 37.8 MINUTES

ORBIT: 400 KM, 57° INCLINATION

Table 5-3. MWCE Operating Time Over Rosman, N.C. for 5° Ground Station Elevation Angle

DAY 1		DAY 2		DAY 3		DAY 4		DAY 5		DAY 6	
ORBIT	TIME (MIN.)	ORBIT	TIME (MIN.)	ORBIT	TIME (MIN.)	ORBIT	TIME (MIN.)	ORBIT	TIME (MIN.)	ORBIT	TIME (MIN.)
1	7.5	16	4.9	33	5.0	48	6.7	64	1.3	79	5.0
2	6.7	17	7.5	36	2.8	52	7.0	67	5.4	82	2.8
6	7.0	18	1.3	37	7.8	53	6.8	68	8.0	83	7.8
7	6.8	21	5.4	38	3.5	62	4.9	78	8.0	84	3.5
		22	8.0	47	7.5	63	7.5				
		32	8.0								
TOTAL	28.0		35.1		26.6		32.9		22.7		19.1

SIX DAY TOTAL: 164.4 MINUTES

ORBIT: 400 KM, 57° INCLINATION

Table 5-4. MWCE Operating Time Over Austin, TX. for 5^{o} Ground Station Elevation Angle

DAY 1		DAY 2		DAY 3		DAY 4		DAY 5		DAY 6	
ORBIT	TIME (MIN.)	ORBIT	TIME (MIN.)	ORBIT	TIME (MIN.)	ORBIT	TIME (MIN.)	ORBIT	TIME (MIN.)	ORBIT	TIME (MIN.)
1	3.0	17	7.8	32	6.9	48	7.8	64	4.7	79	6.8
2	7.8	18	4.7	33	6.8	53	7.7	68	6.2	83	3.6
7	7.7	22	6.2	37	3.6	54	4.6	69	7.2	84	8.0
8	4.6	23	7.2	38 47	8.0 3.0	63	7.8	78	6.9		
TOTAL	23.1		25.9		28.3		27.9		25.0		18.4

SIX DAY TOTAL: 148.6 MINUTES

ORBIT: 400 KM, 57^{o} INCLINATION

Table 5-5. MWCE Two-Station Operating Time Over Austin, TX. - Rosman, N.C. for 5° Ground Station Elevation Angle

DAY 1		DAY 2		DAY 3		DAY 4		DAY 5		DAY 6	
ORBIT	TIME (MIN.)	ORBIT	TIME (MIN.)	ORBIT	TIME (MIN.)	ORBIT	TIME (MIN.)	ORBIT	TIME (MIN.)	ORBIT	TIME (MIN.)
1	8.1	16	4.9	33	9.0	48	10.2	64	5.9	79	9.0
2	10.2	17	10.8	36	2.8	52	7.0	67	5.4	82	2.8
6	7.0	18	5.9	37	7.8	53	8.2	68	8.0	83	7.8
7	8.2	21	5.4	38	8.0	54	4.6	69	7.2	84	8.0
8	4.6	22	8.0	47	8.1	62	4.9	78	9.8		
		23	7.2			63	10.8				
		32	9.8								
TOTAL	38.1		52.0		35.7		45.7		36.3		27.6

SIX DAY TOTAL: 235.4 MINUTES

ORBIT: 400 KM, 57° INCLINATION

Table 5-6. Transponder Mode of Operation

SIGNAL-TO-NOISE RATIO

REQUIRED FOR BER = 10^{-5}

(TOTAL LINK)

REQUIRED E_b/N_o (IDEAL)	=	9.6 dB
CONVERSION TO QPSK*	=	3.0 dB
DIGITAL DEMODULATION LOSS**	=	3.1 dB
		15.7 dB

* NUMBER OF BITS/SYMBOL

** INTERSYMBOL INTERFERENCE, CARRIER RECOVERY PHASE ERRORS, SAMPLING JITTER NOISE, MODULATOR AMPLITUDE IMBALANCE, ETC.

down-link shuttle transmission and ground station reception. The total received signal-to-noise ratio for the transponder mode of operation is given by

$$(S/N)_{TOTAL} = \frac{S}{N_{UPLINK} + N_{DOWNLINK}} \quad (10)$$

or

$$(S/N) = \frac{1}{1/(S/N)_{UPLINK} + 1/(S/N)_{DOWNLINK}} \quad (11)$$

The uplink signal-to-noise ratio is given by

$$(S/N)_{UPLINK} = (EIRP)_E - L_T + (G/T)_{S/C} - BW - N_o \quad (12)$$

where

$(EIRP)_E$ is the effective isotropic radiated power of the ground station

L_T is the total path loss for the up-link transmission

$(G/T)_{S/C}$ is the ratio of the gain of the MWCE spacecraft antenna to the noise temperature of the MWCE receiver

BW is the received signal bandwidth

N_o is the thermal background noise power density for unit temperature.

Similarly, the downlink signal-to-noise ratio is given by

$$(S/N)_{DOWNLINK} = (EIRP)_{S/C} - L_T + (G/T)_E - BW - N_o \quad (13)$$

where

$(EIRP)_{S/C}$ is the effective isotropic radiated power of the MWCE on-board the spacecraft

L_T is the total path loss for the downlink transmission

$(G/T)_E$ is the ratio of the ground station antenna gain to the noise temperature of the ground station receiver.

The total path loss is the sum of four components and is given as

$$L_T = L_f + L_p + L_A + L_{po} \tag{14}$$

where

L_f is the free-space loss

L_{po} is the pointing loss and is caused by the transmit and receive antennas not being pointed on boresight

L_p is the polarization loss due to polarization alignment mismatches between the receive and transmit antennas

L_A is the atmospheric loss due to oxygen and water vapor absorption

An empirical formula[3] for the atmospheric loss is

$$L_A\,(20\ \text{GHz}, \theta) = .71\,(.6)/\sin\theta \tag{15}$$

$$L_A\,(30\ \text{GHz}, \theta) = .71\,(.45)/\sin\theta \tag{16}$$

where θ is the elevation angle.

The effective isotropic radiated power is given by

$$(\text{EIRP}) = G - L_\ell - P_T \tag{17}$$

where

G is the antenna gain referred to an isotropic antenna

L_ℓ is the total line loss between the transmitter and the antenna

P_T is the total transmitted signal power.

The total system noise temperature of a receiver is

$$T_S = T_a + T_o (L_\ell - 1) + L_\ell T_o (NF-1)$$

where

T_a is the antenna temperature.

T_S is the total receiver system noise temperature referred to the input antennas terminals

T_o is the standard noise reference temperature = $290^{\circ}K$

L_ℓ is the total line loss between the antenna and the receiver

NF is the noise figure of the receiver.

The uplink and downlink transmission parameters employed in the analysis are presented in Figures 5-10 and 5-11. The transmitter powers, the antennas, and the receiver noise figures employed were the same parameters recommended in a previous report (Reference 3). The total line losses employed represent worst-case values. The EIRP's and (G/T)'s of the transmitter and receiver systems is also indicated. The complete system performance calculations for the transponder mode for ground station elevation angle of 45°, 20°, and 5° is presented in Tables 5-7, 5-8 and 5-9 respectively The complete system performance summary is given in Table 5-1.

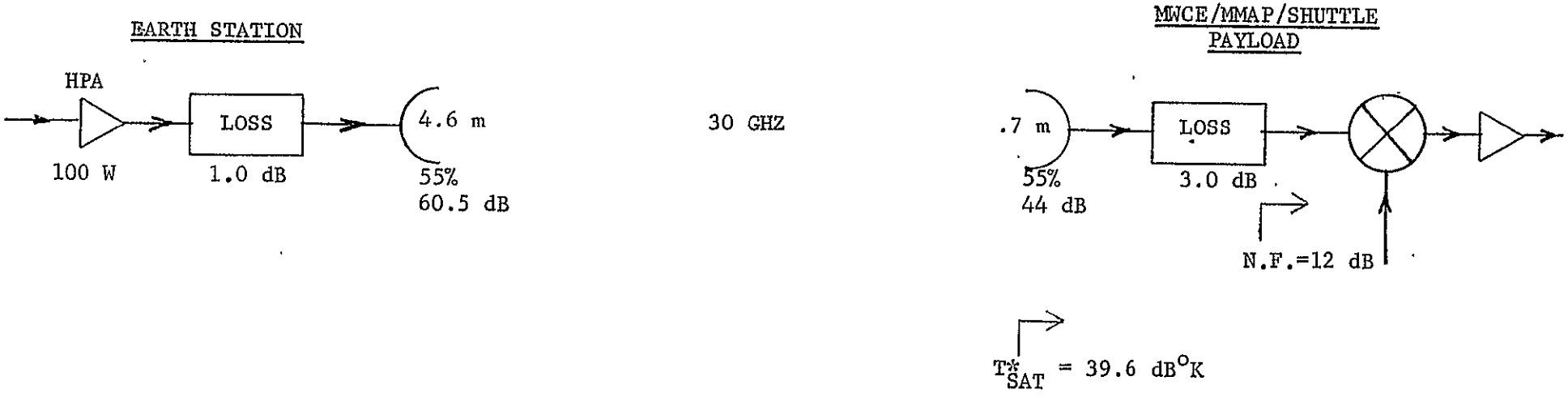

$(EIRP)_E = 78.5$ dBW

$L_T = L_f + L_p + L_A + L_{po}$

L_T = TOTAL LOSS
L_f = FREE SPACE LOSS
L_{po} = POINTING LOSS
L_p = POLARIZATION LOSS
L_A = ATMOSPHERIC LOSS

$(G/T)_{SAT} = 4.4$ dB/°K

$$(S/N)_{UPLINK} = (EIRP)_E - L_T + (G/T)_{S/C} - BW - N_o$$

* INCLUDES LINE LOSS

Figure 5-10. Uplink Transmission Parameters

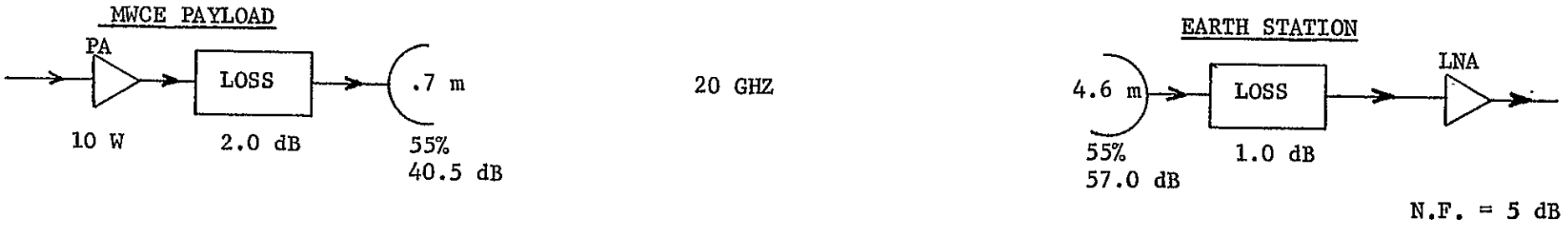

$$T_E^* = 29.5 \text{ dB}^\circ\text{K}$$

$$L_T = L_f + L_p + L_A + L_{po}$$

$$(EIRP)_{S/C} = 48.5 \text{ dBW}$$

$$(G/T)_E = 27.5 \text{ dB}/^\circ\text{K}$$

$$(S/N)_{DOWNLINK} = (EIRP)_{S/C} - L_T + (G/T)_E - BW - N_o$$

Figure 5-11. Downlink Transmission Parameters

Table 5-7. 30 GHz Uplink Budget for a 45° Elevation Angle

EARTH STATION TRANSMITTER POWER (dBW)	20.0
EARTH STATION RF LOSSES (dB)	2.0
EARTH STATION ANTENNA GAIN (dBi)	60.5
EARTH STATION EIRP (dBW)	78.5
LOSSES	
FREE SPACE LOSS (dB)	176.8
POLARIZATION (dB)	.5
ATMOSPHERIC (dB)	.5
POINTING LOSS (TX ANT.) (dB)	.5
TOTAL LOSSES (dB)	178.3
SATELLITE RECEIVE SYSTEM G/T* (dB/°K)	4.4
SIGNAL BANDWIDTH (dB-Hz)	84.0
BOLTZMAN'S CONSTANT (dBW/Hz-°K)	-228.6
C/N UPLINK TOTAL (dB)	49.3

$T_{SAT} = T_a + T_o (L\ell - 1) + L\ell\ T_o(NF-1)$
$T_{SAT} = 290^o + 290^o\ (1) + (2)\ (290^o)\ (14.8)$
$T_{SAT} = 9192^oK = 39.6\ dB^oK$
*INCLUDES LINE LOSS

Table 5-7. 20 GHz Downlink Budget for a 45˘ Elevation Angle (Cont'd)

TRANSMITTER POWER (dBW)	10.0
RF LOSSES (dB)	2.0
ANTENNA GAIN (dBi)	40.5
EIRP (dBW)	48.5
LOSSES	
FREE SPACE LOSS (dB)	173.3
POLARIZATION (dB)	.5
ATMOSPHERIC (dB)	.6
POINTING LOSS (dB)	.5
TOTAL LOSSES (dB)	174.9
EARTH STATION RECEIVE SYSTEM G/T* (dB/^{o}K)	29.5
SIGNAL BANDWIDTH (dB-Hz)	84.0
BOLTZMAN'S CONSTANT (dBW/H_z-^{o}K)	-228.6
C/N DOWNLINK TOTAL (dB)	45.7
C/N UPLINK (dB)	49.3
C/N TOTAL (UP LINK + DOWN LINK) (dB)	44.1

$T_E = T_a + T_o (L_\ell - 1) + L_\ell T_o (NF-1)$
$T_E = 35^{o}K + 290^{o} (.26) + 290^{o} (1.26) (2.16)$
$T_E = 900^{o}K = 29.5\ dB^{o}K$
*INCLUDES LINE LOSS

Table 5-8. 30 GHz Uplink Budget for a 20^{o} Elevation Angle

EARTH STATION TRANSMITTER POWER (dBW)	20.0
EARTH STATION RF LOSSES (dB)	2.0
EARTH STATION ANTENNA GAIN (dBi)	60.5
EARTH STATION EIRP (dBW)	78.5
LOSSES	
FREE SPACE LOSS (dB)	181.8
POLARIZATION (dB)	.5
ATMOSPHERIC (dB)	.9
POINTING LOSS (TX ANT.) (dB)	.5
TOTAL LOSSES (dB)	183.7
SATELLITE RECEIVE SYSTEM G/T* ($dB/^{o}K$)	4.4
SIGNAL BANDWIDTH (dB-Hz)	84.0
BOLTZMAN'S CONSTANT ($dBW/Hz-^{o}K$)	-228.6
C/N UPLINK TOTAL (dB)	43.8

$T_{SAT} = T_a + T_o\ (L_\ell - 1) + L_\ell\ T_o (NF-1)$
$T_{SAT} = 290^{o} + 290^{o}\ (1) + (2)\ (290^{o})\ (14.8)$
$T_{SAT} = 9192^{o}K = 39.6\ dB^{o}K$
*INCLUDES LINE LOSS

Table 5-8. 20 GHz Downlink Budget for a 20° Elevation Angle (Cont'd

TRANSMITTER POWER (dBW)	10.0
RF LOSSES (dB)	2.0
ANTENNA GAIN (dBi)	40.5
EIRP (dBW)	48.5
LOSSES	
FREE SPACE LOSS (dB)	178.3
POLARIZATION (dB)	.5
ATMOSPHERIC (dB)	1.3
POINTING LOSS (dB)	.5
TOTAL LOSSES (dB)	180.6
EARTH STATION RECEIVE SYSTEM G/T* (dB/°K)	29.5
SIGNAL BANDWIDTH (dB-Hz)	84.0
BOLTZMAN'S CONSTANT (dBW/H_z-°K)	-228.6
C/N DOWNLINK TOTAL (dB)	40.0
C/N UPLINK (dB)	43.8
C/N TOTAL (UP LINK + DOWN LINK) (dB)	38.5

$T_E = T_a + T_c (L_\ell - 1) + L_\ell T_o (NF - 1)$
$T_E = 35°K + 290° (.26) + 290° (1.26) (2.15)$
$T_E = 900°K = 29.5\ dB°K$
*INCLUDES LINE LOSS

Table 5-9. 30 GHz Uplink Budget for a 5° Elevation Angle.

EARTH STATION TRANSMITTER POWER (dBW)	20.0
EARTH STATION RF LOSSES (dB)	2.0
EARTH STATION ANTENNA GAIN (dBi)	60.5
EARTH STATION EIRP (dBW)	78.5
LOSSES	
FREE SPACE LOSS (dB)	187.2
POLARIZATION (dB)	.5
ATMOSPHERIC (dB)	3.7
POINTING LOSS (TX ANT.) (dB)	.5
TOTAL LOSSES (dB)	191.9
SATELLITE RECEIVE SYSTEM G/T* (dB/°K)	4.4
SIGNAL BANDWIDTH (dB-Hz)	84.0
BOLTZMAN'S CONSTANT (dBW/Hz-°K)	-228.6
C/N UPLINK TOTAL (dB)	35.6

$T_{SAT} = T_a + T_o (L_\ell - 1) + L_\ell T_o (NF-1)$
$T_{SAT} = 290^o + 290^o (1) + (2) (290^o) (14.8)$
$T_{SAT} = 9192^oK = 39.6\ dB^oK$

*INCLUDES LINE LOSS

Table 5-9. 20 GHz Downlink Budget for a 5° Elevation Angle (Cont'd)

TRANSMITTER POWER (dBW)	10.0
RF LOSSES (dB)	2.0
ANTENNA GAIN (dBi)	40.5
EIRP (dBW)	48.5
LOSSES	
FREE SPACE LOSS (dB)	183.7
POLARIZATION (dB)	.5
ATMOSPHERIC (dB)	4.9
POINTING LOSS (dB)	.5
TOTAL LOSSES (dB)	189.6
EARTH STATION RECEIVE SYSTEM G/T* (dB/°K)	29.5
SIGNAL BANDWIDTH (dB-Hz)	84.0
BOLTZMAN'S CONSTANT (dBW/H_z-°K)	-228.6
C/N DOWNLINK TOTAL (dB)	31.0
C/N UPLINK (dB)	35.6
C/N TOTAL (UP LINK + DOWN LINK) (dB)	29.5

$T_E = T_a + T_o (L_\ell - 1) + L_\ell T_o (NF-1)$
$T_E = 35°K + 290° (.26) + 290° (1.26) (2.16)$
$T_E = 900°K = 29.5\ dB°K$
*INCLUDES LINE LOSS

SECTION 6

NEW TECHNOLOGY

Work on this contract during the interim period of September 1976 through March 1977 has not resulted in the evolution of new technology.

SECTION 7

WORK PLANNED FOR NEXT PERIOD

Work planned for the next interim period includes continuing effort on the three major experiments being defined: AMPA, EEE, and MWCE. In addition work, as directed, will be done on OSP and another experiment concerning an on-board Interferometer for earth-position location purposes, Position Location Interferometer (PLI). Work will also be done on MMAP contractual deliverable items which involve generic considerations to the major experiments. The specific tasks to be started or continued within the next period are discussed in the following paragraphs.

7.1 MMAP

1. Revise, if necessary, Study on R&QA Criteria (draft submitted, Contract Item 16)
2. EMC Test Plan (draft started, Contract Item 17)
3. Ground Handling and Test Operations Man (Contract Item 7)
4. Payload Specialist Functions Plan (Contract Item 8)
5. Mission Operations Plan (Contract Item 9)
6. Data Handling Plans (Contract Item 10)
7. MMAP Schedules (Contract Item 11)
8. List of Critical and Long Lead Items on AMPA, EEE, and MWCE (Contract Item 12)
9. Cost Estimates on AMPA, EEE, and MWCE (Contract Item 13)
10. Level A and B Data (Payload Data Sheets) on AMPA, EEE, and MWCE (revise or update as required, Contract Item 14)
11. Instrumentation Mock-ups on AMPA, EEE, and MWCE (Contract Item 15)
12. MMAP Systems Block Diagrams (to be revised or defined per work-to-date, Contract Item 4)

7.2 AMPA

(Part of Contract Items 3, 7, 10, 13, 14, and 18).

1. User Terminal Design
    a. Identify Requirements
    b. Equipment Design
    c. Specify Calibration Beacons
2. Ground Control Terminal Design
    a. Identify Requirements
    b. Equipment Design
3. Data Reduction Requirements
    a. During Flight (real time)
    b. After Flight (recorded data)
    c. Data Format
    d. Data Volume
    e. Method of Data Reduction and Anal

7.3 EEE

(Part of Contract Items 3, 9, 10, 13, 14, and 18).

1. Phase B Definition of MOD II Design (2.7 to 43 GHz)
    a. Functional Block Diagrams
    b. Mechanical Layout Drawing,
    c. Instrument Payload Descriptions (Level A and B)
    d. Mission Profiles

e. Definition of Data Acquisition Equipment

f. Definition of Data Reduction Techniques

g. Define Software Requirements

h. Prepare Cost Estimates for a Typical Spacelab Flight.

3. Review potential sub-contract proposals on a Frequency, EIRP, and Geographical Listing Task for terrestrial emitters. (Proceed with this contract after review with NASA and as directed).

7.4 MCWE

(Part of Contract Items 3, 7, 10, 13, 14 and 18).

1. Design of MCWE Using a Fixed Antenna and Single Transponder

   a. Functional Block Diagram

   b. Mechanical Layout Drawings

2. Implementation Plan for Fixed Antenna

   a. Identify Long Lead Items

   b. Key Milestones

   c. Ground Support Equipment Definition

   d. Cost Estimates

3. MWCE Test Plan

   a. Define Major Elements for Ground Support and Testing

   b. Identify Facilities Including Modifications

4. Project Plan Definition

   a. Provide Information on System Concepts

   b. Identify Users

   c. Provide Instrument Description

5. Operational Support Definition

   a. Mission Operations

   b. Ground Processing and Data Handling

   c. Payload Specialist Functions

   d. Experiment Integration

7.5 OSP

1. Begin Preliminary User Requirement Study as directed, following outputs from OT/ITS (Office of Telecommunications/Institute for Telecommunications Sciences study.

7.6 PLI

1. Define the experimental objectives and justifications for its need

2. Define the technical approach and analyze problem areas (i.e., earth position accuracy, antenna gain, receiver sensitivity, ground transmitter power, etc.)

3. Perform a conceptual design considering:

   a. Frequency Band Used

   b. Electrical Block Diagram

   c. Mechanical Configuration

   d. Size, Weight, and Power Needed

4. Perform a User Survey based on assumed earth transmitter/antenna configurations.

SECTION 8
CONCLUSIONS

At this point of the MMAP Systems Definition Study only preliminary conclusions may be drawn. The effectiveness of the study is benefited by the highly flexible and responsive posture General Electric has maintained during the course of the contract with the Technical Officer, J. Woodruff, the various Principal Investigators, and with NASA support personnel. Examples include timely responses to the Spacelab Experiment Announcement of Opportunities (AO's) which resulted in the preparation of several Spacelab proposals written in NASA's context. Also included is the detailed technical consideration of a multiplicity of experiment design and system variations, many suggested by the principal investigators.

Work completed during the interim period September 1976 to March 1977 has resulted in two experiment designs, the EEE MOD I and the MWCE. Operational parameters were studied and applied to the AMPA experiment. A 400 km 57^{o} inclination orbit profile was selected as a typical one to define the operational parameters for the experiments.

Progress on the definition of these three experiments has reached the preliminary milestones or beyond. The AMPA and EEE MOD I instruments have been completed in concept design and may now move to the next phase of NASA's experiment hardware procurement. As a cost effective technique some of the work during this period was based on completed contracts [1,2] and on current AMPA contractual work being conducted for NASA by the Airborne Instrument Laboratories. The General Electric studies provided the basis for the Concept Review held at NASA-GSFC in February 1977.

The MWCE has progressed to a preliminary design phase for a system using a steerable antenna mount. This system represents a full-up MWCE and uses a high data rate (500 Mbps). An analysis of the MWCE radius of operation reveals that operation to ground terminals with at least a 5^{o} ground-elevation angle is needed to achieve practical operational times, in the order of 6-8 minutes. Therefore it appears essential to employ a high gain ground antenna in order to achieve a satisfactory carrier-to-noise (C/N) ratio at low antenna elevation angles.

System definition of the EEE MOD I (121.5 to 2700 MHz) is essentially complete. Equipment layouts indicate the requirement for one standard pallet and a moderate size receiver package in the Spacelab Module on AFD. Data handling should be accommodated by the on-board magnetic tapes and real-time data via the TDRSS links. Flexibility of experiment control is afforded by three optional operational modes: remote control via TDRSS, automatic programmed control, or manual control by the Payload Specialist.

Work on defining the AMPA experiment's operational modes has shown that at least a $\pm 70^{\circ}$ viewing angle from the Shuttle is needed to provide an experiment operating time of 6-8 minutes. Details of the experiment operation are included in Section 3 of this report along with a trade-off study of viewing angle versus operating time.

SECTION 9

RECOMMENDATIONS

At the conclusion of this MMAP Systems Definition Study, it is anticipated that there will be conclusions and specific recommendations which will aid in an orderly transition from system design concept to actual experimental system hardware. To date there are three preliminary recommendations offered for NASA's consideration.

As a result of the EEE aircraft flight test R. Taylor is conducting out of NASA-Ames, it will be possible to get measured data on EMI from the Convair 990 aircraft and Model 101 Receiver. The results of these flight tests should improve the EMI data base and help in providing more quantative data for Shuttle EMC studies. In addition, there will be the measured EIRP versus frequency data which adds to the data base and experimental technique.

For the MWCE the use of a high gain spacecraft antenna and a GFE steerable antenna mount would enable a greater operating time for the experiment.

The methodology and results of Reliability versus Cost employed in the R&QA criteria study should be useful in the Shuttle Payload Program for cost effectiveness trade-offs.

SECTION 10

REFERENCES

1. J.B. Horton, M.S. Afifi, G.A. Dorfman, H. Jankowski, Shuttle/Spacelab Electromagnetic Environment Experiment, Phase B Definition Study, Final Report, NAS 5-22469, April 1976 (GE).

2. C.C. Allen, S.P. Applebaum, W.J. Papowsky, G. Wouch, Adaptive Multibeam Antennas for Spacelab, Phase A Feasibility Study, Final Report, NAS 5-22425, February 1976.

3. R. Kaul, Experiment Definition Report on the Millimeter Wave Communications Experiment, Final Report, NAS 5-24034, January 1976 (ORI).

4. Space Shuttle Level II Program Definition and Requirements, JSC-07700, NASA, JSC, Houston, Texas, July 3, 1974.

VIII	Mission Operations
IX	Ground Operations
X	Flight and Ground Specifications
XI	Crew Operations
XII	Integrated Logistics Requirements
XIV	Space Shuttle System Payload Accommodations
XVIII	Computer Systems Software

5. Spacelab Payload Accommodation Handbook, NASA/ESRO, ESTEC REF. No. SLP/2104, May 1975.

6. R.E. Taylor and J.S. Hill, "0.4 to 10 GHz Airborne Electromagnetic Environment Survey of U.S.A. Urban Areas," IEEE International Symposium on Electromagnetic Compatibility (EMC), Session 2B, Washington, D.C., 13-15 July 1976, NASA Accession No. N76-23460.

APPENDIX

MWCE ANTENNA POINTING SYSTEM PRELIMINARY DESIGN

APPENDIX

MWCE ANTENNA POINTING SYSTEM PRELIMINARY DESIGN

1.0 Functional Description

The MWCE Antenna Pointing System (APS) has two modes of operation - acquisition and tracking. The APS functional block diagrams for the acquisition and tracking modes are shown in Figures 1 and 2 respectively. In the acquisition mode the gimbal orientation required to point the monopulse antenna at the desired ground station is determined by the MWCE controller and applied to the APS controller. The commanded gimbal orientation is compared with the actual gimbal orientation as measured by the gimbal potentiometer. The gimbal orientation error is then used to command the gimbal torquer such that the gimbal orientation error is nulled.

When the monopulse system has acquired and is tracking the ground station, the MWCE controller switches the APS from the acquisition to the tracking mode. In the tracking mode (see Figure 2), the monopulse processing electronics generate signals that are proportional to the antenna pointing error relative to the ground station. These signals are processed to generate the appropriate gimbal commands to null the antenna pointing error.

The APS is comprised of two major components - the gimbal assembly and the APS controller. The gimbal assembly contains the gimbal structure, drive motors, bearings, and potentiometers. The APS controller contains the electronics required to process the gimbal pointing error signals and generate the appropriate gimbal motor drive signals.

The APS gimbal assembly mounted in the Spacelab pallet is shown In Figure 3. The gimbal concept is a two axis, X-Y direct drive gimbal similar to that used on the S-193 Skylab experiment. The MWCE mounting arrangement allows the MWCE to be

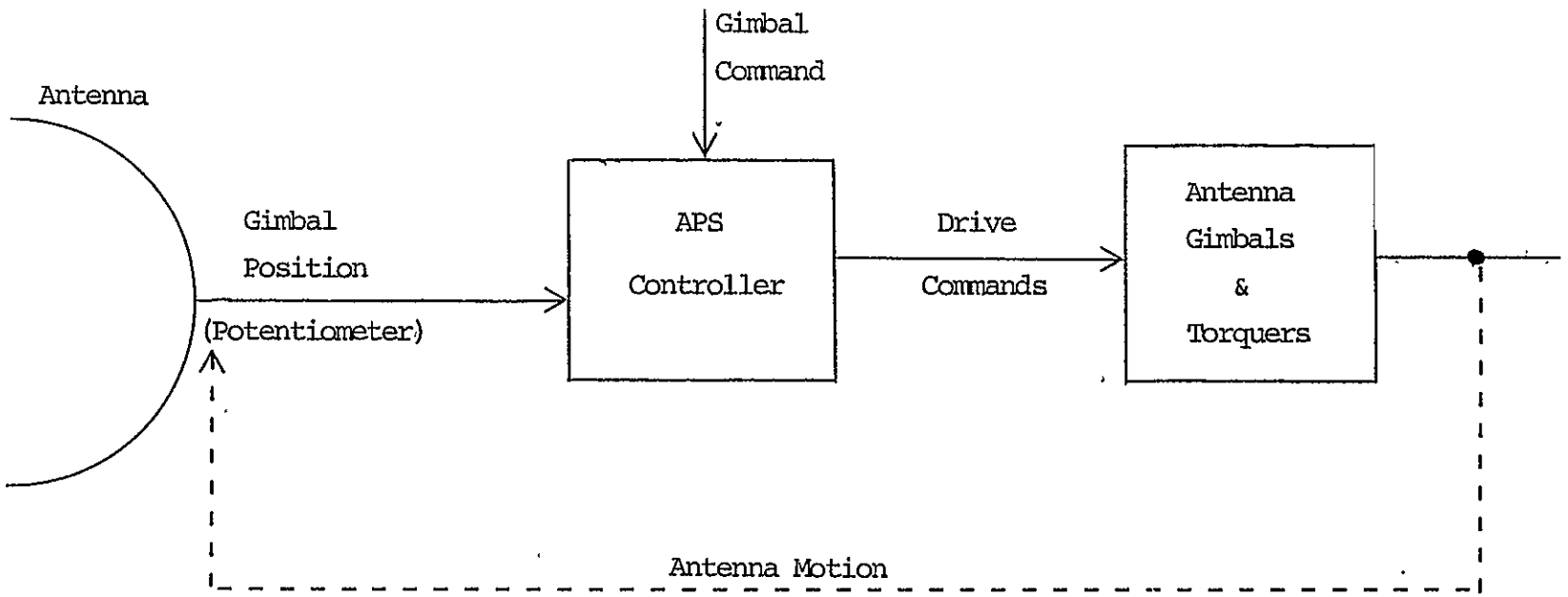

Figure 1 MWCE APS Acquisition Mode Functional Block Diagram

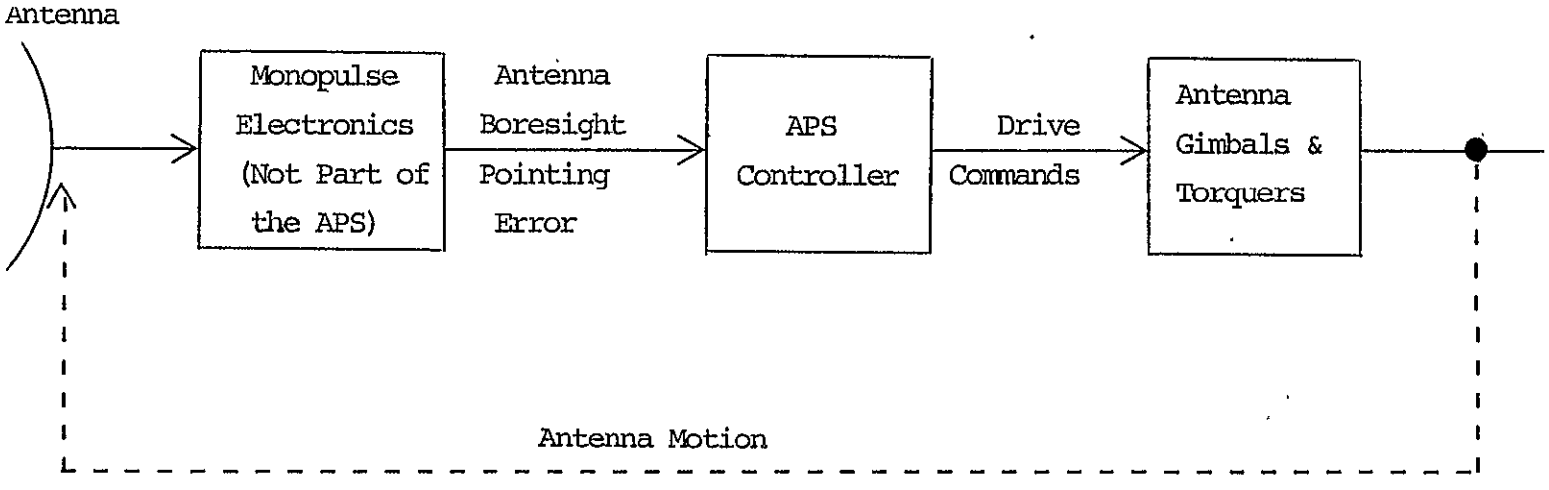

Figure 2 MWCE APS Tracking Mode Functional Block Diagram

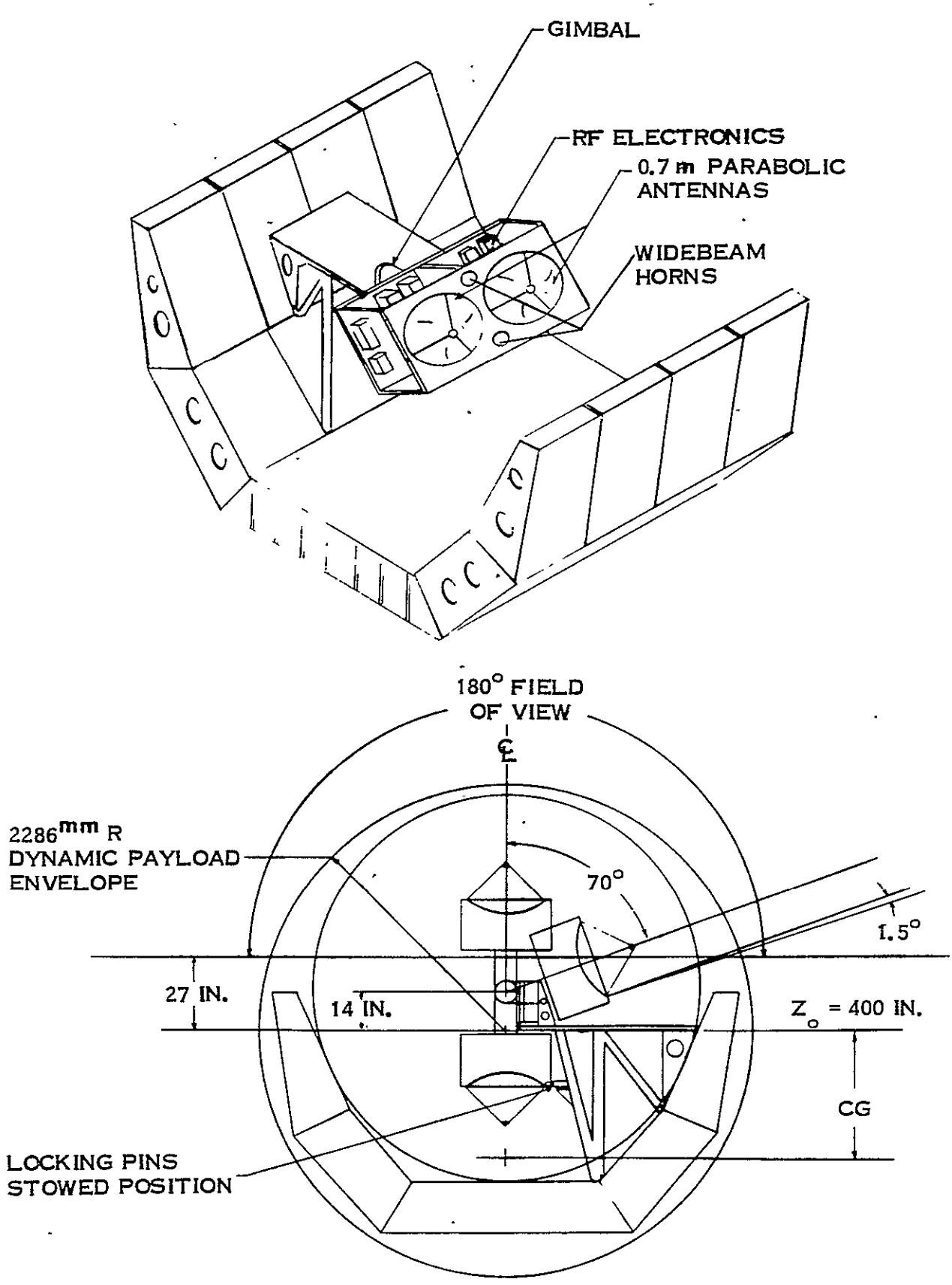

Figure 3 . MWCE Pallet Mounting Configuration

stowed with a low c.g. relative to the shuttle but swing up to obtain the ±70 deg (in both directions) clear field-of-view required for the MWCE.*

A cutaway drawing of the gimbal assembly is shown in Figure 4. Two Inland 7200 DC torque motors provide gimbal control torques. For the nominal mass properties, this results in a 0.34 rad/sec^2 angular acceleration capability*

The APS controller functional block diagram is shown in Figure 5. This APS controller design is based upon the design analysis described in Section 3. The same control loop compensation is used for both the acquisition and tracking modes. Thus, mode selection consists essentially of specifying the pointing error source. It is assumed that the mode commands and acquisition gimbal commands are generated external to the APS.

2.0 Requirements

This section contains the preliminary MWCE APS requirements that were used to guide the design effort. All requirements are 3σ. It can be anticipated that these requirements will be modified as the MWCE design is refined.

2.1 Acquisition Mode

Pointing Accuracy

The APS shall point the antenna boresight within 2 deg of the commanded attitude after the slew and settling time.

Slew Duration

The APS shall execute a commanded 60 deg reorientation with a total slew and settling time less than 10 sec.

2.2 Tracking Mode

Tracking Accuracy

When using the narrow beamwidth monopulse, the antenna boresight shall point within 0.10 deg of the ground station.

Transient Response

An initial 10 deg attitude error at monopulse acquisition shall be reduced to within the tracking accuracy limits within 10 sec.

3.0 Design and Performance Analysis

3.1 Acquisition Mode

The preliminary acquisition mode single axis gimbal control loop is shown in Figure 6. For the preliminary design no slew command shaping/feedforward control has been included. For large angle slews, the gimbal drive motor will be saturated

---

* The MWCE gimbal and support structure configuration was designed by John Zemany; the detail gimbal design was provided by Rae Stanhouse.

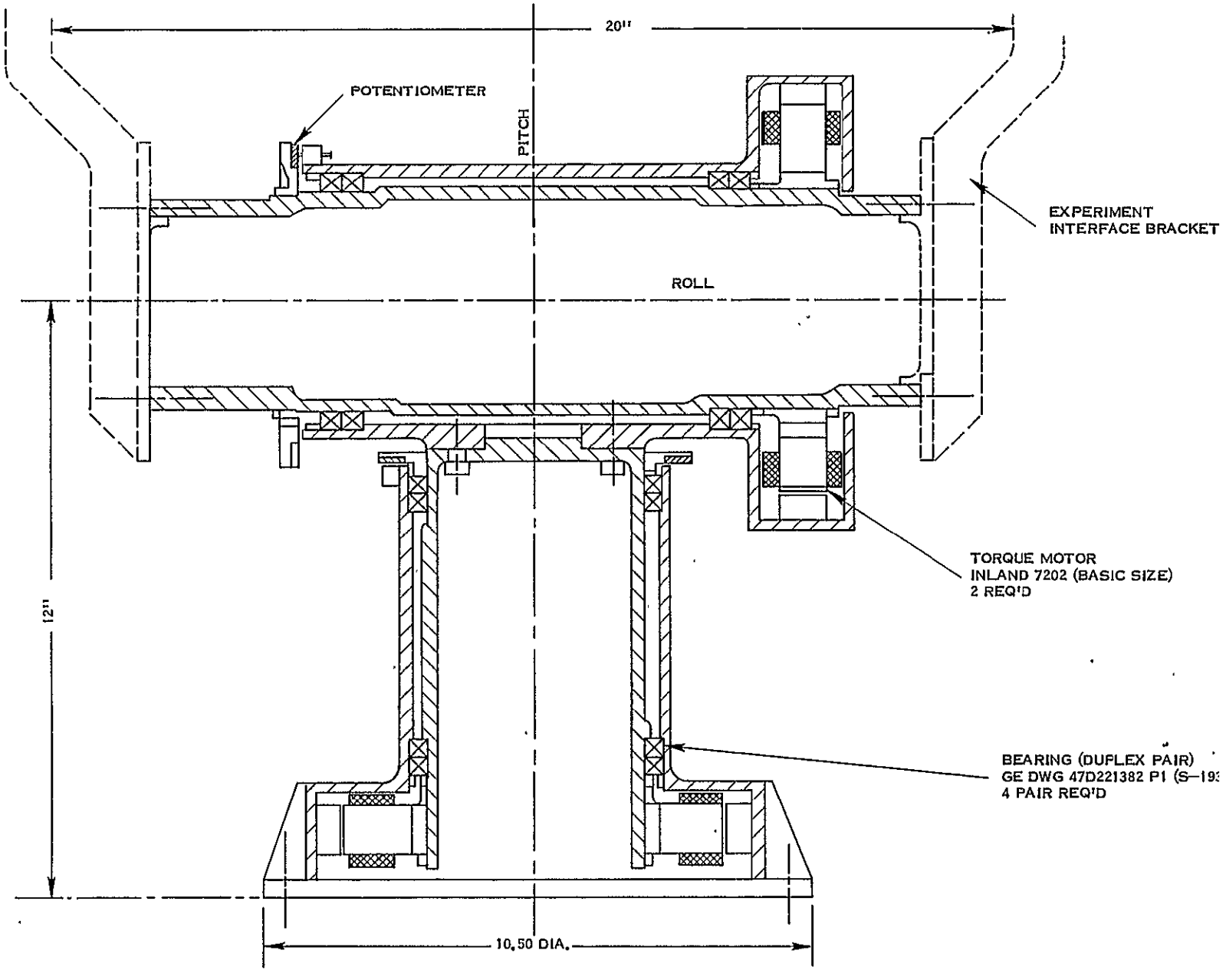

Figure 4. MWCE Gimbal Concept

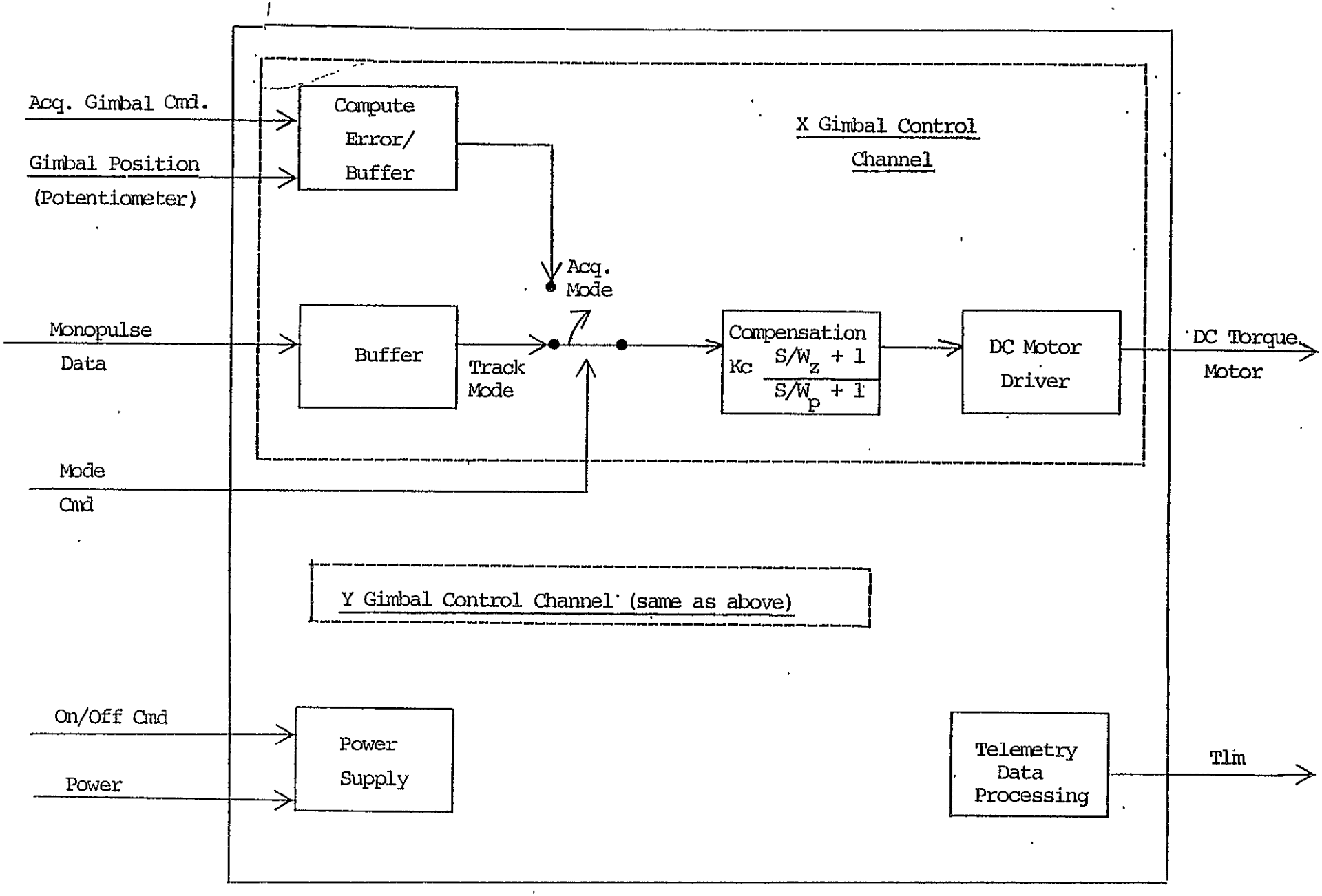

Figure 5 MWCE APS Controller Functional Block Diagram

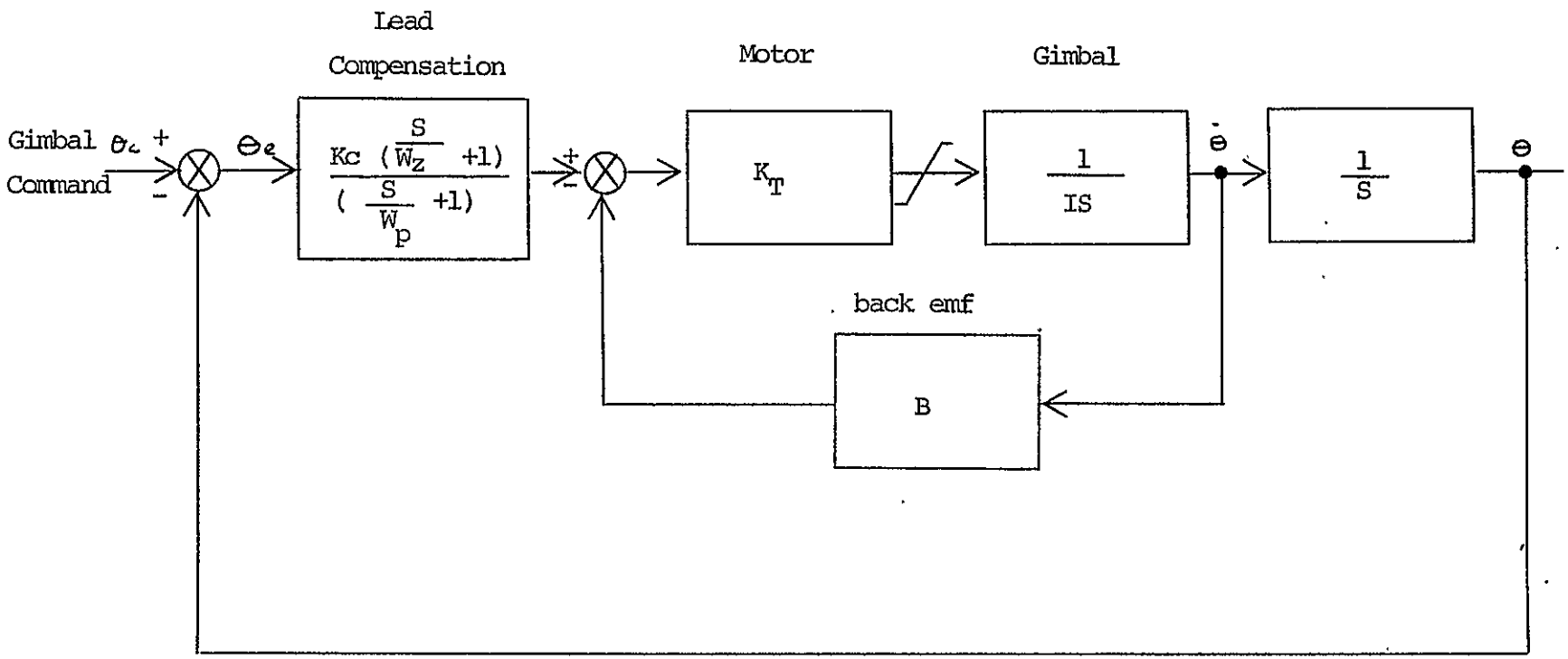

Figure 6 Acquisition Mode Gimbal Control Loop Block Diagram

yielding a maximum gimbal acceleration of 0.34 rad/sec^2. With this acceleration capability, an optimal 60 deg slew can be completed in 3.5 sec. The acquisition control loop shown in Figure 6 will not yield an optimal (i.e., minimum time) slew maneuver; however, it is anticipated that the 60 deg slew maneuver can be completed well within the 10 sec requirement.

The accuracy of the slew maneuver is determined by the gimbal potentiometer angular readout accuracy. Meeting the 2 deg acquisition mode pointing requirement should not present a problem. It should be realized that other attitude error sources external to the gimbal servo loop (e.g. shuttle attitude errors, gimbal command errors, etc.) will also cause errors in the antenna boresight pointing.

3.2 Tracking Mode

There are several conflicting factors in the design of the tracking mode APS. Low tracking errors, fast response and the reduction of the effects of disturbance torques, gimbal bearing friction, and shuttle motion are accomplished with a high gain, high bandwidth control loop. On the other hand, the undesirable effects of monopulse noise on pointing error are agravated by increasing the control loop bandwidth. A preliminary tracking mode control loop design was performed to evaluate these conflicting factors and evaluate the feasibility of the APS design approach.

The tracking mode gimbal control loop block diagram is shown in Figure 7. A series compensated control loop has been selected for the baseline design. This represents the simplest (and least expensive) approach for the APS design. The parameter values for the baseline control loop design are given in Table 1. The motor parameters are based on similar DC torque motors. The MWCE moment of inertia is based on preliminary mass properties data. Single axis, rigid body dynamics have been used for the preliminary design analysis. In view of the relatively low angular rates and control loop bandwidth for the APS, gimbal cross coupling and flexible structure dynamics should not significantly impact the baseline design.

Summary

The principle conclusion of the preliminary design and performance analysis is that the 0.1 deg tracking mode pointing accuracy requirement can be satisfied by the baseline APS design. Table 2 contains a summary of the baseline APS performance.

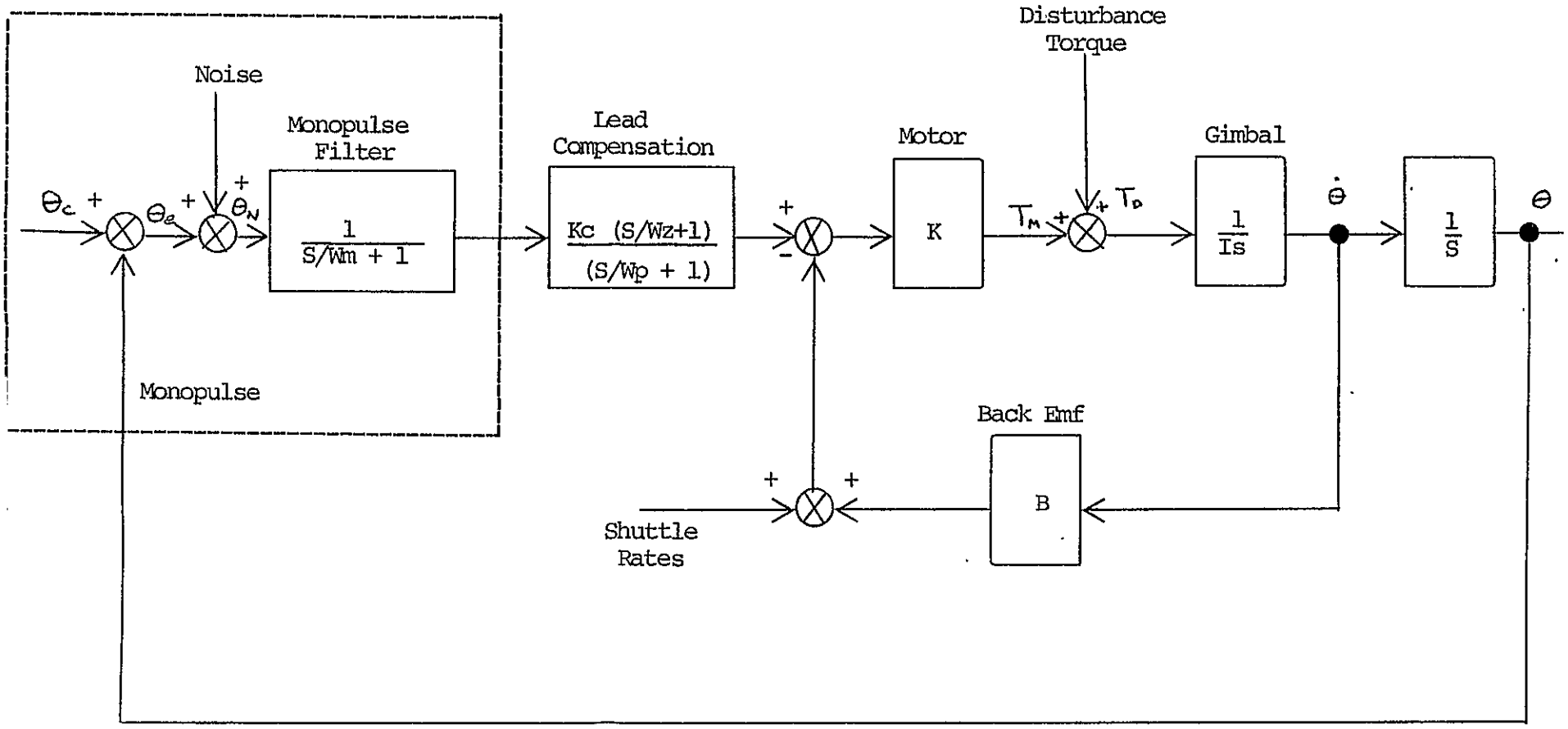

Figure 7 Tracking Mode Gimbal Control Loop Block Diagram

Table 1 Antenna Pointing System Parameters

Symbol	Definition	Value	Units
I	Moment of inertia of gimbal and experiment	31.	slug ft^2
K_c	Compensation gain	1000	volts/rad
W_z	Compensation lead break frequency	1	rad/sec
W_p	Compensation lag break frequency	40	rad/sec
W_m	Monopulse noise filter break frequency	not used	rad/sec
K_T	Motor torque constant	0.25	ft.lb/volt
B	Motor back emf coefficient	1	volt/rad/sec

Table 2 Baseline APS Performance Summary

Performance Criteria	Performance Level	Comments
Steady state pointing error caused by 1 deg/sec ramp input	0.001 deg	Indicates that tracking error due to relative ground station motion will be small
Pointing error caused by monopulse noise	0.001 deg	Based on monopulse noise level of 0.00048 deg (3σ)
Response to disturbance torques cause by shuttle motion	0.06 deg	Can be reduced by increasing loop gain/bandwidth; however, this increases the effects of monopulse noise and flexible structure, control loop interaction
Linear step response settling time (time to move within $\pm$5% of final value)	1.2 sec.	Represents nulling of initial error (i.e., acquisition). Large initial errors (> 1.5 deg) will cause motor saturation and an increase in the response time.
Pointing error cause by bearing friction	0.03 deg	Based on 0.2 ft. lb. bearing friction. Can be reduced by integral compensation
Response to shuttle angular rate	TBD	Not yet evaluated; however, the relatively low shuttle angular are not expected to cause significant control disturbances.

Stability

Of prime consideration in any control loop design is stability. Figure 8 shows the open loop bode plot for the baseline APS. The lead compensation break frequencies have been selected to yield a relatively large phase margin of 72 deg. This results in an overdamped control loop response which has the advantage of reducing the effects of monopulse noise. The possibility of including a monopulse noise filter was incorporated in the baseline design (see Figure 7). The preliminary analysis indicated that the noise filter did not significantly improve performance and consequently it is not included in the final baseline design

The closed loop frequency response for the baseline APS is shown in Figure 9. The closed loop bandwidth is 11 rad/sec.

Step Response

The unit step response is shown in Figure 10. In general, the step response shows the manner in which an initial error is nulled; i.e., it describes the acquisition response. However, the loop gain is such that motor torque saturation will occur when the initial error is greater than about 1.5 deg. If the motor saturates, the step response rise and settling time will be increased. However, the motor acceleration capacity is such that the 10 sec requirement for nulling an initial 10 deg acquisition attitude error should be satisfied.

Bearing Friction Effects

S-193 gimbal experience indicates that the gimbal bearing friction will be on the order of 0.2 ft. lb. For the baseline APS gains, the pointing error required to overcome the friction is 0.03 deg. This value appears acceptable; however, it desired, it could be reduced by the incorporation of an integral compensation term in APS control compensation. If the friction level goes up, then it will be necessary to add the integral compensation. This will not be a significant impact to the design.

Steady State Tracking Error

For the baseline APS, the steady state pointing error response to a ramp input is given by:

$$\Theta_{es} = \frac{B}{K_c} \dot{\Theta}_c$$

where $\dot{\Theta}_c$ is the gimbal command ramp rate.

The maximum tracking angular rate for the MWCE is about 1 deg/sec. For the baseline APS, a constant 1 deg/sec angular rate input causes a steady state error of 0.001 deg. During actual operation, the input to the APS will not have

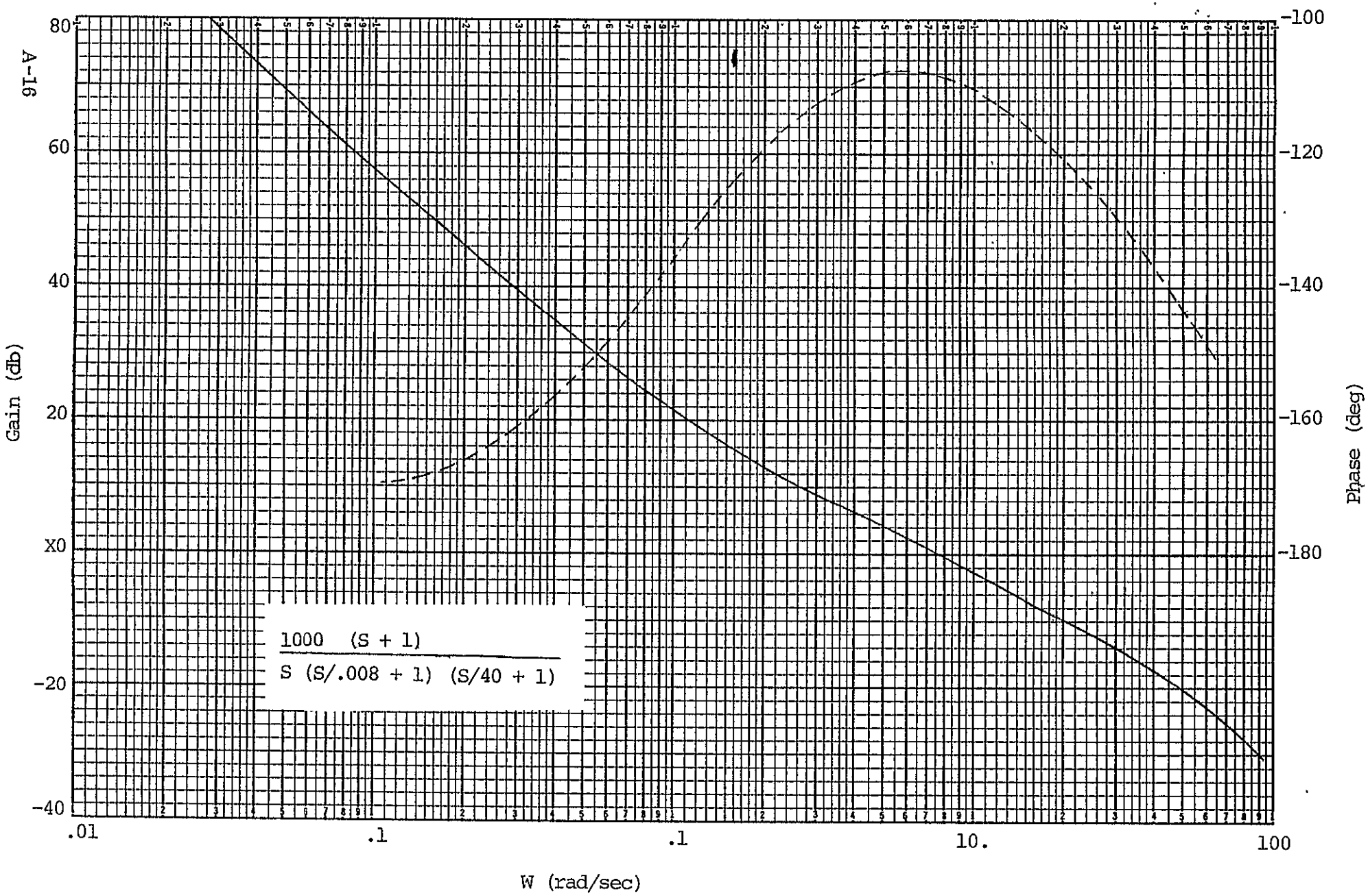

Figure 8 Baseline APS Open Loop Frequency Response

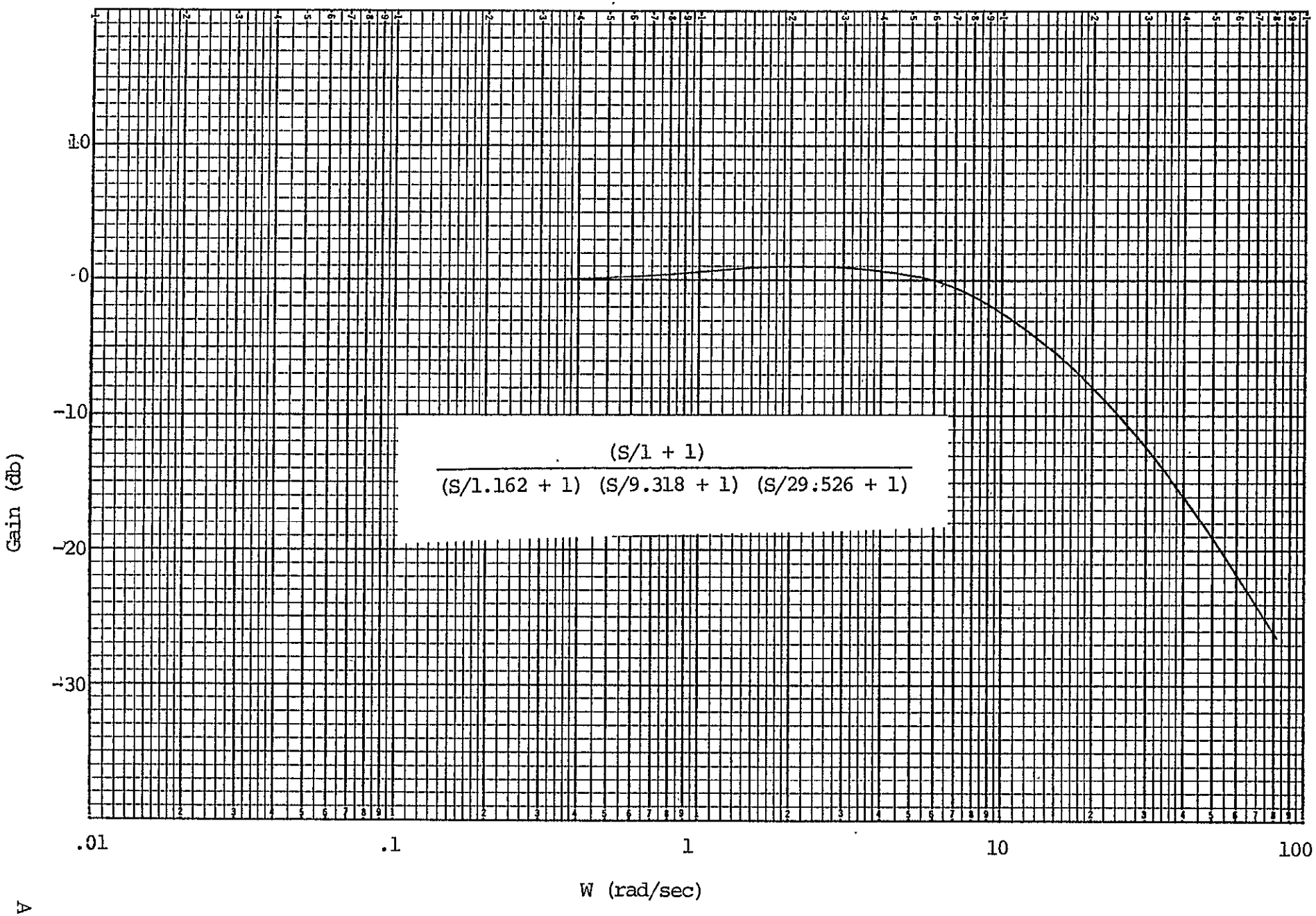

Figure 9 Closed Loop Frequency Response

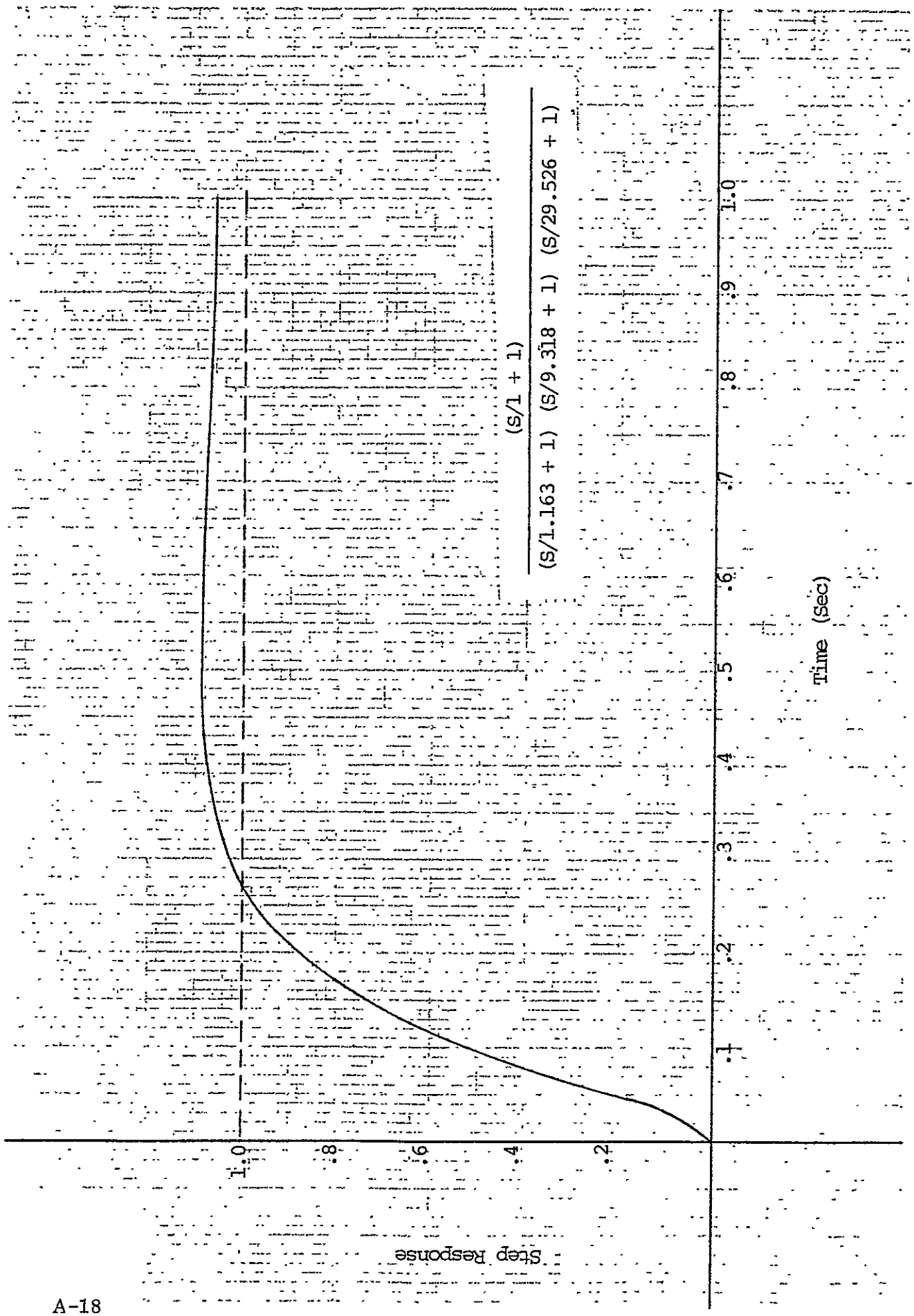

Figure 10 Unit Step Response

a constant angular rate; i.e., keeping the antenna boresight aligned with the ground station will require some angular acceleration. This angular acceleration will cause some increase in the tracking error; however, the angular acceleration is low and the above result indicates that the tracking error caused by the target motion will be small.

Disturbance Torque Response

An important consideration in the MWCE APS is the effect of disturbance torques introduced by shuttle motion. It is assumed that the shuttle is limit cycling between attitude error limits. When the attitude error limit is reached, thrusters are fired to reverse the shuttle angular rate. These thruster pulses generate shuttle motion that results in disturbance torques being applied to the APS gimbals.

The disturbance torque caused by shuttle motion can be shown to be:*

$$Td = l_E \, m \, \ddot{Z}g$$

where Td is the disturbance torque

l_E is the distance from the experiment center of mass and the gimbal axis

m is the mass of the experiment

$\ddot{Z}g$ is the gimbal acceleration.

$\ddot{Z}g$ depends on the shuttle motion and is given by:

$$\ddot{Z}g = \left(\frac{1}{m_s} + \frac{l_g \, l_t}{I_s} \right) F_t$$

where F_t is the thruster force used to control the shuttle attitude.

l_t is the moment arm from the thruster to the shuttle c.g.

l_g is the moment arm from the shuttle c.g. to the gimbal axis.

I_s is the shuttle moment of inertia.

m_s is the shuttle mass.

---

*This disturbance torque analysis is based on a similar analysis performed by Ball Bros. Research Corp. for the shuttle Small Instrument Pointing System (SIPS).

The following numberical values are used:

m_s = 5925 slugs

I_s = 5.8099 E6 slug ft^2

F_t = 36 lb.

l_t = 66 ft.

l_g = 30 ft.

l_E = 3 ft.

m = 6 slugs

yielding

$\ddot{Z}_g$ = 0.0184 ft/sec^2

and

T_d = .33 ft.lb.

The disturbance torque is not a step but rather a short duration pulse. The duration of the pulse can be determined from the time required to change the shuttle angular rate from +0.01 to -0.01 deg/sec. which yields a pulse duration of 0.86 sec.

To find the approximate gimbal attitude error caused by the shuttle motion, the disturbance torque pulse will be approximated by an impulse with strength (.33) (.86) = .28 ft. lb.

The response to the shuttle induced 0.28 ft. lb. disturbance torque impuls is shown in Figure 11. It can be seen that the peak antenna pointing error is about 0.06 deg. This is acceptable; however, for the preliminary design phase it would be desirable to have a slightly lower disturbance torque response. The disturbance torque induced pointing error can be reduced by increasing the control loop gain and bandwidth. This also increases the errors introduced by monopulse noise; however, the monopulse noise analysis indicates that there is some margin for increasing the bandwidth.

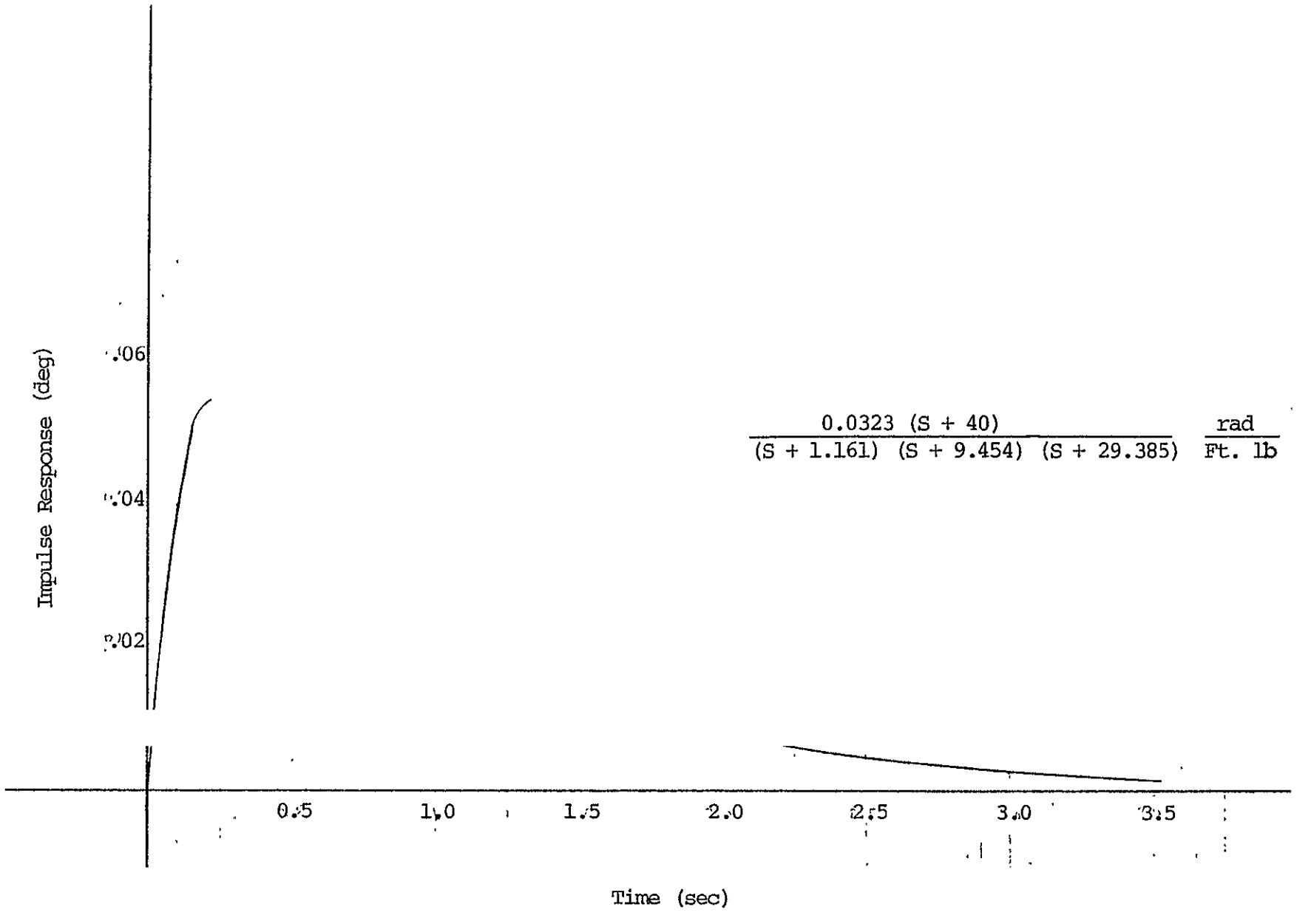

Figure 11 Disturbance Torque Impulse Response

Monopulse Noise Response

The antenna pointing error response to monopulse noise is given by the APS closed loop response.

$$\frac{\theta}{\theta_n}(s) = G_c(s)$$

It will be assumed that the monopulse noise is white with strength σ_n^2; thus the monopulse noise power spectral density (PSD) is uniform with frequency and has magnitude σ_n^2.

The 1σ pointing error caused by the monopulse noise, σ_θ, is then computed by:

$$\sigma_\theta = \sigma_n \left[\frac{1}{2\pi} \int_{-\infty}^{\infty} |G_c(j\omega)|^2 d\omega \right]^{1/2}$$

The integral in the brackets has been tabulated for rational algebraic transfer functions. For the baseline APS, the monopulse noise response can be computed to be:

$$\sigma_\theta = 2.15\, \sigma_n$$

A preliminary analysis of the MWCE monopulse tracking accuracy indicates that the monopulse noise will be quite low - 0.00016 deg (1σ). Thus, the 3σ antenna pointing error caused by monopulse noise is 3 (2.15) (.00016) = .001 deg for the baseline APS.

Other Considerations

1. Effects of Shuttle Angular Rate

Shuttle angular rates cause antenna pointing disturbance through the motor back emf (as shown in Figure 7) and through the bearing friction (not shown in Figure 7). Because of the relatively low shuttle angular rates, these disturbanc are not expected to produce significant antenna pointing errors.

2. Antenna Stowing Maneuver

The MWCE antenna must be stowed and latched prior to shuttle deorbit and landing. The important requirement for the stowing maneuver is that the antenna be guided into the proper position for engaging the retention mechanism without striking any of the support structure. It appears that the baseline APS can support this requirement by employing the acquisition mode control configuration (i.e., control using the potentiometer) and selecting a proper sequence of contro commands.

First the antenna would be oriented such that a single gimbal axis maneuver is required to complete stowing. The final stowing maneuver would then be executed as a series of small steps or a slow rate ramp until the antenna is in the desired position. This approach would avoid any significant control loop overshoot that would bump the antenna into the support structure.

An alternate approach for the final (i.e., single axis) stowing maneuver would be to modify the control loop compensation such that the loop is highly overdamped and responds to command inputs with zero overshoot. This approach would complicate the APS controller somewhat but simplify the stowing maneuver commanding.

3. MWCE/Spacelab Cable

The current MWCE design employs a flexible cable to provide power and signal communication between the gimbal mounted MWCE and the Spacelab. Care must be taken in the design of this cable to ensure that the cable induced disturbance torques do not generate large pointing errors.

GENERAL ELECTRIC

Space Division

Headquarters: Valley Forge, Pennsylvania ☐ Daytona Beach, Fla. ☐ Evendale, Ohio

☐ Huntsville, Ala. ☐ Bay St. Louis, Miss. ☐ Houston, Texas ☐ Sunnyvale, Calif.

☐ Beltsville, Md. ☐ Tacoma, Wash. ☐ Palmdale, Calif. ☐ Bedford, Mass.

☐ Washington, D.C. Area